Sede Amministrativa: Università degli Studi di Padova
Dipartimento di *Biologia*

SCUOLA DI DOTTORATO DI RICERCA IN : BIOSCIENZE E BIOTECNOLOGIE

INDIRIZZO: BIOTECNOLOGIE

CICLO XXVI

FATTORI PATOGENETICI DELL'HELICOBACTER PYLORI

Direttore della Scuola : Ch.mo Prof. Giuseppe Zanotti

Coordinatore d'indirizzo: Ch.mo Prof.ssa Fiorella Lo Schiavo

Supervisore :Ch.mo Prof. Giuseppe Zanotti

Dottorando : Marco Salamina

UNIVERSITY OF PADOVA

DEPARTMENT OF BIOLOGY

PhD School : Bioscience and biotechnology

Curriculum: Biotechnology

CYCLE XXVI

HELICOBACTER PYLORI

PATHOGENIC FACTORS

School Director : Prof. Giuseppe Zanotti

PhD address coordinator : Prof. Fiorella Lo Schiavo

Supervisor : Prof. Giuseppe Zanotti

PhD Student : Marco Salamina

Content

SUMMARY

From 1994, ***Helicobacter pylori*** was classified by WHO (**W**orld **H**ealth **O**rganization) as a class I carcinogen and its infection has been associated to gastroduodenal disease. It colonizes more than half of worldwide population, with a prevalent infection rate in developed countries. In spite of the majority of infected people are asymptomatic, around 20% develop severe pathologies like peptic ulcers and the 1% lymphoma of the mucosa-associated lymphoid tissue (MALT) and stomach cancer. This significant epidemiological study both of the unique characteristics of *H. pylori* inspired many scientists, as bacteriologist, gastroenterologists, cancer and pharmaceutical scientists to understand physio-pathological aspects of this bacterium, and also microbiologist, taxonomist, microbial ecologist and molecular biologist, for a more detailed molecular approach.

H. pylori, a Gram negative, microaerophilic bacteria that colonize human gastric mucosa. It is not an acidophilus bacterium and even if the stomach lumen presents inhospitable condition for most microbes, it is able to survive for a short period, sufficient to enter in the highly viscous mucosa, reach gastric epithelium, and colonize the gastro-enteric tract. *H. pylori* colonization is mediated by a predominant virulence factor, the flagellar motility associated to chemotaxis. To avoid its discharge in the intestinal tract by peristalsis, the bacteria establish a persistent infection inside the viscous gastric mucus film that covers the gastric epithelium. A nickel containing enzyme, the urease, hydrolyzes the urea present in the stomach to ammonia and CO_2, buffering the pH of the periplasm. The most severe clinical outcomes are always associated to cag^+ strains. **cag-*PAI*** is defined as the "Cytotoxic Associated Genes Pathogenicity Island" and it consists of a characteristic chromosome, flanked by transposable elements. Another important virulent factor is the vacuolating cytotoxin A, known as **VacA,** which induces the formation of large cytoplasmic vacuoles in gastric cultured cell lines. Moreover the iron and nickel acquisition is essential grow factors and a large number of genes are responsible of this mechanism.

While the development of an efficient vaccine against *H. pylori* is now the aim of many researchers, the search for new specific antibiotics as a new pharmaceutical target is required for the complete eradication of *H. pylori*.

In this thesis has been investigate the structural and function role of different pathogenic proteins involved in the *H. pylori* colonization of human gastric mucosa. These potential drug targets have been cloned, 8 out of 11 were expressed in a heterologous expression system, after

purification, 2 of them generate protein crystals and only one was possible to characterize the molecular structure. In particular it has been elucidated a possible physiological role of CeuE (HP1561), a Class III SPB (**S**ubstrate **B**inding **P**rotein), crystalized with $Ni(His)_2$ complex and it was determined its affinity to the complex by an *in vitro* approach. The *H. pylori* flagella play a key role during infection allowing the bacterium to move through the mucous layer. The *H. pylori* hook scaffolding protein FlgD were cloned, expressed, purified and crystalized. A study of other purified pathogenic *H. pylori* factors belonging to flagellar component apparatus and transcriptional factors involved in cellular stress response has been reported.

To obtain these results, different experimental approaches has been used. Bioinformatics analysis of target proteins has been performed to predict the best candidates for a crystallographic study and for genetic construction design. Molecular cloning in plasmid vectors has been performed from PCR amplification. The expression conditions were optimized and performed in *E. coli,* a heterologous system. The solubility of recombinant proteins were checked and obtained also with protein refolding methods. Different purification techniques were used in order to obtain pure protein. Target characterization was performed due analytical gel filtration, UV spectroscopy, DLS (**D**ynamic **L**ight **S**cattering) and CD (**C**ircular **D**ichroism). The proteins were concentrated to crystallization trials. The protein crystals obtained were analyzed at ESRF synchrotron (Grenoble, France). Functional *in vitro* approaches were performed using fluorescence spectroscopy, SPR (Surface Plasmon Resonance) and Mass spectroscopy.

In the second chapter is described the three dimensional structure of a *H. pylori* pathogenic protein crystalized in presence with its possible physiological substrate. **HP1561 (CeuE)** is a *H. pylori* protein predicted to be an ABC transporter component, periplasmic iron-bind transporter. Recently it was published that CeuE and fecDE genes of *H. mustelae* encode for a nickel and cobalt acquisition system. In Gram-negative bacteria, nickel uptake is guaranteed by multiple and complex systems that operate at the membrane and periplasmic level. *H. pylori* employs other yet uncharacterized systems to import the nickel required for the maturation of key enzymes, such as urease and hydrogenase. To understand this contradiction of the data about Ni^{2+} acquisition system in *H. pylori* CeuE was cloned, expressed, purified, crystallized and its structure determined. Identity between the sequences of the two *Helicobacter* is 44%. The two Histidine residues (H103 and H197), potentially involved in Siderophores/Ni^{2+} binding coordination in *H. pylori* CeuE, are partially conserved. The His corresponding to *H. pylori* position 103 is conserved, whilst His197 is replaced by a Leucine. In order to check, if this

substitution influence the binding of siderophores/Ni^{2+}, the mutant of *H. pylori* CeuE H197L was than produced and purified. The crystal structure of *H. pylori* CeuE has been determined at 1.65Å resolution using the SAD method, in Apo-form and in complex with $Ni(His)_2$. It comprises two structurally similar globular domains, each consisting of a central five-stranded β-sheet surrounded by α-helices, an arrangement commonly classified as a Rossmann-like fold. Structurally, *H. pylori* CeuE belongs to the class III periplasmic substrate-binding protein. Crystallographic data, fluorescence binding assays and SPR analysis allow to exclude a role of the protein in the transport of VitB12, heme, enterobactin and isolated Ni^{2+} ions. On the contrary, the crystal structure of the protein/$Ni(L\text{-}His)_2$ complex and dissociation constant obtained by SPR technique suggests that *H. pylori* CeuE binds and transport nickel *in vivo* thanks to the formation of a Ni^{2+}/histidine complex or to some ligand that mimics it.

In the third chapter is presented the study of **FlgD**, a flagellar component involved in the formation the extracellular complex, the flagellar hook. The motility of *H. pylori* is considered a colonization factor, due the fact that less motile strains are less able to colonize or survive in the host than full motile strains. In the flagellum machinery are involved more than 50 genomic genes for regulation and assembly. The three major components are the filament, the hook and the basal body. FlgD is not present when the flagellum is completed, but plays a key role during the assembly. Therefore, it has been classified as the hook-scaffolding protein, considering it also as the hook capping protein, interacting with FlgL and FlgK and the basal body rod – modification protein. In *H. pylori* G27 strain FlgD correspond to the gene *hp0858* that was amplified from purified genomic DNA and cloned in an expression plasmid vector. The protein was produced in *E. coli* BL21 in reach medium ad it resulted to a soluble protein. DLS and analytical gel filtration confirm the oligomeric state of FlgD that resulted to be a tetramer in solution. The protein was concentrated to 30g/l and crystalized after a couple of month of incubation. The crystals had diffracted at 2.7Å of maximum resolution. For molecular replacement approach was used homology modeling. Different molecular models were built to fit experimental diffraction data. The secondary structure of the generated models was fitted with experimental CD spectra, where FlgD resulted to have around 12% of helices and 45% of β-sheets (190-260nm). Crystallographic statistics do not properly converged to a positive molecular refinement with the tested models. To solve FlgD structure are necessary crystals of recombinant Selenomethionine FlgD that was expressed, purified and crystalized.

In the fourth chapter are reported *H. pylori* pathogenic proteins that had been characterized. These proteins could be divided in two groups, the first one of flagellar proteins and the second

of cellular stress response factors, in collaboration with Professor V. Scarlato of the department of Biology of Bologna University.

FliN is a cytosolic protein, localized in the C ring of the flagellar basal body. It interacts with the other two components FliM and FliG. Missense or mutation of *fliN* had been associated to non-motile strains. It has been reported that regulates the clockwise/counterclockwise switching of flagella. *H. pylori* FliN was cloned, expressed and purified from the inclusion body after refolding. Oligomerization after refolding was tested by DLS and analytical gel filtration. The protein resulted to be poly-disperse in solution and no protein crystals have been obtained.

FliD is the filament capping protein and it was observed that interact with **FliT** that is not only a flagellar type III substrate specific export chaperone but also inhibits the expression of *fliD* thought its specific interaction with the master regulator $FlhD_4C_2$ complex. In order to analyze possible structure of the co-crystalized FliD-FliT, it was plan to co-express these proteins. Both were cloned with a different affinity purification system, but only FliT was possible to express and purify from inclusion bodies. The CD spectra presented a strong β-sheet component in the secondary structure. DLS and analytical gel filtration revealed that this protein is poly-disperse in solution and no protein crystals were be obtained.

FlgN is a type III secretion chaperone and it has been reported to interact with the two hook junction protein **FlgK** and **FlgL** preventing the protein proteolysis when the flagellum is not assembled. These proteins have been cloned in different type of plasmid vectors for a co-expression experiment, but only FlgN was properly expressed in *E. coli.* Recombinant FlgN was purified by Ni-IMAC and resulted to be soluble in solution. The protein was characterized by analytical gel filtration, DLS and CD. The protein resulted to be a monomer in solution with a 30% of not defined secondary structure (190-260nm). FlgN was concentrated and different crystallization conditions were tested.

In the latter group there are three proteins related to Heat shock response, produced when bacteria encounter stress such as the elevated temperatures, ethanol, H_2O_2 and acid. It was demonstrated that *H. pylori* Hsps play an important role during the host infection. **HrcA** and **HspR** are negative repressor of *groESL* and *dnaK* machinery. HrcA activity depends by the presence of HspR, because it is demonstrated that HrcA is not able to bind DNA in absence of HspR. These two proteins were expressed in *E. coli* and purified by Ni-IMAC affinity. During the concentration step, these proteins present a solubility limit influenced by the concentration.

Mutagenesis of a Cys in HspR and detergent solubility screening with HrcA has been performed, but no suitable protein for crystallization trials has been obtained.

Hp1026 is a gene present in the same operon of HspR (*hp1025*). The function of this gene has not been reported. From sequence homology was possible to identify a helicase domain and ATP-binding domain. This protein, **ORF**, has been expressed in *E. coli* and purified by Ni-IMAC affinity. Analytical gel filtration and CD has been performed to characterize this protein. The protein was a dimer in solution with a 35% of α-helices component. Crystallization trials have been performed at different protein concentrations and also in presence of its possible cofactor, ATPγS. No crystals have been obtained in tested condition.

Appendix:

*Structural and functional study on a human protease **S1P/ SKI1***

The study of human **S1P/SKI1** protease was performed in collaboration with Professor S. Kunz of the Institute of Microbiology, University Hospital Center and university of Lausanne, Switzerland. S1P/SKI-1 is a serine protease that belongs to the mammalian family of Proprotein Convertases (PC). The aim of this family member is to mediate the activation of different important substrates for cell live. Among these proteases, S1P has been shown to have unique substrate specificity, preferring cleavage after non-basic amino acids. Known S1P cellular targets are SREBP-2, involved in the biosynthesis and uptake of lipids and cholesterol, BDNF, ATF-6 and the surface glycoprotein of viruses belonging to the family of *Arenaviridae*. S1P is 118 kDa multi-domain protein; two regions of S1P have been investigated, the "Prodomain", involved in the regulation of S1P catalytic activity, and the so called "catalytic domain", which include the residues responsible for the cleavage reaction itself. Moreover it was analyzed an inactive mutant of cS1P: H249A. Also for ProD was chosen one constructs (ProD_AB and ProD_AC) involved in the affinity of the protease substrate. Hence, the sequences corresponding to the domains were synthesized as optimized genes for the expression in *E. coli* and sub-cloned in expression plasmids in order to obtain C-term His-tagged fusion proteins. These constructs have been expressed in *E. coli,* purified by Ni-IMAC and positive fractions have been collected and concentrated in order to perform crystallization trials. Unfortunately no protein crystals have been obtained in tested condition. To elucidate the role of a mutated variant of the cleavage site “C” of Pro Domain, it was performed a mass spectrometry analysis. Secreted S1P/SKI1 mutant C was purified from culture medium of HEK293 cell line was isolated by IMAC-Co. The sample,

loaded in RP-HPLC, was denatured in 6 M Guanidine-HCl. The chromatographic fractions corresponding to the major HPLC peaks were dried out in a speed-vac concentrator and directly injected in the ESI source. Mass measurements were performed with a quadrupole-TOF spectrometer. Analysis of mass spectra, compared with wild-type form of S1P, allows generating a preliminary Pro Domain auto-processing profile.

SOMMARIO

Dal 1994 il batterio *Helicobacter pylori* è stato classificato come organismo cancerogeneno di prima classe e la sua infezione è associata a patologie gastroduodenali. Più di metà della popolazione mondiale ne è infettata con una maggiore prevalenza nei paesi sviluppati. Nonostante la maggior parte dei casi le infezioni sono asintomatiche, il 20% sviluppa gravi patologie come ulcere peptiche e nell'1% dei casi genera linfomi e gastro carcinomi. L'incidenza e le caratteristiche di questo batterio hanno ispirato batteriologi, gastroenterologi, oncologi e farmacologi per indagare gli aspetti fisiopatologici legati all'infezione, così come microbiologi, ecologi, biologi molecolari hanno cercato i fattori di virulenza coinvolti in nell'infezione.

H. pylori è un batterio microaerofilico Gram negativo che colonizza la mucosa gastrica. Non è un batterio acidofilo, anche se è in grado di sopravvivere nel lume dello stomaco per un breve periodo necessario per raggiungere le cellule epiteliali spostandosi attraverso la mucosa gastrica. La colonizzazione è mediata da fattori di virulenza predominanti come la motilità flagellare associata alla chemiotassi. Per evitare che sia espulso dal tratto intestinale dalla peristalsi, il batterio *H. pylori* stabilisce un'infezione cronica. L'ureasi, che è un enzima nickel dipendente, che idrolizza l'urea presente in ammoniaca e CO_2 tamponando il pH acido dello stomaco. I casi più gravi sono associati ai ceppi che esprimono l'isola di patogenicità *cag-PAI,* che consiste in un cromosoma delimitato da elementi trasponibili. Un altro importante fattore di virulenza è la tossina vacuolizzante VacA, che induce la formazione di vacuoli citoplasmatici. Anche il meccanismo di acquisizione di ferro e nickel è fondamentale per la colonizzazione batterica e dunque finemente regolata da un gran numero di geni.

Lo sviluppo di un vaccino e nuovi antibiotici nutrono una costante ricerca di nuovi possibili bersagli farmacologici, necessari per completa ed efficiente eradicazione del batterio *H. pylori*.

In questa tesi sono stati analizzati il ruolo e la struttura di alcune proteine patogenetiche del *H. pylori*. Questi potenziali target farmacologici sono stati clonati, otto su undici sono stati espressi in un sistema eterologo, due proteine di quelle purificate hanno generato cristalli e di una sola ne è stata definita la struttura molecolare. In particolare è stato definito un possibile ruolo della proteina CeuE (HP1561), appartenete alla famiglia delle proteine che legano un substrato, cristallizzata in presenza del complesso $Ni(His)_2$ e definita l'affinità con lo stesso *in vitro.*

Del flagello, che svolge un ruolo chiave durante l'infezione, ne è stata studiata la proteina coinvolta nella formazione dell'uncino FlgD che è stata clonata, espressa, purificata e cristallizzata.

Inoltre è stato riportato anche uno studio di altri fattori del flagello e di alcune proteine coinvolte nella risposta allo stress cellulare.

Per ottenere tali risultati sono stati utilizzati approcci differenti. Per individuare le migliori proteine candidate per uno studio cristallografico e progettare costrutti funzionali sono state effettuate predizioni bioinformatiche. Gli amplificati di PCR sono stati clonati in vettori plasmidici. Le condizioni di espressione sono state ottimizzate e fatte in *E. coli,* un sistema di espressione eterologo. La solubilità delle proteine ricombinanti è stata analizzata e ottenuta anche mediante refolding. Sono stati usati diversi sistemi di purificazione per ottenere un buon grado di purezza. Per la caratterizzazione proteica sono state usate come tecniche la gel filtrazione analitica, spettroscopia UV, DLS (Dynamic Light Scattering) e dicroismo circolare. Le proteine sono state concentrate e sottoposte a esperimenti di cristallizzazione. I cristalli sono stati analizzati al sincrotrone ESRF (Grenoble, France). Spettroscopia di fluorescenza, SPR (surface plasmon resonance) e spettroscopia di massa sono le tecniche utilizzate per la caratterizzazione *In Vitro.*

Nel secondo capitolo viene decritta la struttura tridimensionale di una proteina patogenetica di *H. pylori,* cristallizzata in presenza del suo possibile substrato fisiologico. **HP1561 (CeuE)** è una proteina di *H. pylori* annotata come componente periplasmatico di un trasportatore ABC che lega e trasporta il ferro. Recentemente è stato pubblicato chele *ceuE* e *fecDE* di *H. mustelae* codificano per proteine coinvolte nel acquisizione del nickel e cobalto. Nei Gram negativi, l'acquisizione del nickel è garantita da sistemi di proteine che operano a livello di membrana e periplasmatico. Per l'acquisizione del nickel, l' *H. pylori* integra diversi sistemi non ancora caratterizzati, necessari per la maturazione di enzimi chiave come l'ureasi e l'idrogenasi. Per chiarire tale contraddizione nel sistema di acquisizione del nickel nell'*H. pylori,* CeuE è stata clonata, espressa, purificata, cristallizzata e la sua struttura è stata risolta. L'identità di sequenza tra i due *Helicobacter (pylori e mustelae)* è del 44%. Le due Istidine (H103 e H197), potenzialmente coinvolte nel legame di coordinazione del sistema sideroforo/Ni^{2+} nel *H. pylori* CeuE, risultano essere parzialmente conservate. L'His corrispondente alla His103 di *H. pylori* è conservata, mentre His197 è sostituita da una Leucina. Al fine d'identificare se tale mutazione possa influenzare il legame sideroforo/Ni^{2+}, è stato prodotto e purificato il mutante *H. pylori* CeuE H197L. La struttura molecolare di *H. pylori* CeuE è stata determinata con una risoluzione di 1.65 Å mediante metodo SAD, sia nella forma apo, che in complesso col $Ni(His)_2$. Essa è costituita da due domini globulari simili, ognuno costituito da cinque foglietti-β circondati da α-eliche, comunemente classificato come Rossman fold. Strutturalmente *H. pylori* CeuE appartiene alla Classe III della famiglia di proteine che legano un substrato specifico (SBPs). Dati cristallografici,

saggi di fluorescenza e analisi all'SPR ci permettono di escludere il coinvolgimento della proteina nel trasporto della VitB12, eme, entrobactina, e ioni Ni^{2+} isolati. Al contrario la struttura della proteina/complesso $Ni(His)_2$ e le costanti di dissociazione ottenute mediante SPR suggeriscono che *H. pylori* CeuE lega e trasporta il nickel *in vivo* mediante il complesso Ni^{2+}/His o altro ligando che lo mima.

Nel terzo capitolo viene presentato lo studio su **FlgD,** una proteina flagellare fondamentale nella formazione di un complesso extracellulare, l'uncino del flagello. La motilità dell'*H. pylori* è considerata un fattore di colonizzazione, attraverso il quale ceppi meno motili hanno minori possibilità di colonizzare e sopravvivere nell'ospite di ceppi più motili. Per la formazione del flagello sono coinvolti più di 50 geni per la regolazione e l'assemblaggio delle varie componenti. Le tre componenti principali sono il filamento, l'uncino e il corpo basale. FlgD non è presente quando il flagello è maturo, ma ha un ruolo chiave durante l'assemblaggio. Perciò, è stato classificato come proteina necessaria per l'impalcatura dell'uncino (*hook scaffolding protein*), considerata anche proteina di testa dell'uncino (*capping protein*) in quanto interagisce con FlgL, FlgK e le proteine del corpo basale. Nel ceppo *H. pylori* G27, FlgD corrisponde al gene *hp0858* che è stato amplificato dal DNA genomico purificato e clonato in un vettore plasmidico. La proteina è stata prodotta in *E. coli* BL21 e la proteina è risultata essere solubile. Gel filtrazione analitica e misure al DLS confermano il suo stato di oligomerizzazione, che risulta essere un tetramero in soluzione. La proteina è stata concentrata fino a 30 g/l e cristallizzata dopo un paio di mesi d'incubazione. I cristalli hanno diffratto a una risoluzione massima di 2.7 Å. Per la sostituzione molecolare è stata usata la tecnica del *homology modelling*. Sono stati costruiti diversi modelli molecolari per fittare i dati sperimentali. La struttura secondaria dei modelli generati è stata comparata con gli spettri di dicroismo circolare, dove FlgD è risultata essere composta da un 12% di eliche e complessivamente da un 45% di foglietti beta (190-260nm). Le statistiche cristallografiche non hanno dato convergenza positiva negli esperimenti di sostituzione molecolare con i modelli testati. Per risolvere la struttura di FlgD sono necessari cristalli di FlgD derivatizzata con Selenometionine, che è stata espressa, purificata e cristallizzata.

Nel quarto capitolo sono riportate le proteine patogenetiche di *H. pylori* che sono state caratterizzate in questa tesi. Queste proteine possono essere divise in due gruppi, il primo delle proteine flagellarli ed il secondo delle proteine coinvolte nella risposta allo stress cellulare in collaborazione con il Prof. V. Scarlato del dipartimento di Biologia dell'università di Bologna.

FliN è una proteina citosolica localizzata nell'anello C del corpo basale del flagello ed interagisce con altri due componenti FliM e FliG. Mutazioni missenso di *fliN* sono state associate a ceppi non-motili ed è stato riportato che regola la rotazione oraria/antioraria del flagello. *H. pylori* FliN

è stata clonata, espresso e purificata dai corpi d'inclusione dopo refolding. Lo grado di oligomerizzazione è stato analizzato mediante DLS e gel filtrazione analitica. La proteina è risultata essere polidispersa i soluzione e non sono stati ottenuti cristalli di proteina.

FliD è la proteina "capping" del filamento cellulare ed è stato osservato che interagisce con **FliT**, che non è solo un chaperon substrato specifico del sistema III di esporto flagellare, ma inibisce anche l'espressione di *fliD* attraverso l'interazione con il complesso $FlhD_4C_2$. Al fine di analizzare la struttura del complesso FliD-FliT, è stata pianificata la co-espressione di queste proteine. Entrambe sono state clonate con un sistema di purificazione differente, ma solo la purificazione di FliT è stata possibile dai corpi d'inclusione. Lo spettro di dicroismo circolare ha rivelato una forte componente di foglietti-β nella struttura secondaria. Secondo le misure di DLS e gel filtrazione analitica FliT è polidispersa in soluzione e perciò non stati ottenuti cristalli della stessa.

FlgN è una proteina del sistema secrezione tipo III ed è stato osservato che interagisce in maniera specifica con le proteine di giunzione dell'uncino con il filamento FlgK ed FlgL, prevenendone la proteolizzazione prima della maturazione del flagello. Queste proteine sono state clonate in differenti tipi di vettori plasmidici, ma solo FlgN è stata efficacemente espressa in *E. coli.* FlgN ricombinante è stata purificata mediante Ni-IMAC è risultata essere solubile. La proteina è stata caratterizzata con gel filtrazione analitica, DLS e CD. La proteina è un monomero in soluzione con un 30% di struttura secondaria non definita (190-260 nm). FlgN è stata concentrata e sottoposta a test di cristallizzazione.

Nell'ultimo gruppo ci sono tre proteine HSPs (Heat Shock Response), prodotte dal batterio quando incontra stress come elevate temperature, etanolo, H_2O_2 e acidi. E' stato accurato che le HSPs di *H. pylori* svolgono un ruolo importante durante l'infezione dell'ospite. **HrcA** e **HspR** reprimono la trascrizione di *groESL e dnaK.* L'attività di HrcA è influenzata dalla presenza di HspR, in quanto è stato dimostrato che HrcA non è in grado di legare il DNA in assenza di HspR. Queste due proteine sono state espresse in *E. coli* e purificate con Ni-IMAC. Durante le fasi di concentrazione hanno mostrato un limite di solubilità. Mutagenesi mirata sul costrutto di HspR e screening di detergenti su HrcA sono hanno migliorato il sistema, senza però riuscire ad ottenere una condizione ottimale per la formazione di cristalli di proteina.

HP1026 (ORF) è un gene presente nello stesso operone di HspR (*hp1025*), ma con funzione non nota. Dall'analisi della sequenza è stato identificato un dominio con attività elicasica ed un dominio legante l'ATP. La proteina è stata espressa in *E. coli* e purificata con Ni-IMAC. Per la caratterizzazione sono state effettuate gel filtrazione analitica e dicroismo circolare. La proteina

risulta essere un dimero in soluzione con un 35% di α-elica. I test di cristallizzazione son stati effettuati scrinando diverse concentrazioni e anche in presenza del possibile cofattore, ATPγS in forma non idrolizzabile. Nessun cristallo è stato ottenuto dalle condizioni testate.

Appendice:

Studio strutturale e funzionale della proteasi umana S1P/SKI1

Lo studio di questa proteasi umana è stato effettuato in collaborazione con il Prof. S. Kunz dell'Istituto di Microbiologia, del Centro Universitario Ospedaliero e dall' Univ. Di Lausanne, Svizzera. **S1P/SKI1** è una serina proteasi della famiglia delle Proprotein Convertasi (PCs). Lo scopo di membri di questa famiglia è quello di mediare l'attivazione di diversi importanti substrati per la vita cellulare. Tra queste proteasi, S1P presenta una specificità di substrato, con un sito di taglio dopo un residuo non basico. Tra i target cellulari di S1P sono stati identificati SREBP-2, coinvolto nella biosintesi dei lipidi e del colesterolo, BDNF, ATF-6 e glicoproteine superficiali di virus appartenenti alla famiglia delle *Arenaviridae.* S1P pesa 118kDa ed è una proteina multidominio; quindi 2 regioni di S1P sono state studiate, il "Prodomain" (ProD) che regola l'attività catalitica, ed il "cathalytic domain" (cS1P) che include i residui responsabili per la reazione proteasica. Inoltre è stato analizzato un mutante inattivo (cS1P_H249A) e due costrutti per il dominio di regolazione (ProD_AB e ProD_AC). Le sequenze nucleotidiche dei corrispettivi costrutti sono state sintetizzate come geni ottimizzati per l'espressione in *E. coli* e subclonati in vettori plasmidici per l'espressione ottenendo proteine in fusione con una coda di 6-His. Questi costrutti sono stati espressi in *E. coli*, purificati con Ni-IMAC e le frazioni positive sono state raccolte e concentrate per test di cristallizzazione. Sfortunatamente non sono stati ottenuti cristalli di proteina nelle condizioni testate.

Per chiarire il ruolo di una variante mutata nel sito di taglio "C" del dominio di regolazione è stata effettuata una analisi di spettrometria di massa. La proteina secreta S1P mut C (sS1P_MutC, 116kDa) è stata purificata dal medium di coltura di una linea di HEK293 trasfettate e isolata con Co-IMAC. Il campione è stato denaturato in Guanidinio 6M e caricato in HPLC. Le frazioni corrispondenti ai picchi predominanti sono stati essiccati ed iniettati in spettrometro di massa (ESI-TOF). L'analisi delle masse, confrontate con la forma nativa (sS1P_WT) ha permesso di generare un profilo preliminare del pattern di processamento del dominio di regolazione (ProD)

with a quadrupole-TOF spectrometer. Analysis of mass spectra, compared with wild-type form of S1P, allows generating a Pro Domain auto-processing profile.

Chapter 1

Helicobacter pylori

General aspects

Transmission

Genetic Variability

Acid resistance and adaptation

Colonization and interaction with epithelium cells of gastric mucosa

Virulence factors

H. pylori and gastroduodenal disease

Therapy of *H. pylori* infection

Helicobacter pylori

General aspects

Helicobacter pylori is a non-spore forming gram-negative bacterium that colonizes the human gastric mucosa of more than half of the world's population (Rothenbacher and Brenner, 2003).

The presence of microbes in human stomach was firstly described by Bizzozero in the XIX century, but only in 1983 Warren and Marshall isolated and characterized *H. pylori* (Marshall and Warren, 1984; Nobel Prize, 2005).

The interest of the scientific community spread when Barry Marshall demonstrated that *H. pylori* provokes gastritis, drinking a suspension of *H. pylori* during a congress.

In the scientific literature in the year 2000 more article have been published on *Helicobacter* than on *Salmonella* or *Bacillus,* just behind *Escherichia coli*, the most cited bacteria, demonstrating how biological research has focused on this field.

Fig. 1.1 ***Helicobacter pylori***

The organism isolated by Warren and Marshall was initially classified as *Campylobacter pylori* for its curved morphology. It is characterized by its ability to grow under microaerophilic condition, and by G + C content of 34% (Syst. Bacteriol. 1985;35:223–225). 16S rRNA sequence analysis revealed its distance from *Campylobacter* genus (Romaniuk P.J., 1987), so it was renamed as *Helicobacter pylori* (Goodwin C.S., 1989).

Most of the strains of *H. pylori* are clinically asymptomatic, but some are pathogenic and they can induce gastritis or more sever diseases: 10% of the infected subjects may present peptic ulcer and atrophic gastritis. In 1994, the World Health Organization classified it as the first bacterial class 1 carcinogen, since 1% of infected individuals may develop gastric adenocarcinoma and lymphoma of mucosa-associated lymphoid tissue (MALT) (Blaser, 1998; Peek, 2002, Suerbaum, 2002).

Animal models of infection, such as *H. felis* and *H. mustelae,* have been very useful to characterized *H. pylori* virulence factors, together with *H. pylori* Sydney strain (SS1), which present a reproducible mice infection, very useful for the development of new vaccines. Further gastric *Helicobacter* species have been found in humans and animals, particularly in non-human primates and domesticated mammals; in particular, enterohepatic *Helicobacter,* that was for the first time isolated by Philips and Lee in 1983 (Robertson B.R., 1987).

The small genome size of the bacterium, 1,7 Mb, reveals a profile of an organisms that was fine

tuned for its niche of gastric mucosa: it is an example of co-evolution with the host system, compared to the larger *E. coli* genome, that conserves many regulatory features leaking in *H. pylori* genome.

1.2 Transmission

H. pylori infection is ubiquitous worldwide, with significant differences in the prevalence of infection within and between countries (Goh K. L., 1997; Malaty H. M., 1992). The studies on the transmission of *H. pylori* suggest a human-to-human oral-oral and fecal-oral route (Blaser, 1998), but do not exclude common environmental sources, in particular water (Klein P., 1991) and animals (Morris A., 1986). The acquisition of *H. pylori* happens mainly during childhood (Bardhan N., 1993) and the prevalence of infection is higher in developing countries (Mitchell H.M., 1992).
Some studies suggest, from the geographic subdivision of *Helicobacter* strains, that the bacterium has accompanied humans for ten thousands of year during migrations (Kersulyte, 2000). This could be the reason why *H. pylori* is a very common human pathogen. It has used humans as carrier, possibly providing them with benefits for surviving during long period of human history (Suerbaum, 2002).
The association of *H. pylori* to different severe pathologies such as peptic ulcer, gastric cancer, and B-cell MALT lymphoma requires a quick development of molecular strategies to prevent the spread of the bacterium and of antibiotic resistant strain formation.

Genetic variability of *H. pylori*

H. pylori genome consists of a circular chromosome, sequenced in 1997 using a random shotgun approach. The first strain sequenced was the 26695 strain, which size is 16,667,867 base pair, with 39% of G + C content and 1,590 predicted coding sequence (Tomb, 1997). The sequence of other strains revealed extensive genetic heterogeneity, possibly caused by the selective pressure that had operate on this microorganism together to its specific capability for diversification by mutation and recombination. It has been shown that different strains could colonize the same individual and thereby the primitive fingerprinting of the host changes during chronic colonization (Suerbaum, 2007). The polymorphisms of *H. pylori* are caused by cumulative events of chromosome rearrangements, such as point mutations, recombination, insertions and deletions. This adaptation process is reflected on three major group of bacterial cluster genes: *i*) genes involved in the biosynthesis of the DNA machinery uptake, repair and recombination; *ii*) genes that favor bacteria-bacteria interaction and genetic exchange and *iii*) genes that regulate the host interaction. A particular group of polymorphism of DNA, contingent to 5’ of some

genes, involves short tandem repeats, which are the responsible for this type of recombination improving the heterogeneity among *H. pylori* strains. This type of slippage provokes the shifting in- and out- of frame during the transcription, presenting antigenic variation of the same protein (Saunders, 1998). This mechanism is used by bacteria to improve adaptation to changes of the host inhospitable living conditions. *H. pylori* uses its genetic plasticity for persistent infection, even if the immune response generated by the host is not sufficient to its eradication, and therefore the gastritis pathogenesis of *H. pylori* is still poorly understood (Suerbaum, 2007). The recombination among different strains, correlated to the colonization of different macro-niches of human stomach, increase *H. pylori* fitness, and explain the levels of complexity found in its sub-population (Kang, Blaser, 2006).

Acid resistance e virulence aspects

Helicobacter pylori is not a acidophilus bacterium and even if the stomach lumen presents inhospitable condition for most microbes, it is able to survive for a short period, sufficient to enter in the highly viscous mucosa, reach gastric epithelium, and colonize the gastroenteric tract (Suerbaum, 1999). To complete this sequence of events, it activates a gene cluster (ureAB and ureEFGHI) for the biosynthesis of a nickel containing enzyme, the urease, that hydrolyzes the urea present in the stomach to ammonia and CO_2, buffering the pH of the periplasm (Weeks, 2000). It was demonstrated that urease-deficient *H. pylori* are not able to colonize the stomach (Eaton, 1991). Even if urease is a cytoplasmatic protein, is it possible to found it on bacterial surface, due the lysis of some organisms (Phadinis, 1996), and the protein amount may reach as much as 10% of total bacterial protein (Montecucco, 2001). Therefore, urease is one of the most common bacterial antigens (Del Giudice, 2001). It has been suggested that the external urease protects the bacteria from the low pH of the stomach, creating a cloud of ammonia around it (Scott, 1998; Stingl, 2002). The activity of cytoplasmic urease is regulated by a urea channel (UreI). This regulation is necessary to avoid over-alkalization, lethal for the bacteria (Clyne, 1995). Urease is a dodecamer composed by six subunit of **UreaA** (HP0073) and six of **UreaB** (HP0072), forming a 600kDa molecular complex (Ha, 2001). The formation of this complex and its activation/inhibition is regulated by **UreaE** (HP0070), **UreaF** (HP0069), **UreaG** (HP0068) and **UreaH** (HP0078). Another characteristic system, which regulates the activity of urease and is a low pH sensor (Pflock, 2004), is the **ArsRS** system, essential for growth in *vivo* (Schar, 2005). **ArsS** (HP0165) is a histidine kinase that, in acidic stress conditions, phosphorylates an OmpR-like reponse regulator, **ArsR** (HP165). The genes regulated by this system are membrane proteins, Ni^{2+} storage proteins, detoxifying enzymes and *H. pylori* specific proteins of unknown function.

Other well characterized transcription regulators for acidic resistance are **NikR** (HP1338) and **Fur** (HP1027). Fur is a ferric uptake protein and is a transcriptional factor that controls intracellular iron homeostasis through the expression of iron-uptake and iron-storage genes (van Vilet, 2002; Delany, 2001). At low pH and in the presence of Ni^{2+}, NikR acts as a nickel-regulator that directly represses several genes such as Fur (van Vilet, 2002), but also activates other genes (Contreras, 2003), preventing the emergence of toxic nickel concentrations (Dosanjh, 2006). In general, the outer membrane composition of *H. pylori* plays a key role in acid adaptive response, thanks to a pH sensor system (Pflock, 2006).

Colonization and interaction with epithelium cells of gastric mucosa

H. pylori colonization of human gastric mucosa is mediated by a predominant virulence factor, the flagellar motility associated to chemotaxis (Kavermann, 2003). To avoid its discharge in the intestinal tract by peristalsis, the bacteria establish a persistent infection inside the viscous gastric mucus film that covers the gastric epithelium. For this reason *H. pylori* requires more than fifty putative proteins for the expression, secretion and assembly of polar helicoidal-shaped flagella, composed by a basal body, which include the rings, motor and switching proteins, a hook and a filament. The major proteins involved are **FlaA** and **FlaB** that are the copolymer filament subunits (Haas, 1993). Even if their genes are located in different positions on the chromosome (Suerbaum, 1993), both are necessary for full motility (Josenhans, 1995). **FlgE** is the structural component of the hook, as well as **FliD** that constitutes the capping of the filament. Many other proteins are involved in flagella biosynthesis, assembly and chemotaxis, but little is known about them (O'Toole, 2000). The chemotactic factors, such as urea and bicarbonate ions (Yoshiyama, 1999) associated to the enzymatic ability to disrupt the oligomeric structure of mucin (Windle, 2000), allow *H. pylori* to move and colonize its gastric niche. To bind to epithelial cells, *H. pylori* uses fucosylated glycoproteins and sialylated glycolipids as cellular receptors (Mahdavi, 2002). **BabA** (HP1243) and **SabA** (HP0725) are two outer membrane proteins that present strong allelic variation, producing different bonding models to modulate the adhesion molecules by multiple mechanisms. It has been shown that BabA heterogeneity among *Helicobacter* strains was associated to different clinical outcomes, while SabA positive status has been inversely related to the ability of the stomach to secrete acids (Yamaoka, 2006). The adherence of *H. pylori* could be regulated to avoid regions of stomach epithelium where the host defense response is more vigorous. Another phase variable outer membrane protein, **OipA** (HP0638), identified as a potential colonization factors, is associated to severe outcomes, duodenal ulceration and gastric cancer.

The ability of *H. pylori* to move through the mucus layer by its flagella facilitates a better access to nutrients and the delivery of effectors molecules, that are fundamental steps in the colonization of human gastric mucosa.

Virulence factors

The most severe clinical outcomes are always associated to cag^+ strains (Parsonnet, 1997). **cag-*PAI*** is defined as the "Cytotoxic Associated Genes Pathogenicity Island" and it consists of a characteristic chromosome region of about 40 kb containing around 28-29 genes, flanked by transposable elements (Censini, 1996; Tomb, 1997; Haker, 2000). Some cag-PAI genes encode proteins that form the "Type four secretion system" (T4SSs), which allows the delivery of proteins and/or DNA in the host, influencing its homeostasis. The best characterized secreted protein is CagA, which becomes phosphorylated by endogenous kinases and modulates host cell functions by interfering with cell signaling. CagA is considered a bacterial oncoprotein (Hatakyama, 2004 and 2006) because the interaction of CagA with host proteins induces multiple cellular events that include morphogenetic changes and may lead to malignant transformations (Tummuru, 1993; Covacci, 1993; Hatakeyama, 2005).

Another important virulent factor, which gives a competitive advantage to *H. pylori,* is the vacuolating cytotoxin A, known as **VacA** (HP0887). When secreted, it induces the formation of large cytoplasmic vacuoles in gastric cultured cell lines (Leunk, 1988; Cover, 1992). VacA is a multi-globular protein composed by two domains, p33 and p55, forming a mature toxin whose structure seems a "flower" with a central ring surrounded by "petals". In condition of low pH, the dissociation of this complex is observed, favoring the entrance of the monomer in lipid host cellular membranes by forming a hexameric anion-specific channel (Cover, 1997). The effects produced by this toxin are related to the alteration of antigen presentation (Molinari, 1998), inhibition of T-cell activation and proliferation (Boncristiano, 2003) and apoptosis induction (Galmiche, 2000).

H. pylori pathogenic strains express a protein that is able to activate neutrophiles, **HP-NAP**. This protein promotes the adhesion of human neutrophiles to endothelial cells and simulates the production of reactive oxigen species (ROS) (Yoshida, 1993). The structure of this protein reveals a four-helix bundle protein that oligomerizes to form a dodecamer containing a negatively charged cavity (Zanotti, 2002). In spite the protein ability to store up to 500 iron atoms, it has functionally evolved as a leukocyte activator able to induce mucosal damage, though neutrophils activation (Montecucco, 2001).

H. pylori and gastroduodenal disease

H. pylori infection is usually associated to an increase of the risk of different severe pathologies including peptic ulcers, non-cardia gastric adenocarcinoma and gastric mucosa-associated lymphoid tissue (MALT) lymphoma, even if most of *H. pylori* infected individuals are asymptomatic (Cover, Blaser 2009). The risk of a severe outcome, as peptic ulcers or adenocarcinoma, is strongly correlated to the specific infecting strain. In fact, some *H. pylori* strains present typical protein polymorphism associated to the expression of characteristic virulence factors that usually interacts with host epithelial cells, increasing the risks for some disease. It was demonstrated in different studies that, in particular in Western countries, cag-PAI positive *H. pylori* strains are associated to a high risk of peptic ulcers disease, premalignant gastric lesion, and gastric cancer (Basso, 2008). A more particular protein pattern analysis was performed to the major pathogenic protein factors. The correlation with the number of CagA tyrosine phosphorylated (EPIYA) motifs, as well as the expression of an active form of vacuolating cytotoxin VacA in *vivo* is predictive of gastric cancer risk (Higashi, 2002). Often strains that express BabA and OipA OMPs are associated to a higher risk of disease than the strains that lack these factors (Cover, 2009).

The stomach cancer is usually diagnosed between the ages of 50 and 70 years, excluding hereditary cases in which is possible to observe younger cases more frequently. The geographical distribution of this disease also reflects a higher prevalence in certain world areas, such as Japan, Korea and China (Hatakeyama, 2009). The gastric cancer has been histologically classified in two types, the first one associated to environment perturbations and the second more related to host genetic predisposition. It has been demonstrated that *H. pylori* plays a key role in both type of gastric carcinomas (Uemura, 2001), and that there is a correlation between the dominant form of intestinal-type and *H. pylori* cag^+ strains (Blaser, 1998).

During *H. pylori* infection, there is an activation of the immune response of the host that attracts and activates neutrophils, which release ROS. This response provokes a perpetuation of inflammation, and oxygen radicals may cause a wide range of cellular damages that can be associated to the stimulation of malignant B cells growth in MALT lymphoma (Farinha, Gascoyne 2005).

Gastroesophageal reflux has also been associated to *H. pylori* infection. In fact, motor alteration of esophageal sphincter (Penagini, 2002) should be correlated to esophagus cells damage. The increase of gastric juice secretion, hydrochloric acid and pepsin were identified as the most important factors in the induction of reflux esophagitis. The secretion of gastrin by endocrine G cells is stimulated by gastric mucosal interleukins IL-8 and IL-1b, as a consequence of *H. pylori*

inflammatory response (Souza, 2009).

Recently it was also demonstrated that the motility of *H. pylori* is a critical virulence determinant, since it enhances the effects of SabA, during the adherence of the bacteria to the epithelial gastric cells, increasing the bacterial density to trigger higher inflammatory response (Chen-Yen K, 2012).

Therapy of *H. pylori* infection

The first-line therapy, in population with less than 15-20% clarithomycin resistance rate, consists of a triple therapy, constituted by a proton pump inhibitor (PPI), clarithromycin and moxicillin or metronidazolein (Malfertheiner, 2007). The most serious problem is represented by the increase of *H. pylori* resistant strains (D'Elios, 2007). To avoid this problem, the development of a vaccine represents a possible solution. Several approaches have been devised to generate an effective vaccine against the bacterium. Two generations of vaccine have been generated, the first consisting in the whole bacterial sonicated cells, and the second by *H. pylori* isolated proteins that are processed and used by antigens to simulate immunity in host. They latter needs adjuvants to elicit effective protection. Even if the studies on animal models have been extensive, the human successful cases are limited. About human trials, the most successful trial used the bacterium *Salmonella typhi* carrying *H. pylori* antigens or inactivated *H. pylori* cells. In this case *S. typhi* was deleted of virulence genes and modified to consecutively express *H. pylori's* urease, then this vector was orally administrated to 8 uninfected volunteers, but it was ineffective in producing any detectable mucosal or humoral immune response to urease antigen (DiPetrillo, 1999). Changing the bacterial vector in *S. tiphimurium,* better results were observed in some human volunteers, who produced some antibody against urease (Angelakopulos, 2000). Another vaccine against *H. pylori* tested on human uninfected volunteers was a *Salmonella* prophylactic Ty21a(pDB1), which displayed moderate efficacy but no major adverse effects (Bumann, 2001). Oral inactivated *H. pylori* whole cell vaccine induced a specific B-cell response, but could not eradicate the bacterium from infected individuals, showing prophylactic but not therapeutic efficacy (Losonsky, Kotoloff, 2003).

Vaccinologists are now going to test new forms of vaccine based on live vectors, for instance DNA vaccines, which carry DNA sequences encoding *H. pylori* antigens, increasing safety and efficacy. The microsphere vaccines are able to induce humoral and mucosal immunity as well as mediated immunity. Bacterial ghost vaccines simulate the native antigenic structures, since they are constituted by empty cell envelopes without cytoplasmic contents, preserving cellular morphology (Agarwal, 2008).

While the development of an efficient vaccine against *H. pylori* is now the aim of many researchers, the search for new specific antibiotics as a new pharmaceutical target is required for the complete eradication of *H. pylori*.

Chapter 2

Mol Microbiol. 2013 Dec 12;PubMed PMID: 24330328.

Helicobacter pylori periplasmic receptor CeuE (HP1561) modulates its nickel affinity via organic metallophores

Md Munan Shaik,[†§] Laura Cendron,[‡§] Marco Salamina, Maria Ruzzene and Giuseppe Zanotti*

Department of Biomedical Sciences, University of Padua, Viale G. Colombo 3, 35131 Padua, Italy.

Abstract

In Gram-negative bacteria, nickel uptake is guaranteed by multiple and complex systems that operate at the membrane and periplasmic level. *H. pylori* employs other yet uncharacterized systems to import the nickel required for the maturation of key enzymes, such as urease and hydrogenase. *H. pylori* CeuE protein (HP1561), previously annotated as the periplasmic component of an ABC-type transporter apparatus responsible of heme/siderophores or other Fe(III)-complexes uptake, has been recently proposed to be on the contrary involved in nickel/cobalt acquisition. In this work, the crystal structure of *H. pylori* CeuE has been determined at 1.65Å resolution using the SAD method. It comprises two structurally similar globular domains, each consisting of a central five-stranded β-sheet surrounded by α-helices, an arrangement commonly classified as a Rossmann-like fold. Structurally, *H. pylori* CeuE belongs to the class III periplasmic substrate-binding protein. Both crystallographic data and fluorescence binding assays allow to exclude a role of the protein in the transport of VitB12, enterobactin, heme and isolated Ni^{2+} ions. On the contrary, the crystal structure of the protein/Ni^{2+}(L-His)$_2$ complex suggests that *H. pylori* CeuE binds and transport nickel *in vivo* thanks to the formation of a Ni^{2+}/histidine complex.

Introduction

In gastric *Helicobacter* species nickel represents an essential cofactor of key enzymes, such as urease and NiFe-hydrogenase. Reduced availability of nickel causes urease inactivation and consequent reduced capability of buffering the acidic pH of the gastric lumen, one of the primary bacterial defenses against such hostile environment. On the other hand, hydrogenase inactivation due to nickel paucity impairs the opportunity of *Helicobacter* to use the hydrogen available in the gastric mucosa as a respiratory substrate and strongly limits its colonization efficacy (Olson *et al.*, 2002). The availability of such transition metal should be guaranteed by uptake systems at the outer membrane level implying the capture of nickel ions and transport trough the membranes. The subsequent incorporation of metal ions into nickel-dependent enzymes requires complex assembly processes and multiple accessory proteins. While a class of porins guarantee the uptake of complexed nickel ions at the outer membrane level (OMPs), two main routes are known to be used by bacteria to import nickel over the inner membrane, one involving an integral membrane high-affinity permease, the other defined by specific ABC-type transporter systems (Mulrooney *et al.*, 2003). *H. pylori* NixA permease has been identified (HP1077) and demonstrated to mediate the import of nickel through the cytoplasmic membrane (Bauerfeind *et al.*, 1996), whilst NikH guarantees at the outer membrane level the availability of nickel to the permease (Stoof *et al.*, 2010a). NixA expression is regulated by NikR (nickel-responsive regulator) and repressed in the presence of high nickel concentrations, to avoid toxic overload (Wolfram *et al.*, 2006). However, urease activity in a NixA deletion mutant is reduced but not abolished, thus implying the presence of an alternative nickel transporter (Nolan *et al.*, 2002). It has been also postulated that *H. pylori* uses the ExbB/EsbD/TonB transport system to import nickel complexed by an unknown nickelophore captured from the environment (Schauer *et al.*, 2007). Very recently, the $Ni(L\text{-}His)_2$ complex has been identified as a substrate for the NikABCDE-dependent uptake of nickel in *Escherichia coli* (Chivers et al., 2012; Lebrette et al., 2013).

Recently it has been proposed, using *H. mustelae* as a model of gastric species that colonizes ferrets stomach, that CeuE and FecD/E proteins represent an ABC-type transporter system that mediates an alternative route for the nickel/cobalt acquisition (Stoof *et al.*, 2010b). Indeed, despite being previously classified as proteins involved in the iron uptake, inactivation mutants of each of them did not alter significantly the iron levels in the bacterial cells and, on the contrary, clearly reduce urease activity and nickel content.

The protein coded by gene hp1561 (CeuE) was annotated as periplasmic iron-binding protein and as a component of an Fe(III) ABC transporter. Contradictory experimental data concerning a putative involvement in the iron acquisition processes have been accumulated in the literature: it was found to be iron-regulated during the stationary-phase, along with many other genes (Merrell *et al.*, 2003), but the transcription of such genes as well as those coding for the cytoplasmic ABC-transporter components FecD and FecE is not repressed by iron, and is also not affected by mutation of gene *fur* (Delany *et al.*, 2001a; Delany *et al.*, 2001b; van Vliet *et al.*, 2002). In a recent work aimed at identifying the presence of natural antisense transcripts in *H. pylori*, a new small non-coding RNAs complementary to mRNAs of CeuE have been discovered (Xiao *et al.*, 2009), suggesting that metal homeostasis can be regulated by alternative strategies, as hypothesized in other cases such as ferritins (Bereswill *et al.*, 2000; Xiao *et al.*, 2009). Following the recent model of a novel nickel/cobalt specific ABC-type transporter working independently from NixA, a role of nickel receptor could be hypothesized for CeuE protein in this contest. Indeed, due to its sequence similarity to periplasmic substrate-binding proteins present in both Gram-negative and Gram-positive bacteria, it can be proposed that CeuE could capture nickel/cobalt ions (Ni^{2+}/Co^{2+}) or nickel/cobalt complexes, available in the periplasm thanks to outer membrane porins and deliver the substrate to the translocator, defined by the FecD/E inner membrane importer. However, a direct proof of such a role is lacking and the nature and specificity of the actual CeuE ligands remain unclear.

To elucidate the structural features of this periplasmic ABC-type transporter binding protein and possibly characterize the nature and affinity toward putative substrates, CeuE receptor coded by gene *hp*1561 from *H. pylori* has been cloned in *E. coli*, expressed, purified, crystallized, and its structure determined both in the absence and presence of nickel ions. *In vitro* binding activity with different possible metal ions and metal-containing compounds has been characterized.

Materials and Methods

Molecular cloning

HP1561 gene was amplified by PCR from *H. pylori* G27 genomic DNA, using proofreading *pfu* DNA polymerase (Finnzymes, Finland), with the following primers: 5'- CAC CAT GGA AGT CAA AGT TAA GGA TTA TTT CG (Forward) and 5' CCA TAA GAA TGG CTC AAC TTC TGC GTC (Reverse), which amplify from 33 to 332 amino acids from total length 333 amino acids with N-terminal signal peptide/transmembrane helix deletion (32 amino acids) and one His deleted from C-

terminal. The amplified fragment was cloned into the pET101vector (Invitrogen) in frame with a C-terminal His-tag, using a TOPO® Cloning kit by Invitrogen to obtain the pET101-HP1561 plasmid. Right insertion in the cloned vector was confirmed by colony PCR and by sequencing with T7 forward and reverse primer.

Overexpression and affinity purification

E. coli BL21(DE3) cells (Novagen) were transformed with the pET101-HP1561 plasmid and grown in LB media at 37° C, supplemented with Ampicillin (100 µg/ml). Protein expression was triggered by 1 mM isopropyl-β-D-thiogalactoside (IPTG, Inalco) till the culture reached an optical density (OD_{600}) of 0.7. After 4h incubation at 28° C, bacteria were collected and resuspended in a lysis buffer (30 mM Tris, pH 8.0, 150 mM NaCl) and then disrupted by a One Shot Cell breakage system at 1.35psi (Constant System Ltd., UK). The lysate was centrifuged to remove cell debris (18,000 g for 25 min) and loaded into a column containing 5 ml of Ni^{2+} charged Chelating Sepharose™ (GE Healthcare, UK). After extensive washing using the lysis buffer, supplemented with 20mM imidazole, the protein was eluted by a linear gradient from 80 to 300 mM imidazole. The protein was further purified by gel filtration, using a Superdex 200™ 16/60 GL (GE Healthcare) equilibrated with 30 mM Tris pH 8.0, 150mM NaCl. HP1561-His tagged eluted as a single peak. All the protein samples collected throughout the purification were separated and analyzed on 15% sodium dodecyl sulfate–polyacrylamide gel electrophoresis (SDS–PAGE). The resolved gels were stained with 0.25% Coomassie Brilliant Blue R250 reagents.

Molecular mass of CeuE protein was determined by analytical gel filtration using an analytical column Superdex 200™ 10/300 GL (GE Healthcare), operated on an AKTA FPLC instrument (GE Healthcare).

To prepare the seleno-methionyl protein, the plasmid pET101 containing the HP1561 gene was transformed into the methionine auxotrophic *E. coli* strain B834. The transformed bacteria were grown in M9 minimal medium supplemented with 0.4% (w/v) glucose, salts and all the amino acids except Met, substituted by Se-Met (50mg/L). About 30 minutes before induction with 0.3 mM IPTG, a further solution of Se-Met plus Leu, Ile, Val, Phe, Lys and Thr was added to the medium to inhibit the *E. coli* methionine pathway and to force the incorporation of Se-Met. The HP1561 Se-Met derivative was purified as the native protein, with enhanced content of reducing agent in buffer (5 mM DTT), to prevent oxidation. CeuE-H197L mutant was expressed and purified in the same conditions applied for the wt protein, obtaining analogous yield and pureness.

Crystallization and structure determination

The purified protein was concentrated to 50 g/l and used for crystallization tests, partially automated using an Oryx 8 crystallization robot (Douglas Instruments). Crystals grew in several conditions. The best native crystals were obtained at 293 K by vapor diffusion technique using a 20 g/l protein stock solution and, as precipitant, a solution containing 0.1 SPG Buffer pH 8.0, 25% (w/v), PEG 1500 (The PACT Suit, solution n. 5, Qiagen, USA). Crystals could be processed as orthorhombic, space group $P2_12_12_1$, with unit cell dimensions **a**=67.37 Å, **b**=87.02 Å, **c**=105.90 Å. Two monomers are present in the asymmetric unit, with V_M= 2.3Å^3/Da, corresponding to an approximate solvent content of 47%. A diffraction data set was measured at the beamline ID29 of the European Synchrotron Radiation Facility (ESRF), Grenoble, France. Crystals of Se-Met derivative were grown in the same condition and a SAD dataset was measured at the beamline ID14-4 of ESRF. To explore the metal coordination in the metal binding site, CeuE crystals were grown in the presence of 10mM $NiSO_4$ in the precipitant solution (0.5 M Sodium Formate, 0.1 M Bis Tris Propane, pH 7.5, 20 % (w/v) PEG 3350), by sitting-drop vapor diffusion at 20^{0}C. They belong to the monoclinic $P2_1$ space group with unit cell dimensions a= 60.18 Å, b=76.95 Å, c=72.78 Å, β=94.52 Å. Nickel anomalous data were measured at the beamline ID 23-1 of ESRF at the wavelength of 1.48520 Å. Furthermore, a purified CeuE protein solution (0,006 mM) was treated with a buffered $NiCl_2$ solution (0,6 mM), in the presence of a three fold excess of L-histidine, in order to obtain a Ni(L-His)$_2$ complex. The sample was concentrated to 10 g/l, further enriched with the metal complex to maintain a 10 fold excess and tested by sparse matrix crystallization screenings (Structure Screen I and II, Molecular Dimension Limited, and PEG's Screen, Qiagen) at 293 K, in a vapor-diffusion setup. Diffraction quality crystals were obtained in multiple conditions, the best resulting PEGsII n.45 (0,2M Lithium Cloride, 0,1M Tris pH 8,5 30% w/v PEG 4000) and PEGsII n.72 (0,1M Lithium Cloride, 0,1M Tris pH 8,5 32% w/v PEG 4000). The CeuE Ni^{2+}-histidine containing crystals belong to the same space group as those grown with $NiSO_4$, with analogous cells parameters.

All the datasets were indexed and integrated with software Mosflm (Leslie,2006) and merged and scaled with Scala (Evans,2006), contained in the CCP4 crystallographic package (Collaborative Computational Project, Number 4,1994). The structure was solved by experimental phasing using the selenium dataset, in which position of selenium was explored by Autosol and further model building with extension to high resolution native dataset with Autobuild (Adams *et al.*, 2009). Model building was further extended with Buccaneer (Cowtan,2006) and manual rebuilding with graphic software Coot (Emsley *et al.*, 2004). Refinement was carried on using package Phenix (Adams *et al.*, 2010), and Refmac (Murshudov

et al., 1997). The final crystallographic R factor is 0.198. (R_{free} 0.239). All the putative complexes including the different nickel compounds were solved by molecular replacement using the software Phaser (McCoy *et al.*, 2007) or Molrep (Vagin *et al.*, 1997), starting from a monomer model of HP1561 and refined by Refmac. Solvent molecules were added with the automated procedure of Phenix, followed by manual inspection and small adjustments with the software Coot. Geometrical parameters of the models, checked with software Procheck (Laskowski *et al.*, 1993), are as expected or better for this resolution.

CeuE site-directed mutagenesis

Single point mutation of the *CeuE* gene was performed with the QuickChange Site-Directed Mutagenesis Kit (Stratagene), using pET101-HP1561 plasmid as template. Oligonucleotides to introduce the mutation were designed as following (Sigma-Aldrich): mutH197Lfw (5'- AAA GGG GTG GAG CTT TTC CTT AAG GCC AAT AAG ATT AGC -3') and mutH197Lrv (5'- GCT AAT CTT ATT GGC CTT AAG GAA AAG CTC CAC CCC TTT -3'). The insertion of the required mutation in the resulting plasmid (pET101-HP1561-H197L) was verified by sequencing.

Fluorescence measurements

Tryptophan fluorescence quenching upon ligand binding was measured with a Perkin Elmer LS50B Fluorescence Spectrophotometer. Each titration was performed in a 2 ml quartz-cuvette thermostated at 298 K, using an excitation wavelength of 295 nm and an emission wavelength of 340 nm and slits width adjusted to 5 nm. An equilibration time of 3 minutes has been applied after each substrate addition, before acquiring the fluorescence signal. Both CeuE wild type protein and CeuE H197L mutant have been diluted to 0.5µM in Tris 30mM, NaCl 150mM, pH 7.5 before titration, while increasing amounts of each ligand were added stepwise, exploring a concentration range between 1 and 100 µM for hemin, enterobactin and Vitamin B12, while nickel chloride, nickel-EDTA and nickel-$(His)_2$ were added till 50µM. Iron-enterobactin complex was prepared starting from iron-free enterobactin dissolved in DMSO and a $FeCl_3$ stock solution according to Zawadzka *et al.* (Zawadzka *et al.*, 2009). $Ni(His)_2$ and nickel-EDTA were prepared treating a nickel chloride stock solution with a large excess of EDTA or histidines (molar ratio 1:2). Fluorescence data were fitted using a non-linear regression analysis by the software GraphPad Prism version 6. Best fitting of the fluorescence curves and the corresponding dissociation constants were calculated using a one-site and single type of binding model for all the substrates tested, using the general quadratic equation as reported in van de Weert and Stella (van de Weert *et al.*, 2011). The molar fluorescence of the free ligands was estimated by linear regression, in the same conditions of the binding tests.

Surface Plasmon Resonance Analysis

A Biacore™ T100 (GE Healthcare) instrument was used. CeuE was covalently coupled to a CM5 (series S) sensor chip (carboxymethylated dextran surface) by amine-coupling chemistry to a final density of 3700 resonance units (RU), as described in (Ruzzene et al., 1999); a 10 mM acetate, pH 5.0 buffer was used for the immobilization. A flow cell with no immobilized protein was used as control. Binding analysis was carried out in a running buffer consisting of 10 mM HEPES, pH 7.4, 150 mM NaCl, 0.05 % (v/v) Tween-20, applying a flow rate of 10 µl/min. Each sensorgram (time course of the surface plasmon resonance signal) was corrected for the response obtained in the control flow cell and normalized to baseline. After each injection the surface was regenerated by a double injection of 1M NaCl for 30 sec; this treatment restored the baseline to the initial resonance unit value. For kinetics experiments, a Biacore method program was used that included a series of three start up injections (running buffer), zero control (running buffer) and 5 different concentrations (ranging between 0.05 and 10 µM, one of which in double) of Ni-(L-His)$_2$ or vitamin B12. Serial dilutions of the analyte were performed in running buffer from a 25 mM top concentration. High performance injection parameters were used; the contact time was of 480 s followed by a 480 s dissociation phase. The kinetic data were analyzed using the 2.0.3 BIAevaluation software (GE Healthcare). Curves were fitted with the classical Langmuir 1:1 model; the quality of the fits was assessed by visual inspection of the fitted data and their residual, and by chi-square values. Two independent experiments were performed.

Results and Discussion

The overall Model

The crystal structure of *H. pylori* CeuE (HP1561) was determined at 1.65Å resolution using phases obtained from single anomalous dispersion method. The model could be built from amino acids 33 to 335 (the protein expressed starts at residue 33, since the first 32 amino acids represent a putative secretion signal). The electron density for main chain atoms is always continuous and very well defined, with the exception of few residues (103-107) in the loop that connects strand β5 to helix α6. This happens for both molecules present in the asymmetric unit, an indication that this area is intrinsically flexible. *H. pylori* CeuE consists of two structurally similar globular domains, a N-terminal (33-165) and a C-terminal domain (187-335), each consisting of a central five-stranded β-sheet surrounded by α-helices, also known as a Rossmann-like fold (Figure. 2.1). The two domains are topologically similar and a long, rigid α-helix (α10, 166-186) acts as an inter-domain linker (Figure. 2.2). *H. pylori* CeuE was classifies as a

class III periplasmic substrate-binding protein (SBP). Its overall fold shares structural features in common with PhuT and ShuT, two heme-transport proteins from *Pseudomonas aeruginosa* (PDB ID: 2R79) and *Shigella dysenteriae* (PDB ID: 2R7A), respectively (Ho *et al.*, 2007). Other structures of the same family include BtuF, a vitamin B12 transport protein from *E. coli* (PDB ID: 1N2Z, (Borths *et al.*, 2002)), FhuD, a periplasmic siderophores binding protein from *E. coli* (PDB ID: 1K7S, (Clarke *et al.*, 2000)) and HmuT, a periplasmic heme binding protein from *Yersinia pestis* (PDB ID: 3NU1, (Mattle *et al.*, 2010)). Two hemes are bound in the heme-binding cleft of the latter, which also presents a more extended groove to accommodate the heme.

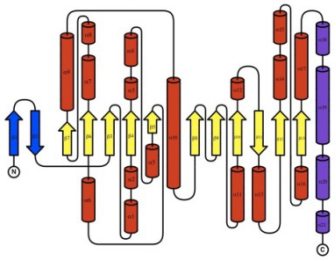

A

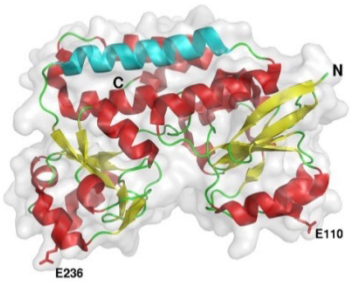

B

C

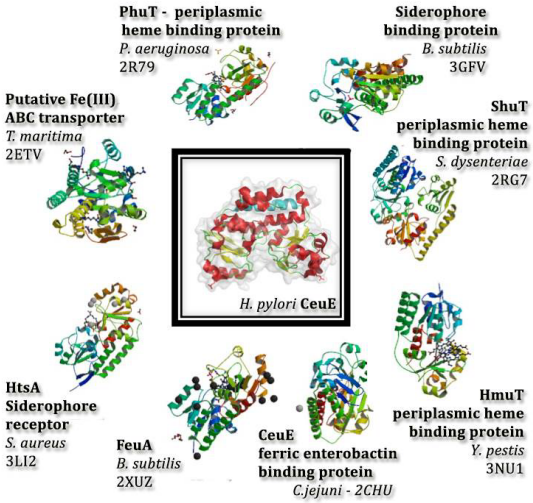

r.m.s.d. Å	PDB ID
4.2 (292)	2ETV
2.5 (246)	2R79
3.0 (261)	3GFV
2.7 (238)	2RG7
3.1 (254)	3LI2
2.3 (231)	1N2Z
2.6 (252)	2XUZ
3.0 (253)	2CHU
3.3 (231)	3NU1

Figure. 2.1 A) Topology diagram of *H. pylori* CeuE. B) Overall cartoon of the monomer. α-helices are in red, β-strands in yellow, others in green, the long α-helix connecting the two domains in cyan. C) *H. pylori* CeuE 3D Structure alignment (Dali) with other SBPs family members.

The three-dimensional structures of the members of the periplasmic binding proteins family most similar to *H. pylori* CeuE are listed in Figure 2.1 C. The r.m.s.d. between equivalent Cα atoms ranges from 2.3 Å to 4.2 Å. The sequence similarity among members of the family is quite low and only five residues are fully conserved: two surface-exposed glutamates (E110 and E236), one in each lobe, and three other

residues (Pro 117, Glue 118 and Pro 243) (Figure 2.2). They could possibly denote the structural features of this family. Although almost all of the secondary structure elements described in the other members of the protein family are conserved in *H. pylori* CeuE, some extra features are present in the latter. Two antiparallel β-strands (34-49), present in the N-terminal domain, are absent in PhuT, ShuT, and BtuF, but they are present in the putative Fe(III) ABC transporter from *Thermotoga maritima* (tm0189, PDB: 2ETV) and in other siderophore binding proteins, such as FeuA from *Bacillus subtilis* (PDB: 2XUZ, (Peuckert *et al.*, 2011)), HtsA from *Staphylococcus aureus* (PDB: 3LI2, 3EIW, (Grigg *et al.*, 2010)) and ferric enterobactin binding protein from *Campylobacter jejuni* (PDB: 2CHU, (Muller *et al.*, 2006)). There is also a C-terminal extension, present only in 2ETV, containing three α-helices (α18, residues 302-306; α19, 309-323, and α20, 325-330). In fact, *H. pylori* CeuE is longer in sequence (335 amino acids) if compared to ButF (266), PhuT (308) and ShuT (277), but smaller than 2ETV (356).

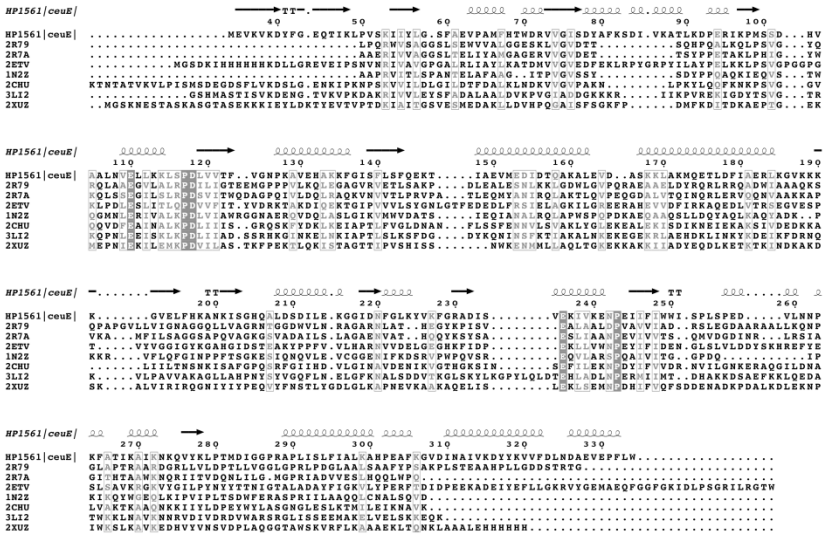

Figure. 2.2 Amino acid sequence alignment of CeuE homologues from different species.

Two loops at the surface of the N-terminal domain of the structure of HP1561 display quite high B-factors. These two loops are composed of residues 101-116 and 126-138 (Figure 2.3). The elevated B-factor was reported to be present in other members of this class III periplasmic binding proteins: three loops with similar features are present at the surface of the C-terminal domain of the crystal structure of siderophore receptor HtsA from *Staphylococcus aureus* (PDB: 3LI2, 3EIW), which is described as an open form of the protein, whilst residues in this three loops have

lower B-factors in a close form of the protein, crystallized in a different space group (Figure 1) (Grigg *et al.*, 2010). Referring to the crystal structure of HtsA, the *H. pylori* structure can be defined as an open form. Similar high B-factors in the residues at the surface of these two loops are present also in the periplasmic heme-binding protein ShuT and PhuT. In addition, the C-terminal domain of ShuT has a small-extended loop (residues 168-173) that presents quite high B-factor and which extends over the substrate binding site. It can be speculated that this loop is flexible, acting as a gate for the substrate-binding site. This extended extra loop is absent in the structure presented here, leaving the gate open for the entrance of the ligand.

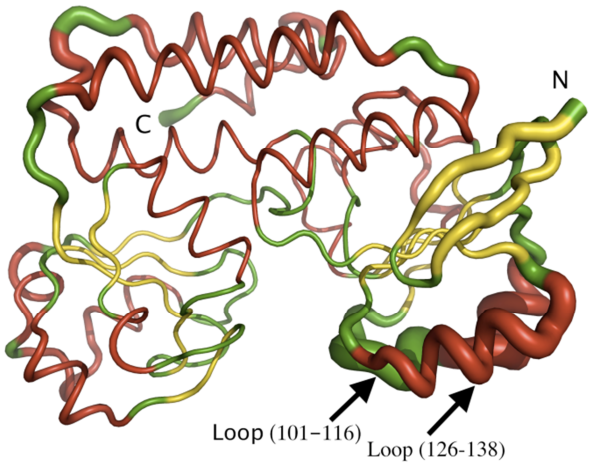

Figure. 2.3 Ribbon drawing of the monomer of *H. pylori* CeuE. The diameter of the ribbon tube is proportional to the thermal parameters of the atoms.

Interaction with the ABC transporter

Two CeuE molecules, oriented face-to-face facing the binding cavity, are present in the asymmetric unit in the orthorhombic space group. Two molecules are also present in the monoclinic crystal cell, but oriented in a different way, a strong indication that the two molecules do not correspond to a physiological dimer.

BtuCD is an adenosine triphosphate–binding cassette (ABC) transporter that translocates vitamin B_{12} from the periplasmic binding protein BtuF into the cytoplasm of *E. coli*. The crystal structure of the overall complex is known (Hvorup *et al.*, 2007). The monomer of *H. pylori* CeuE crystal structure can be superimposed to BtuF in the crystal structure of the complex with a r.m.s.d. of 2.4 Å (Figure 2.4 A). Two conserved, surface-exposed residues, one in each lobe of the protein, Glu110

and Glu236, are present in the same place in the two proteins and they interact with two positively charged residues (Arg295 and Arg59) on the surface of BtuCD (Figure. 2.4 B). In addition, in the theoretical model of HP0889, the putative ABC transporter partner of *H. pylori* CeuE, the two positively charged residues considered crucial for the formation of the BtuF/BtuCD complex are conserved. The flexibility of the exposed surface loops in the N-terminal domain of *H. pylori* CeuE, involved in the interaction with the putative ABC transporter, (residues 101-116, 126-138) might play a role in the interaction and/or in substrate translocation.

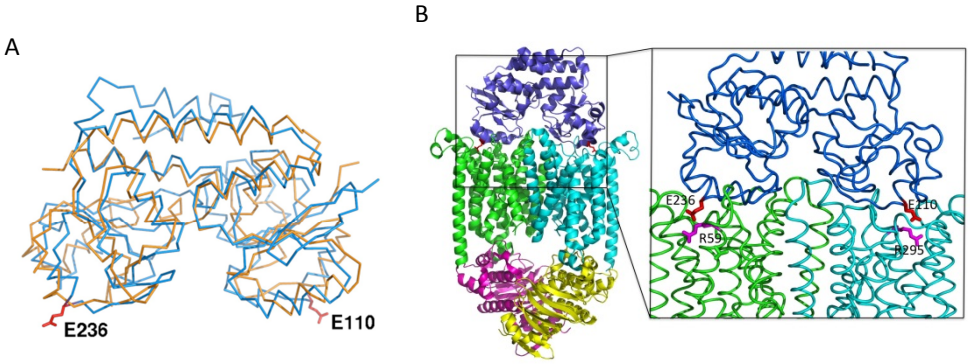

Figure. 2.4 A) Cα trace of *H. pylori* CeuE (blue) superposed to *E. coli* BtuF in complex with BtuCD (PDB ID 2QI9). Side chains of residues Glu110 and Glu236 are shown in red. B) Cartoon view of BtuCD (the four polypeptide chains are represented in different colors) with *H. pylori* CeuE (blue) replacing BtuF. On the right side a detail of the interaction region shows the two negatively charged glutamate residues (red) interacting with the positively charged arginines (magenta).

Ligand-binding Assays

Since the 3D structure of *H. pylori* CeuE presents a similarity to the protein family that includes periplasmic heme-binding proteins, periplasmic siderophore receptors and Vitamin B12 binding proteins, binding assays were performed with the following compounds: hemin, enterobactin and VitaminB12, and with Ni^{2+} ions in the presence of histidine as a chelating agent. Indeed, the possibility to acquire such transition metal if complexed by two histidine ligands, Ni-(L-His)$_2$, has been recently demonstrated for *E. coli* NikA periplasmic receptor (Chivers *et al.*, 2012). Later, the structure of *E. coli* NikA protein has been crystallized either in complex with Ni-(L-His)$_2$ or as purified from the bacterium. In the latter case, a still unidentified nickel containing complex has been found in the substrate binding cleft, suggesting it could represent the physiological nickel chelating ligand (Lebrette *et al.*, 2013). Such results reveal that, analogously to iron uptake, nickel acquisition could be

guaranteed by receptors that recognize specific nickel complexes, either endogenously produced or deriving from the growth medium.

The binding of hemin, enterobactin and VitaminB12 was tested through quenching of intrinsic protein fluorescence, since four tryptophan residues are present in the CeuE protein, two of which in the putative binding cavity. A clear fluorescence quenching was observed after addition of increasing amounts of heme, vitamin B12 or enterobactin. The experimental curves concerning the iron-containing compounds (Figure 2.5) were better fitted by a non-linear regression, assuming a one-site binding model. In the tested conditions, all of the compounds were characterized by modest dissociation constants values, in the micromolar range or worse, the best resulting hemin (18.3 ± 0.4 µM).

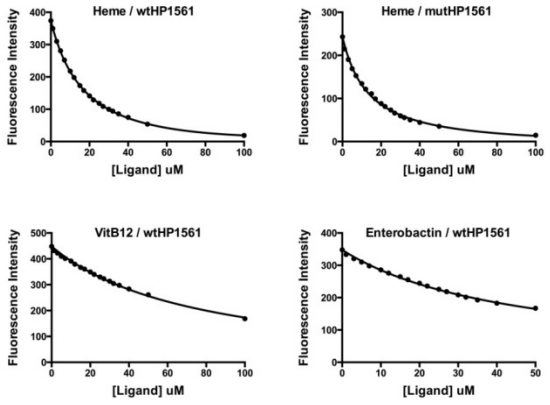

Figure 2.5. Fluorescence titrations with iron-containing complexes, plotted as fluorescence signal against increasing concentration of substrate. Top panels left and right correspond to titration of wt-CeuE and CeuE-H197L mutant with heme, while bottom panels left and right of wt CeuE with vitamin B12 and enterobactin, respectively.

In the case of nickel containing compounds, since the fluorescence quenching values are significantly altered owing to the absorption of the fluorescence signal at 330 nm by nickel ions (Shepherd *et al.*, 2007), the estimation of the binding constant was performed by surface plasmon resonance analysis. Analysis of the sensograms (Figure. 2.6 A) gives for the Ni-(L-His)$_2$ complex a K_D = 0.79 µM (±0,08 µM). In order to derive, using the same technique, a value for the other ligands, the experiment was repeated with heme, enterobactin and vitamin B12. A significant curve could be obtained only with the latter, owing to aggregation phenomena with the others two. The binding curve of Vitamin B12 (Figure. 2.6 B) indicates that this complex is quite labile, such that it was not possible to estimate a reliable value for the binding constant. Since fluorescence data point to values in the same range for Vitamin B12, heme and enterobactin, they allow excluding an involvement of CeuE in the VitB12

transport, as well as a capability to recruit Fe(III) by siderophores analogous to enterobactin or by heme. In addition, crystals grown in the presence of an excess concentration of heme and enterobactin failed to show the ligand bound to the protein in the crystal.

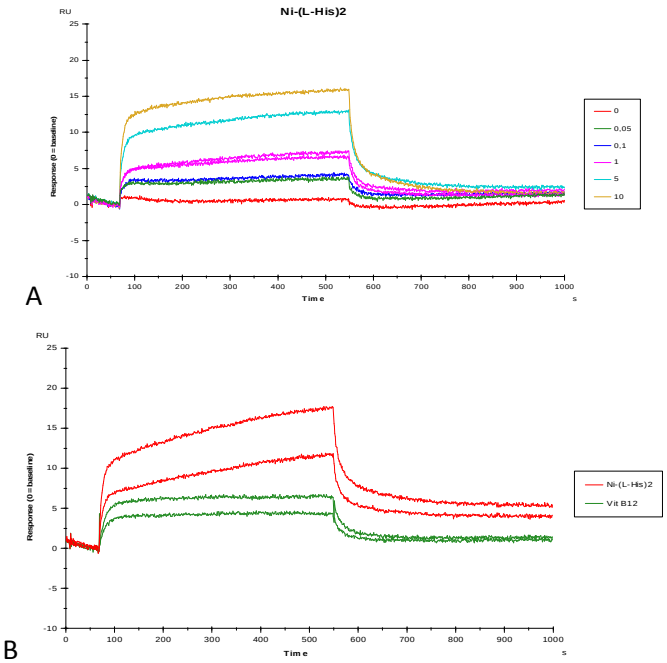

Figure 2.6 Analysis of CeuE interaction with Ni-(L-His)$_2$ and vitamin B12 by means of SPR signal detection. A) Ni-(L-His)$_2$ solutions at the indicated concentrations were injected over the CeuE chip for kinetics determination. B) Comparison between Ni-(L-His)$_2$ and vitamin B12.

Ni^{2+} coordination studies

In order to test if CeuE from *H. pylori* is directly involved in Ni^{2+} binding and/or transport, crystals of the protein were grown also in the presence of 10 mM Ni^{2+}. Three nickel ions were identified in the Fourier-difference anomalous electron density map, one of them present in the potential substrate-binding cleft, and other two close to the protein surface (Figure 2.7). However, none of the three Ni^{2+} ions are characterized by a specific coordination. They are in general close to some negatively charged protein residues (for example, nickel in the substrate-binding site interacts with Glu69), but the remaining coordination sites of the metal are occupied by acetate or water molecules, suggesting an unspecific interaction of positively charged ions with negative side chains of the protein.

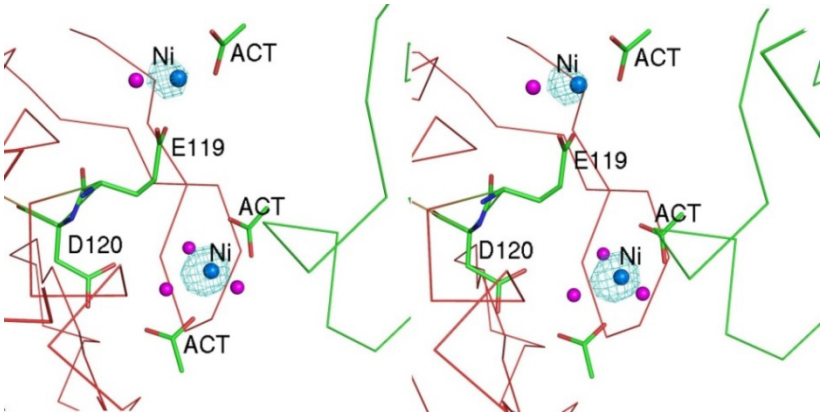

Figure. 2.7 Unspecific nickel binding to the surface of *H. pylori* CeuE

On the contrary, crystals grown in the presence of Ni(L-His)$_2$ show the presence of the complex clearly bound inside the CeuE binding cleft (Figure. 2.8). The Ni^{2+} ion presents a slightly distorted octahedral coordination, where five of the coordinating atoms belong to the two free histidines, whilst the sixth is a nitrogen atom of His 103 of the protein. Interestingly, the two free histidines are asymmetrically bound, in a different manner if compared with the Ni(L-His)$_2$ complex that is stable in aqueous solutions (Lebrette *et al.*, 2013). One of the histidines contributes with three atoms to the coordination, two nitrogens from the imidazole ring and from the amine group and a carboxylic oxygen, whilst only the amine nitrogen and the carboxylic oxygen of the second histidine take part in it. The imidazole ring of this second histidine ligand is not involved in the direct coordination of the metal, but is oriented toward the entrance of the protein's binding cavity and establishes hydrogen bonds with four water molecules trapped in the same environment. This situation leaves the sixth coordination position available to His103 of CeuE. The position of the Ni^{2+} complex inside the protein cavity is stabilized by Arg230, whose NH nitrogen interacts with both the carboxylates of the two free histidines and the side chain of Asp209, which is buried inside the protein cavity (Figure. 2.8 A).

It is worth noticing that the binding of the Ni^{2+} complex, that involves His103, induces an ordering of the region 103-107 (Figure 2.8 B), in the loop that connects strand β5 to helix α6, which is the only area not well defined in the electron density map of the *apo*-protein. Indeed, the structural features emerging from the comparison between *apo*- and Ni(L-His)$_2$ loaded forms of CeuE allow to hypothesize a mechanism where the highly symmetric complex Ni(L-His)$_2$ present in aqueous solutions is trapped and reorganized in the CeuE binding cleft through the

displacement of the imidazole ring of one of the free histidine ligands by His103, which anchors the complex into the binding cavity and breaks the Ni^{2+} coordination symmetry.

Other two structures of the Ni(L-His)$_2$ complex bound to a bacterial transport protein have been determined, NikA from *E. coli* and from *S. aureus* (Lebrette *et al.*, 2013; Minasov et al., PDB ID 3RQT). These two structures present the same fold (the r.m.s.d. for the superposition of 402 equivalent Cα atoms is 2.5Å), but the nickel adduct binds to them in a completely different way (Figure. 2.8C). In *S. aureus* NikA the Ni^{2+} does not directly interact with protein atoms, whilst are the latter that interact with the histidines coordinating the ion. On the contrary, the binding in the case of the *E. coli* protein is reminiscent of that of *H. pylori* CeuE (Figure. 2.8 C). In both cases, a protein's histidine residue replaces one of the coordination of the metal, despite in a different way: instead of the displacement of the imidazole ring of the histidine, in *E. coli* NikA a histidine carboxylate group is displaced. Residues in the two binding cavities are also quite similar, despite differently oriented.

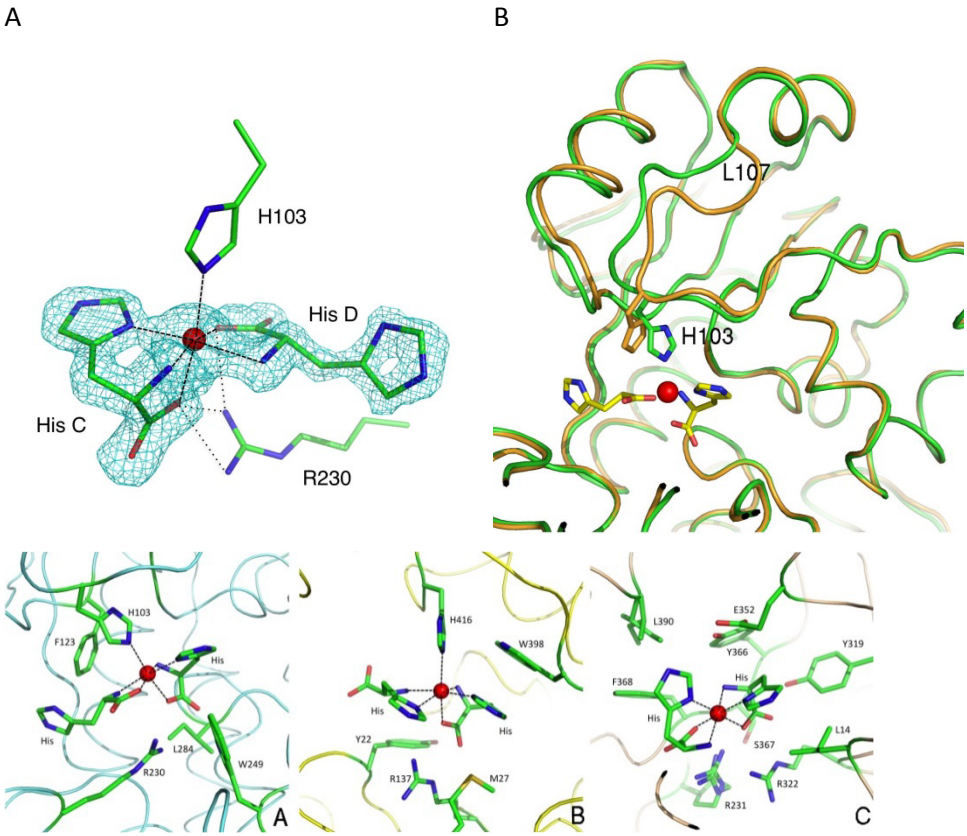

Figure 2.8 A) Ni(His)$_2$ complex binding site of CeuE. B) Chain trace of a portion of apo-CeuE (orange) and in complex with the nickel-His adduct (green). C) Comparison of the biding sites of the Ni(L-His)$_2$ adduct in A) *H. pylori* CeuE, B) *E. coli* NikA and C) *S. aureus* NikA.

The binding cleft and mutagenesis studies

H. pylori CeuE presents significant similarities with heme- or siderophores-binding proteins of known structure. A model of CeuE from *H. mustelae*, the gastric species where the involvement of CeuE in the nickel/cobalt uptake has been discovered, has been built by homology modeling and superimposed to our structure, showing that in the former the His present in the binding cleft and corresponding to *H. pylori* position 103 is conserved, whilst a second histidine present in the biding cavity, His197, is replaced by a leucine. In order to test if this substitution is relevant for the binding of possible ligands, the mutant of *H. pylori* CeuE H197L was produced and purified. Fluorescence quenching assays (Figure. 2.5), as well as co-crystallization trials, shows a behavior very similar to the wild type protein.

Variability among strains

H. pylori is characterized by a large genetic variability, and CeuE does not represent an exception. The amino acid sequence of *H. pylori* CeuE is available for 47 different bacterial strains. In addition, *ceuE* gene is duplicated in three strains, 26695, J99 and 83, bringing to 50 the number of sequences available. They are confined to the superficial area of the protein, and only two residues are relatively close to the putative binding cleft, Pro253, that in two cases is a threonine, and Asp 209, that in some strains is a serine. They both appear not to be in direct contact with the hypothesized position of the ligand. The putative region of contact with the ABC transporter is also quite conserved, and only three residues are sometimes mutated: Val104, that in some strains is threonine, Lys135, that becomes glutamate in strain SNT49, and Pro253.

A special case is represented by strains 908, 2017 and 2018. Strain 908 belongs to a patient suffering of ulcer disease and it was isolated in 1998. Strains 2017 and 2018 represent chronological sub-clones from the same patient isolated about then years later (Devi *et al.*, 2010; Avasthi *et al.*, 2011). The sequence of these three genes shows long deletions in the C-terminal domain of the protein and the analysis of the molecular model suggest that the new protein cannot fold properly, or at least that it cannot be able any more to bind the ligand, since it lacks part of the residues forming the binding grove. We can conclude that most likely nickel uptake in these strains is guaranteed by other routes of metal acquisition that do not imply CeuE protein involvement such as the NixA permease one.

Conclusions

In Gram-negative bacteria, nickel uptake is guaranteed by multiple and complex systems that operate at the membrane and periplasmic level. Together with NixA permease, *H. pylori* employ other yet uncharacterized systems to import the amount of nickel required for the maturation of key enzymes, such as urease and hydrogenase.

The crystal structure presented here demonstrates that *H. pylori* CeuE (HP1561) shows all the distinctive features of the proteins belonging to the class III SBP family. In particular, a putative ligand-binding cavity is clearly present in between the two protein domains and the protein presents other characteristics of these SBP family members, including the residues that define the cleft surface and those that can alter the size of the cavity and thus assure the binding and release of the ligand. Co-crystallization studies in the presence of various potential ligands have shown that only a $Ni(L\text{-}His)_2$ complex was able to bind inside the putative binding cavity, whilst a large excess of nickel ions, despite the presence of three ions bound to different sites of the protein surface, seem to exclude a direct coordination of nickel ions, due to its unspecific and loose coordination features. At the same time, our results exclude specificity of binding toward others ligand of the SBP family, likeVitB12, enterobactin or heme. These results are in line with the study of the corresponding receptor (Stoof *et al.*, 2010b) in *H. mustelae*, a gastric species closely related to *H. pylori*, that indicates an involvement of CeuE protein in nickel/cobalt acquisition, together with the transmembrane ABC-transporter components FecD/E (HP0889/HP0888). Furthermore, a superposition of *H. pylori* CeuE structure with the BtuF VitB12-receptor, whose structure has been solved in complex with the other members of the transporter, BtuC/D, allowed to confirm that CeuE shares two conserved and surface exposed glutamic residues that are properly oriented on the protein surface to interact with two positively charged residues on the periplasmic surface of the transmembrane partner, elements that play a key role in the metal delivery mechanism.

It has been postulated that *H. pylori* uses the ExbB/EsbD/TonB transport system to import nickel complexed by an unknown nickelophore captured from the environment (Schauer *et al.*, 2007). In this paper we have demonstrated that *H. pylori* CeuE selectively binds Ni^{2+} *in vitro* thanks to a two-histidine complex. We have

not demonstrated the exact nature of this ligand *in vivo*, nevertheless the observation that CeuE binds $Ni(L\text{-}His)_2$ in a way similar to *E. coli* NikA, despite the two proteins belong to different families, strongly suggests a more general physiological function for this nickel complex.

Chapter 3

FlgD - Helicobacter pylori hook scaffolding protein

Introduction

Material and methods

Cloning

Overexpression and affinity purification

Circular Dichroism

Analytical gel filtration

Dynamic Light Scattering (DLS)

Crystallization and X-ray diffraction analysis

Bioinformatics

Results and Discussion

Introduction

H. pylori flagellar biosynthesis is tightly coordinated by the activities of σ^{54} (HP0714) and σ^{28} (HP1032) factors that mediate the flagellar genes expression. Flagellar proteins turnover is phase-variable and regulated by a posttranslational mechanisms (Lertsethtakarn P, 2011). The mature flagellum is composed by a hook – basal boy complex and the extracellular filament. In the first complex, the inner membrane base (MS ring base, flagellar type III secretion system, cytoplasmic C ring, the motor) is localized in the cytoplasm, whilst in the periplasm there is the rod (with P ring and L ring) and the hook is extracellular.

The hook components are secreted when the periplasmic rod is completed. To determine the correct *Helicobacter pylori* hook length, FlgD and FliK mediate the assembly of FlgE monomers. Therefore, FlgD plays a critical role during the assembly of flagellar hook (Zhou H, 2011). Immunoelectron microscopy technique has been used to localize FlgD at the distal end of the rod and at the distal end of the hook, acting as a hook capping protein (Ohnishi K, 1994). Hence, it is involved when the rod is completed and discarded when the hook has reached its mature length. The interaction with the hook junction proteins (FlgK and FlgL) blocks the hook maturation and permits the formation of the filament with the filament capping protein, FliD (Homma M, 1986). FlgD has been classified as a member of axial family of exported flagellar proteins. Studies on *Escherichia coli* and *Salmonella enterica* flagellar biosynthesis suggest that FlgD regulates the flagellar hook assembly owing to transient intermediate structure. In fact, FlgD has not been detected in mature flagella (Pallen MJ, 2005). FlgD regulates the hook monomer polymerization, preventing the leakage of hook monomers and controls the correct hook length.

Xantomonas campestris C-term FlgD (Kuo WT, 2008) and *Pseudomonas aeruginosa* FlgD molecular structure (Zhou H, 2011) have been determined at 2.5Å and 2.5Å resolution, respectively. A novel hybrid comprising Tudor-like domain interdigitated with a fibronectin type III domain has been revealed.

In our study *H. pylori* FlgD was cloned, expressed and purified. Oligomerization state and secondary structure components have been experimentally defined. FlgD crystals diffracted to 2.7Å of resolution. The crystal structure has not been solved yet. Low sequence similarity of *Hp*FlgD with *Xc*FlgD and *Pa*FlgD revealed that possible different molecular structure could be present in *Helicobacter pylori* hook

scaffolding protein FlgD.

Materials and Methods

Molecular Cloning

H. pylori flgD is located in genome locus C694_0467 (EMBL AFV42119.1). The corresponding nucleotide sequence (HP0858) has been amplified by PCR using a thermostable Phusion high-fidelity taq polymerase (NEB) starting from the purified genomic DNA of *H. pylori* G27 strain. *FlgD* has been cloned into the pETite (Lucigen) plasmid vector in frame with a C-terminal His-tag, using 5' primer - GGA GAT ATA CAT ATG GCT ATT GAT TTA GCA GAA G – (forward) and 3' - GTG ATG GTG GTG ATG ATG TGC TGT CTC TTT AGG GG –(reverse). The amplified gene has been cloned in pETite (Lucigen) pre-processed linearized free-enzyme plasmid vector, in frame to a C-term His-tag. The cloning has been performed by thermal shock transformation of *E. coli* G10 strain (Lucigen), grown over night on LB medium supplemented of Kanamycin (30µg/ml). The colonies were controlled by colony-PCR using combined primers FlgD forward and T7 reverse primers and vice versa. Purified plasmid of positive colonies have been examined with double digestion restriction enzymes (NdeI and NotI) for 2 hours at 37°C, than inactivated for 20 minutes at 65°C. Positive samples have been sequenced by BMR™ sequencing services with T7 forward and reverse primers.

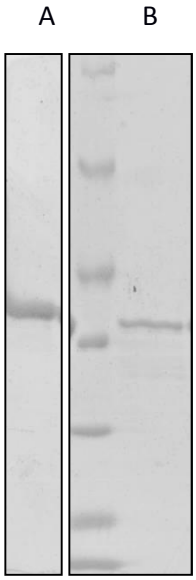

Figure 3.1- (A) SDS PAGE *FlgD, Molecular weight marker (116, 66, 45, 30, 20, 18, 14 kDa), B) SeMet FlgD.*

Overexpression and purification

pETite-FlgD plasmid has been used to transform *E. coli* BL21 (DE3) strain. Protein expression has been performed for 4 hours at 28°C in Luria Bertani medium containing kanamycin resistance at 30 µg/ml, after induction with isopropyl-β-1-thiogalactopyranoside (Sigma). The biomass has been separated from medium by centrifugation for 15 minutes at 11000g, re-suspended in lysis buffer (Tris 20mM pH

7.5, NaCl 150mM, PMSF 2mM) and disrupted with One Shot Cell breakage system (Constant System Ltd., UK). The lysate has been clarified by centrifugation at 40000g for 30 minutes and supernatant was loaded on a 5-ml His-trap column (GE Healthcare) equilibrated with the buffer. After washing step with buffer supplemented with 20mM imidazole, the protein has been eluted in imidazole gradient to 500mM. The protein has been loaded on a Superdex 200 16/60 GL preparative gel filtration chromatography column (GE Healthcare). The eluted protein was concentrate by ultrafiltration (Vivaspin 10000MW 15R, Sartorius) to 30g/l for crystallization purposes. The protein concentration has been determined by UV/Vis spectroscopy (280nm, Cary 50 Bio UV-Visible spectrophotometer, Varian Inc.) using theoretical absorption coefficient. Protein purity has been checked by SDS-PAGE at the end of the purification step and loaded at different concentrations (Figure 3.1 A).

Expression of recombinant seleno-methionine derived FlgD (Figure 3.1 B) has been performed using a *Met* auxotroph *E. coli* strain (B834). The bacteria were grown in 1 liter of minimal medium M9 supplemented of 2% glucose, vitamin B_1, amino acids and seleno-methionine. The purification step was the same as described before.

Circular Dichroism (CD)

To detect secondary structure components of FlgD, a Circular Dichroism analysis has been performed. The instrument used was a JASCO J-715 Spectropolarimeter operated at 298K. 5 runs have been accumulated with 0.14 g/l (Tris 20mM pH7.5, NaCl 150mM) in a 0.05 cm path length cell, in the wavelength interval 190-260 nm (Figure 3.2). Molar ellipticity was estimated by the buffer spectrum, rescaled to a standard solution containing the buffer. The secondary structure was predicted by deconvolution performed with the software "CD Spectra Deconvolution" (CDNN 2.1).

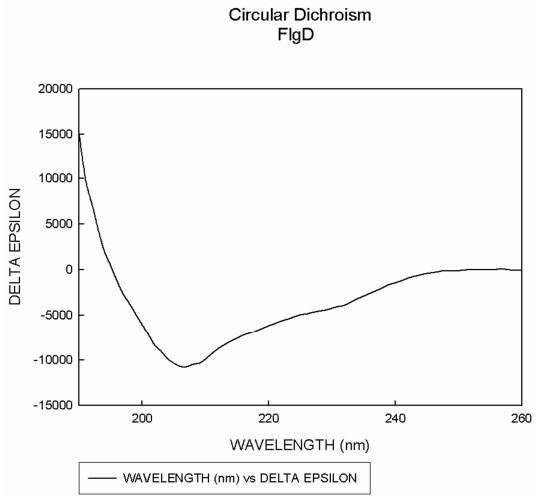

Figure 3.2 – ***Recombinant purified FlgD Circular Dichroism***

Analytical Gel Filtration

FlgD mass has been estimated by analytical gel filtration chromatography using Superose 12 10/300 GL (GE Healthcare), equilibrated with Tris 20mM pH 7.5, NaCl 150mM, with AKTA FPLC instrument (GE Healthcare). Recombinant His tagged FlgD was eluted in a single peak with a retention time of 11.28 ml (Figure 3.3). The molecular mass calculated from analytical gel filtration chromatography analysis was about 141,000 Da. Considering FlgD monomer as His tag fusion protein (2.7 kDa), its molecular mass resulted to be 35468 Da. Therefore, FlgD oligomerization state resulted to be tetrameric in solution.

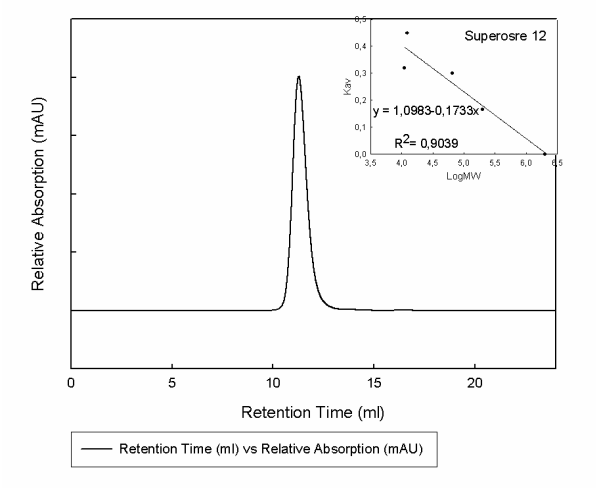

Figure 3.3 – ***Recombinant purified FlgD analytical gel filtration chromatography Superose 12™ 10/300 GL***

Dynamic Light Scattering

Recombinant FlgD has been analyzed with Dynamic Light Scattering instrument at DLS Zetasizer Nano ZS (Malven Instruments). FlgD concentration was determined to be 2.23 g/l. The analysis was performed at 25°C with a temperature equilibration time of 120 sec. The viscosity of the bulk material was of 0.8872 cP. A low volume quartz batch cuvette QS 3.00 mm (Malvern) was used. The measure of Z-Average size (± SD)(d.nm) resulted to be 14,22 ± 8.985 with a polydispersity index of 0.399 (Figure 3.4). The hydrodynamic radius of predominant particle was 10.10 nm ± 3.214 (SD) and estimation of molecular weight was 148,8 kDa ± 51.4 (SD). In the graph the sample distribution of molecular mass (size nm) versus volume (percentage) has been reported. The mass estimated with DLS indicates that the oligomerization state of FlgD is tetrameric.

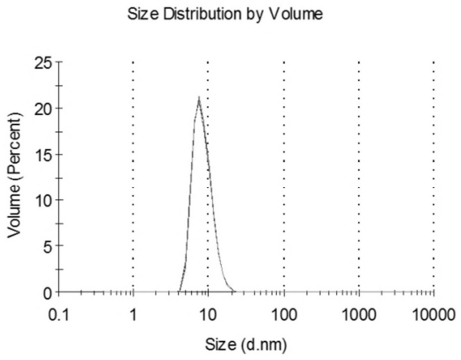

Figure 3.4. ***Recombinant purified FlgD Dynamic Light Scattering analysis***

Crystallization and X-ray diffraction analysis

Recombinant FlgD has been concentrated to 30 g/l and different crystallization kits have been tested. The crystallization plates have been prepared with the partially automated "Oryx Crystallization robot" (Douglas Instruments, UK). The best crystals have been obtained with vapor diffusion technique, at 293 K (Figure 3.5). The precipitant solution correspond to the position A4 (number 4) of PACT suite (Molecular Dimension) containing 0.1M SPG pH 7.0, 25% PEG1500. Other crystals have been obtained with precipitant solution 32 of PEGSII (0.2M NaAcetate, 0.1M Tris pH 8.5, 16% PEG4000) and with solution 80 of PEGS II (0.01M TriSodiumCirate, 16% PEG6000).

Diffraction data have been measured at the ID14-4 beam line of European Synchrotron Radiation Facility of Grenoble, France. One crystal was used to measure an entire data set. The data have been indexed and integrated with Mosflm software (Leslie AG, 2006), merged and scaled with Scala (Evans P, 2006), contained in the CCP4 crystallography package (CCP4, 1994). The crystal belongs to the monoclinic space group P2 or $P2_1$ with cell parameters **a**= 77.25 Å, **b**=34.15 Å, **c**=131.45 Å, β=99.6°. The R_{merge} for all data is 0.073 and the best resolution is 2.75 Å. Statistics on data collection are reported in Table 3.1. Molecular replacement was tried with program Molrep (Vagin AA, 1997).

A B

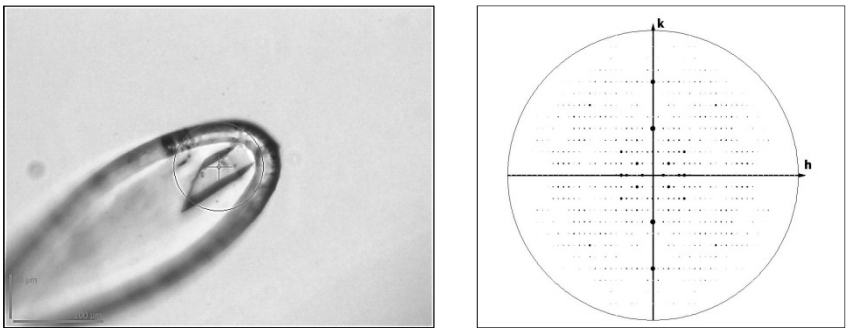

Figure 3.5 (A) FlgD crystal mounted at beam line 14 of ESRF of Grenoble, France. (B) FlgD crystal diffraction pattern.

Data	**FlgD**
Wavelength	0.95372
Space group	P2
a, ***b***, ***c*** (Å), β(°) Z	**a**= 77.25, **b**=34.15, **c**=131.45, β=99.6 Z=2
Resolution (Å)	54.09 - 2.75 (2.90-2.75)
R_{merge}	0.073 (0.503)
R_{pim}	0.045 (0.313)
Unique reflections	18367 (2641)
$\langle I/\sigma(I)\rangle$	11.1 (2.5)
Completeness (%)	99.9 (99.5)
Multipliciy	3.6 (3.5)

Table 3.1 FlgD crystal data

Bioinformatics analysis

The homology modeling has been performed with secondary sequence predictors and molecular model servers. Proteomic website Expasy (www.expasy.org/toos) servers, Jpred (Cole C., 2008), and PSIpred (Buchan D.W.A., 2013) have been used to generate a two-dimensional secondary structure consensus for each residue (Figure 3.6). For molecular modeling SWISS MODEL (Arnold K., 2006), Phyre server (Kelly LA, 2009) and E-Tasser (Zhang Y, 2008) have been used.

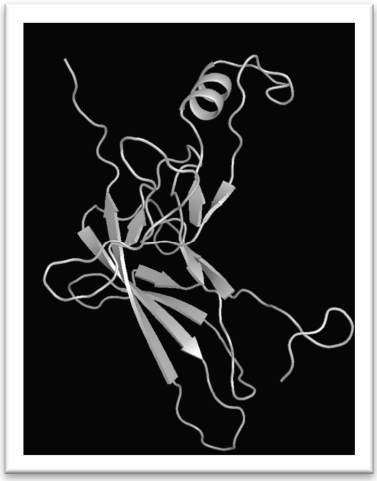

Figure 3.6. ***FlgD homology model generated by Pyre server (Model n.1).***

Results and Discussion

In this thesis, *Helicobacter pylori* FlgD has been investigated. It has been cloned and expressed in *E. coli*. FlgD is classified as a flagellar secreted protein, but no secretion signal has been detected in the sequence analysis (Signal P 2.0 Server). It is annotated as a flagellar basal body modification protein.

The protein expressed in *E. coli* resulted to be cytosolic and soluble. The predicted molecular weight of the monomer (Protparam, Walker JM, 2005) with the His tag (2.7 kDa) resulted to be 35,486 Da. This value was confirmed by the migration of purified FlgD in SDS-PAGE gel, which corresponds to the band of the marker at 35 kDa (Low Molecular Weight, NEB™) (Figure 3.7 A). Recombinant FlgD presented a strong degradation, reduced by the addition during purification of protease inhibitors (PMSF 2mM). Part of FlgD degradation was also removed by preparative gel-filtration chromatography (Figure 3.7 B).

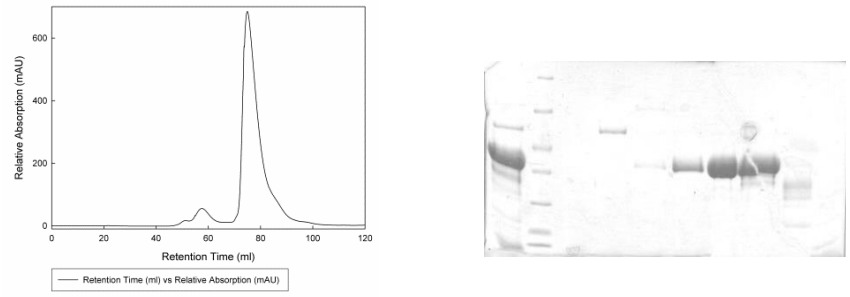

Figure – Recombinant FlgD preparative gel filtration chromatography Superdex 200™ 16/60 GL – SDS PAGE FlgD fraction of gel filtration.

It was possible to purify 10 g/L of nearly pure soluble protein. Analytical gel filtration,

confirmed by dynamic light scattering measurements, suggested a tetrameric oligomerization state for FlgD in solution. Dynamic light scattering measurements presented a predominant particle of FlgD with a diameter of about 10.1 nm, compatible with four-time the molecular weight of the FlgD monomer. The other two FlgD structures known, *Xc*FlgD and *Pa*FlgD are dimers in solution as well as in asymmetric unit in the crystal, however a possible tetrameric oligomerization state has been suggested in physiological conditions.

The protein was concentrated to 30g/l and different crystallization screening kits have been tested. Crystals were grown after months of incubation with a solution containing 0.1M SPG pH 7.0 and 25% PEG1500. The crystals tested diffract at a maximum resolution of 2.7Å.

The crystal structure of *Pseudomonas aeruginosa* FlgD and that of *Xanthomonas campestris* C-terminal FlgD domain have been published. The sequence similarity among these two species and *H. pylori* FlgD is lower than 10%, with only 35 identical positions conserved in the amino acid sequence. It has not been possible, using the FlgD molecular structures already determined, to solve the structure of *H. pylori* FlgD by molecular replacement. Moreover, different possible molecular models have been generated, despite the low sequence similarity. The initial model obtained with the SWISS MODEL PDB Server covered residues from 165 to 251 of *H. pylori* FlgD, which is composed of 316 amino acids. The similarity in the domain is 18%. Moreover, molecular models have been optimized with a homology modelling approach.

A secondary structure prediction consensus has been generated using Jpred and PSIpred. The amounts of secondary structure components of this prediction have been checked through secondary structure prediction and circular dichroism. Several molecular models were generated with E-Tasser and Phyre servers and the ones that present the correct amount of secondary structure have been used for molecular replacement. Despite these efforts, all molecular replacement attempts failed to find a correct solution.

Meanwhile, the recombinant seleno-methionine containing FlgD was expressed and purified, but no protein crystals have been grown till now.

Chapter 4

H. pylori pathogenic factors

Pathogenic Factors

- Flagellar proteins
- Stress response elements

Material and Methods

- *Molecular Cloning*
- *Overexpression and Purification*
- *Solubility test*
- *Circular Dichroism*
- *Analytical gel filtration chromatography*
- *Dynamic Light Scattering*

Results and Discussion

Abstract

H. pylori is the only bacterium discovered able to survive in the hostile environment of human gastric mucosa and establish chronic colonization. The presence of virulence factors often represents the discriminant among pathogenic and not pathogenic strains. The former are associated to severe diseases, such as gastritis and cancer. A preliminary study has been performed on different proteins involved in two important colonization factors, the bacterial flagellum and the heat-shock proteins involved in cellular stress response. In particular, from the flagellar apparatus the C-ring flagellar switch protein FliN, the HAPs proteins (FlgL - FlgK - FliD) with their specific substrate chaperone FlgN and FliT have been investigated. Among the heat shock proteins analyzed, there are the two transcription regulators HspR and HrcA and the associated protein Orf (HP1026), the latter of unknown function. These proteins have been cloned in a plasmid vector to be expressed in *E. coli.* A molecular characterization has been performed on successfully purified proteins using analytical gel filtration chromatography, dynamic light scattering and circular dichroism, defining the oligomerization state in solution and the secondary structure content.

INTRODUCTION

FLAGELLINS

H. pylori is a polar flagellate bacterium. To colonize human gastric mucosa, it has evolved different virulence determinants that are necessary for pathogenesis. Less motile strains are less able to survive in the hostile environment of the human stomach than fully motile strains. Therefore, *H. pylori* motility is considered one of the most important colonization factors (O'Toolle PW, 2000). Complementary studies on *Helicobacter mustelae* suggest that motility plays a key role in the initial colonization for a long-term persistence (Andrutis KA, 1997). Cytokine response has been associated to *H. pylori* motility, in particular IL-8 induction (Watanabe S, 1997), demonstrating that the stage of gastric disease contributes to the maintenance of high motility. *H. pylori* does not present genetic cluster organization of flagellar genes. Gene expression is regulated by σ factors. Nine operons containing 15 flagellar genes characterized by σ^{70} consensus sequence and five operons containing hook basal body genes recognized by σ^{54} promoter region have been identified (Spohn G, 1999).

The structural organization of the *H. pylori* flagellum can be divided in three components: *i*) the basal body, which includes the rings, the motor, the switch proteins and the type III secretion system proteins; *ii)* the hook, a flexible structure that links the filament to drive in the basal body (Macnab RM, 1996); *iii)* the extracellular filament masked by a sheath whose ultrastructure features are relatively uncommon (Goodwin CS, 1985). The sheath contains also phospholipids and LPS similarly to the outer membrane, but with different proteins and fatty acids amount (Geis G, 1993). The possible roles of this sheath are the acid protection, masking of flagellar antigen and cellular adhesion (Jones AC, 1997).

The flagellar proteins secretion system and flagellar switch are regulated by the cytoplasmic C ring. This intracellular complex is composed of FliG, FliM and **FliN** (Lowenthal AC, 2009). FliG is involved in the turning of clockwise or counterclockwise rotation, modifying flagellar switch. CheY is a chemotaxis response regulator (Sarkar MK, 2010) that binds FliM or FliN. When CheY is phosphorylated, a clockwise rotation of *H. pylori* flagellum is observed, and *vice versa*. Moreover, FliN interacts with protein complexes belonging to the type III secretion system components, such as FliH, FliI or with substrate chaperone partners (Thomas J, 2004).

A flagellum-specific secretion pathway exports, through a central channel, the proteins involved in the basal body rod formation, the hook, the hook filament junction and the filament with its cap (Homma 1990). These proteins have been observed to polymerize in order to form the

hollow filamentous axial structure. The expression of flagellar axial substructure is sequential to that of the previous components (Kubori T, 1992), except for the assembly of the filament cap that starts upon the completion of the FlgK-FlgL hook filament junction, to allow the polymerization of the filament (Homma M, 1984). When the hook is completed, **FlgK** and **FlgL,** two hook-junction proteins, bind **FliD**, the filament capping protein, which mediates the filament assembly. The reason why these three proteins have been classified as HAPs (Hook associated proteins) derives by their simultaneous presence, when the hook is completed. Specific interactions with HAPs have been observed by putative export chaperones that facilitate the initiation of filament assembly (Kutsukake K, 1994). In particular, **FlgN** shows a specific affinity for FlgK and FlgL, and **FliT** for FliD, preventing cytosolic axial polymerization (Fraser GM, 1999).

Co-expression experiments have been planned in order to increase recombinant protein solubility expressed in heterologous system. The aim of our study was to determine the molecular structure of FliD-FliT and FlgKL-FlgN complexes and to define their interaction domains using the X-ray single crystal diffraction technique.

Heat Shock Proteins

Heat-shock proteins (Hsps) are produced when bacteria encounter stress such as elevated temperatures, but also ethanol, H_2O_2 and acid. Hsps such as DnaK and GroEL promote the proper folding and increase the survival of the pathogens in harsh environments (Craig, 1993). It was demonstrated that *H. pylori* Hsps play an important role during the host infection (Hoffman, 2003). In fact GroEL and GroES *H. pylori* homologue not only assist the proper protein folding, but also are considered an important modulator of urease enzyme activity (Dunn, 2007; Evans, 1992; Kansau, 1996).

Response to stress is a tool conserved through both eukaryotes and prokaryotes, but the molecular mechanisms between the two species are different. In *E. coli* and most of other gram-negative bacteria there is a positive regulation governed by a specific sigma factor (σ^{32}), which induce the transcription of heat shock genes under stress condition (Bukau, 1993). Negative regulation is also common in *Bacillus subtilis* and other gram-negative and gram-positive bacteria, where there is the involvement of a transcriptional repressor, **HrcA**, which binds a CIRCE DNA region. This transcriptional regulator binds DNA in the promoter region of heat shock genes under non-stressed conditions, inactivating the relative genes (Shulz, 1996; Zuber, 1994).

Another negative mechanism of transcription repression involves **HspR**, which directly controls the transcription of dnaK operon in *Streptomyces,* binding in the promoter region to three partially related inverted repeats of DNA, known as HAIR (HspR as associated inverted repeats) (Bucca, 1995). Moreover, HspR is able to auto regulate its own synthesis by repressing the promoter responsible for the transcription of the DNA region that contains the *hspR* gene itself, *H. pylori* DnaJ homologue, and a third gene named *orf,* of unknown function. Therefore, HspR negatively regulates *groELS* operon and *hrcA-grpE-dnaK* operon, which are also regulated by HrcA. This was demonstrated by *hrcA* deletion, as well as *hspR* and *hrcA*/*hspR* deletions. In non-stress condition, both HspR and HrcA are necessary in order to leave *Pgro* and *Phrc* repressed (Spohn, 2004). HspR binds the operon located far upstream from the promoters (Spohn, 1999), while the DNA binding site of HrcA is closer to the transcription starting point. Recently, another mechanism of HspR and HrcA on *H. pylori* genome regulation has been demonstrated. In fact, the genes regulated by HspR and HrcA are 43: not all are repressors, but they also activate the transcription of 14 genes involved in the biosynthesis and assembly of the flagellar apparatus (Roncarati, 2006). The motility of *H. pylori* has been associated to heat shock proteins expression (Colland, 2001; Niheus, 2004), as well as in *C. jejuni* (Andersen, 2005).

In silico sequence analysis predicts that HrcA presents a trans-membrane domain from residue 146 to 156, suggesting a similarity to the membrane-bound activator ToxR of *Vibro cholerae*, which regulates virulence gene expression by sensing environmental stimuli of periplasmic domain and transmitting them directly to its cytoplasmic DNA-binding domain (Kurukonis, 2000; Skorupski, 1997). HrcA activity depends by the presence of HspR, because it has been demonstrated that HrcA is not able to bind DNA in absence of HspR (Spohn, 2004).

HspR presents an oligomerization domain composed by hepta-repeats of hydrophobic residues, also present in eukaryotic heat shock transcription factors. These repeats could mediate trimerization, forming a coiled-coil structure between monomers (Narberhaus, 1999; Sorger, 1989).

The sequence similarity between *H. pylori* HrcA and structurally solved *T. marittima* is around 30% (Liu J, 2005). *T. marittima* HrcA crystallizes as a dimer. The structure was determined at 2.2Å resolution and the monomer is composed by three domains: a helix-turn-helix N-terminal domain (WH), a GAF like domain, and an inserted dimerization domain (IDD). The IDD, even if composed by hydrophobic residues, presents a unique structural fold with an anti-parallel β-sheet made by three β-strands sided by four α-helices.

Orf (HP1026) is the third gene present in the *cbpA-hspR-hp1026* multicistronic operon. The heat shock response of *H. pylori* is regulated by *groESL, hrcA-grpE-dnaK,* and *cbpA-hspr-orf* operons. They are negatively regulated by HspR. The structural and functional role of Orf is still unclear. Sequence analysis of Orf identifies a possible helicase domain, coupled to an ATP binding site (unpublished data, V. Scarlato and Alberto Danielli, Department of Biology, Bologna University). *H. pylori* Orf knockout does not present growth defects, but preliminary results show a lower capacity of the mutant to return to the basal expression level of the heat shock genes induced after shock with respect to wild type strains.

The proteins described have been cloned, successfully expressed and purified. *In vitro* characterization has been performed using circular dichoism, analytical gel filtration chromatography and dynamic light scattering techniques.

Material and Methods

Molecular cloning and mutagenesis

FliN (HP0584), FliT (HP0754), FlgN (HP1457) nucleotide sequences have been amplified from G27 *H. pylori* strain using forward ('5'-'3') and reverse ('3'-'5') primers reported in table (4.1). FlgN was amplified from residue 29 to residue 210. The amplified DNA fragments have been separated in agarose gel (1%) and DNA was extracted with Gel Extraction kit (Qiagen). The purified DNA was cloned in the C-term His-tag pETite plasmid vector (Lucigen) and positive colonies have been controlled by colony PCR. Extracted plasmids (MiniPrep kit Sigma) have been controlled with restriction enzyme double digestion (NdeI and NotI, NEB) and plasmid sequencing (BMR genomics sequencing service).

FliD (HP0752), FlgK (HP1119), FlgL (HP0295) genomic sequences have been amplified from G27 *H. pylori* strain. Molecular primers have been designed in frame to a N-term strep tag sequence (WSHPQFEK) insertion and cleavage site for restriction enzyme in 5' and 3' (Table 4.1). DNA amplified fragments have been cloned in Zero Blunt® TOPO PCR cloning kit (Invitrogen) plasmid vector. The cloning has been verified with enzymatic digestion and plasmid sequencing (BMR genomics sequencing service).

HspR, HrcA and Orf have been cloned in collaboration with A. Danielli and V. Scarlato, Dept. of Biology, Bologna, Italy. *HspR* (HP1025) nucleotide sequence has been amplified from 26695 *H. pylori* strain and cloned in pET22b(+) plasmid vector (Novagen). HspR mutagenesis has been

performed using '5' – '3' primer HspRC2Y_fw GAT ATA CAT AAT ATC ATA TGT ACG ATT ATG ATG AAC CGC TTT A and HspRC2Y_rev TAA AGC GGT TCA TCA TAA TCG TAC ATA TGA TAT TAT GTA TAT C. *HrcA* (HP0111) has been synthetized as optimized gene from Gene Optimizer Assisted (Life technologies) and cloned in pET22b(+) (Novagen) plasmid vector. *Orf* (HP1026) has been amplified from 26695 *H. pylori* strain and cloned in pET22b(+) (Novagen).

Name	Sequence	Restriction site
FliN_G27_fw	GGA GAT ATA CAT ATG CCA GAA ACA GAA GCT AAT AAG	
FliN_G27_rev	GTG ATG GTG GTG ATG ATG TGA ATT TTT AGC GAG ATA ATA C	
FliT_G27_fw	GAA GGA GAT ATA CAT ATG TTGATAGAGCGCCTTTCTTTAGAGC	
FliT_G27_rev	GTG ATG GTG GTG ATG ATG AGACAAAAATTTTTGAATCTTTTTAG	
FlgN_G27_fw	GAA GGA GAT ATA CAT ATG ACT TAT CAA AAT GTG AAT GAT G	
FlgN_G27_rv	GTG ATG GTG GTG ATG ATG AAACATACGCTTATTGCTAGC	
FliD_G27_fw	GGA TCC ATG GCT AGC TGG AGC CAC CCG CAG TTC GAA AAA GGC GCC GCA ATA GGT TCA TTA AGC	BamHI
FliD_G27_rev	CTC GAG TTA ATT CTT TTT AGC CGC CGC TTG	XhoI
FlgK_G27_fw	GGA TCC ATG GCT AGC TGG AGC CAC CCG CAG TTC GAA AAA GGC GCC GGC GGA ATC TTA TCT TCA CTC	BamHI
FlgK_G27_rev	CTC GAG TTA TTG TTT AAT CCC CAA TAA AGT GTC	XhoI
FlgL_G27_fw	GGA TCC ATG GCT AGC TGG AGC CAC CCG CAG TTC GAA AAA GGC GCC CGC GTT ACC TTT GGC TC	BamHI
FlgL_G27_rev	CTC GAG CTA CAA ATA TTT CGT TAA AGA C	XhoI

Table 4.1 Oligonucleotide design for target gene amplification

Bioinformatics

The Signal P 4.1 Server (Petersen T N, 2011) has been used to predict the presence of a signal secretion peptide in an *in silico* analysis of protein sequence using a combination of neural networks. Gram-negative prokaryotes organism, cleavage site and signal peptide prediction have been selected. From FlgN amino acids sequence analysis, a cleavage site between position 28 and 29 with a probability of 60% has been predicted.

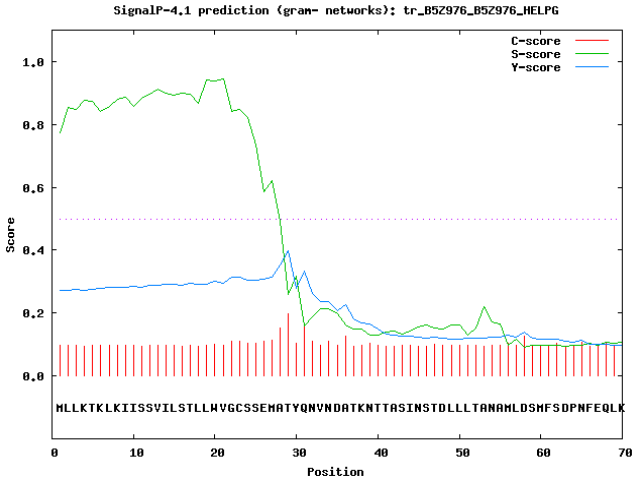

Figure 4.1 FlgN signal peptide prediction made with Signal P 4.1 Server

Overexpression, purification and crystallization trials

Transformation of C-term pETite-**FliN** and pETite-**FliT** have been performed in *E. coli* BL21 (DE3). Bacteria were grown in 2 Liter Luria Bertani medium supplemented of 30µg/ml kanamycin, at 37°C until reach 0.4 OD_{600}. The expression has been inducted with 0.5 mM IPTG (isopropyl-β-1-thiogalactopyranoside, Sigma) and the bacteria have been lied to 28°C for 5 hours under hard shaking. The bacteria have been separated from medium by centrifugation (15 minutes at 11000g), resuspended in LB medium and then disrupted by a One Shot Cell breakage system at 1.35psi (Constant System Ltd., UK). The lysates have been centrifuged for 20 minutes at 10,000g. Insoluble fractions have been washed with TBS buffer supplemented by EDTA 0.5 mM, Urea 0.1M and Triton X1000 2% and then centrifuged again. 18 hours denaturation step in hard shaking have been performed in Tris-HCl 20 mM, Urea 8M, pH 8.0. The solutions have been centrifuged and loaded in a Ni-IMAC column pre-equilibrated with denaturant buffer. Before the elution (TrisHCl 20 mM, NaCl 100 mM, Imidazole 300 mM), different washing steps have been performed with the supplement of Imidazole (20 mM), β-mercaptoethanol (2 mM), Triton X100 (0.1 %) and β-ciclodextrin (5 mM). FliN and FliT have been eluted in a single step of elution at 300 mM Imidazole. A PD-10 Desalting column (Sigma), equilibrated with Tris 20 mM NaCl 100 mM buffer, has been used to remove Imidazole from the protein solution.

Recombinant **FlgN** expression has been performed in *E. coli* BL21 (DE3) for 4 hours alter induction (0.5 mM IPTG) in reach medium supplemented of antibiotic (kanamycin 30µg/ml). The bacteria was collected, disrupted with mechanical system (One Shot Cell breakage system, Constant System Ltd., UK) and clarified by centrifugation (30 minutes at 18,000g). Recombinant FlgN has been purified from the soluble fraction, loading the supernatant on a column containing 5ml of Ni^{2+} charged Chelating Sepharose™ (GE Healthcare). The extensive washing was performed with NaH_2PO_4, 20 mM NaCl, 300 mM and Imidazole 20 mM. The protein was eluted in a linear gradient from 20 to 500 mM Imidazole. Preparative Superdex 200™ (16/60) has been used to filter the purified protein.

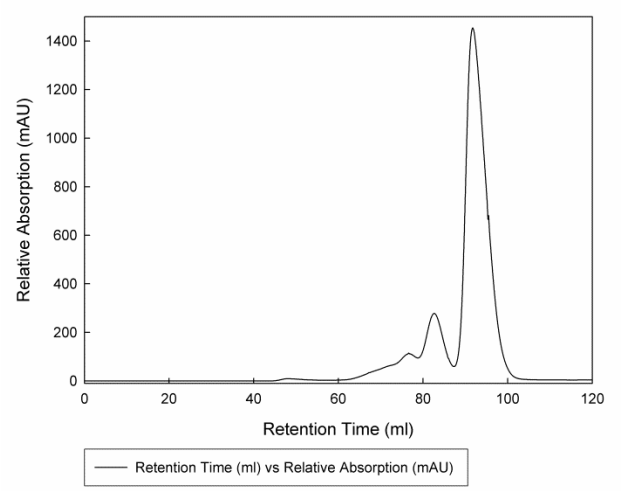

Figure 4.2 Recombinant FlgN preparative gel filtration, Superdex 200

HspR has been expressed in *E. Coli* Arctic (DE3) in 2 liters of LB medium at 37°C until optical density (OD_{600}) 0.6 and then induced with 0.5 mM IPTG overnight at 16°C. The bacteria have been collected and resuspended in lysis buffer (NaH_2PO_4 50 mM, NaCl 300 mM) supplemented of 1mg/ml DNAse (Sigma), 1mg/ml ribonuclease (Sigma), 0.01% NP-40 (Tergitol), 0.2 mM PMSF. The lysis has been performed with a French press (One Shot Cell breakage system, Constant System Ltd., UK) at 1.4 psi and clarified by centrifugation for 30 minutes at 18,000g. The soluble fraction has been loaded in a 1ml Ni^{2+} charged Sepharose™ column (GE Healthcare). After extensive wash with buffer supplemented of 20 mM Imidazole, the protein has been eluted in a linear gradient from 20 to 500 mM imidazole. Preparative gel filtration (Superdex 75 16/60 GL) has been performed to purify the protein and to remove imidazole from the solution.

A PD -10 desalting column has been used to change the buffer into a solution of HEPES 20 mM pH 7.5, NaCl 200 mM, supplemented of EDTA (2 mM), DTT (5 mM).

Recombinant **HrcA** has been expressed in *E. coli* Arctic (DE3) strain. The bacteria were grown at 28°C in Luria Bertani medium supplemented of Ampicillin (100 µg/ml) until 0.5 optical density (OD_{600}) was reached, were induced with IPTG (0.5 mM) and the expression last 18h at 12°C. After centrifugation, lysis was performed using a French press system (1.4 psi) in buffer (NaH_2PO_4 50 mM, NaCl 300 mM) supplemented of 1mg/ml DNAse (Sigma), 1mg/ml ribonuclease (Sigma), 0.01% NP-40 (Tergitol), 0.2 mM PMSF. Clarification has been performed by centrifugation at 18,000 g for 30 minutes and the soluble fraction loaded in a Ni^{2+} charged Sepharose™ column (GE Healthcare). Addition of 20 mM imidazole to the buffer solution has been used to wash the column and the HrcA has been eluted in a linear gradient from 20 to 300 mM Imidazole. HrcA

has been treated with a PD-10 Desalting column (Sigma), equilibrated with Tris 20 mM NaCl 300 mM buffer, to remove imidazole from the protein solution.

Orf has been expressed in *E. coli* BL21 (DE3) for 4 hours after induction (0.5 mM IPTG) in reach medium supplemented of 50µg/ml ampicillin. Bacteria were collected, re-suspended (Tris 20 mM pH 7.5, NaCl 150 mM), lysed (One Shot Cell breakage system, Constant System Ltd., UK) and clarified by centrifugation (30 minutes at 18,000g). Supernatant has been loaded on a 5ml Ni^{2+} charged Chelating Sepharose™ column (GE Healthcare). After extensive washing with imidazole 20 mM added to the buffer, the protein was eluted in a linear gradient from 20 to 300 mM Imidazole. Preparative Superdex 200™ (16/60) has been used to filter purified protein.

The molecular weight of recombinant proteins has been estimated by 15% sodium dodecyl sulfate–polyacrylamide gel electrophoresis (SDS–PAGE) and stained with 0.25% Coomassie Brilliant Blue R250 reagent.

UV/Vis spectroscopy, (280nm, Cary 50 Bio UV-Visible spectrophotometer, Varian Inc.) was used to determine protein concentration, using theoretical absorption coefficient.

For crystallization purposes, purified recombinant proteins have been concentrated at least to 10g/l using ultrafiltration (Vivaspin 5,000 and 10,000 MW, 15R).

Semi-automated Oryx 8 crystallization robot (Douglas Instruments) has been used to prepare different crystallization kits of Hampton (Crystal Screen I and II) and Molecular Dimension (Structure Screen I and II, PACT suite, PEGsII, PGA, JCSG I-IV, $AmSO_4$) at 293 K with sitting drop vapor diffusion technique.

Solubility analysis

Refolding tests screening have been performed on inclusion bodies of HrcA. The bacteria (*E. coli* Arctic strain) that have expressed recombinant HrcA have been resuspended in TBS buffer (8 ml) in the ratio 20 ml of buffer to 1L of culture. The bacteria have been lysed with French press (One Shot Cell breakage system, Constant System Ltd., UK) at 1.4 psi. The lysate has been divided in 4 aliquots and centrifuged for 15 minutes at 18,000g. The soluble fractions have been separated from the pellets that have been gently equilibrated with detergents for 4 hours at 4°C. The detergents that have been used were $C_{12}E_8$ (2.5% w/v), Deossicolate (2.5% w/v) and NP-40 (2.5% w/v). Buffer without detergent has been used as control. The mixtures have been centrifuged (15 minutes at 18,000 g) and the proteins solubility analyzed by 15% sodium SDS–polyacrylamide gel electrophoresis, stained with 0.25% Coomassie Brilliant Blue R250 reagent.

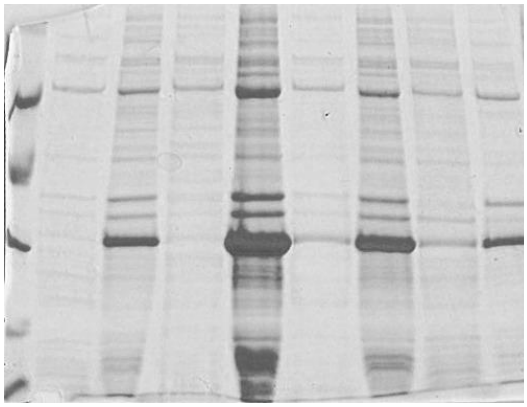

Figure 4.3 SDS-PAGE *HrcA solubility test. LMW (97, 66, 45, 30, 20, 14 kDa), (Supernatant/Pellet) Negative Control,* (S/P) $C_{12}E_8$ 2.5% w/v, (S/P) Deossicolate 2.5% w/v and (S/P) NP-40 2.5% w/v.

Circular Dichroism

Circular Dichoism analysis was performed on *FlgN*, *FliT, HrcA and Orf* to identify the secondary structure components. The instrument used was JASCO J-715 Spectropolarimeter at 298K. It has been accumulated 5 runs with (Tris 20 mM pH7.5, NaCl 150 mM) in a 0.05 cm path length cell. The wavelength interval analyzed was 190-260 nm. A solution containing the buffer was used for data rescaling and for estimating molar ellipticity. The deconvolution has been performed with the software "CD Spectra Deconvolution" (CDNN 2.1).

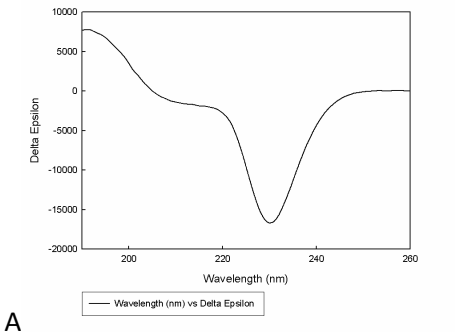

A

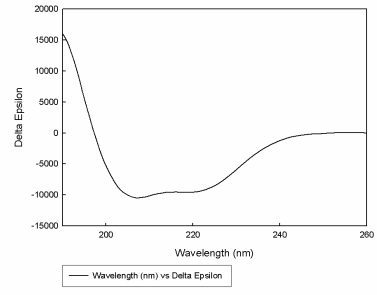

B

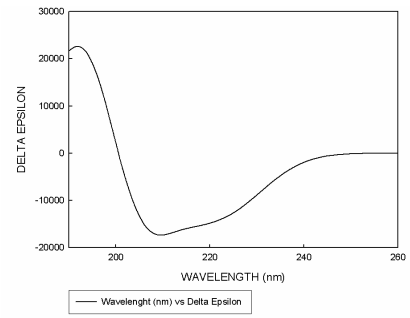

C

190-260 nm	***FliT***	***FlgN***	***Orf***
α-helix	*16.4%*	*21.7%*	*34.8%*
β- sheet	*44.1%*	*27.8%*	*15.5%*
β – turn	*15.8%*	*22.3%*	*16.6%*
Random coil	*27.3%*	*32.3%*	*31.3%*
Total	*103.7%*	*104%*	*98.4%*

D

Figure 4.4 Circular Dichroism of recombinant purified FliT (A), FlgN (B), ORF (C). D) Table 4.2 Secondary structure amounts of CD spectra deconvolution with CDNN2.1

Analytical Gel Filtration

Molecular mass and oligomerization state were estimated by analytical gel filtration using Superose 12 16/60 GL (GE Healthcare™), equilibrated with Tris 20 mM pH 7.5, NaCl 150 mM, with AKTA FPLC instrument (GE Healthcare™). The calibration curve has been performed with Cytochrome C (12.4 kDa), Alcohol Dehydrogenase (29 kDa), Albumin (66 kDa), Carbonic anidrase (150 kDa), β-amiloidase (200 kDa) and Blue dextran (2000). His tag **FliN** and **FliT** were eluted as one single distribution peak. **FlgN** eluted in a single peak with a retention time of 12 ml with molecular mass, estimated by analytical gel filtration analysis, of 20.06 kDa. The theoretical molecular mass of the FlgN monomer with His tag (2.7 kDa) is 21.1 kDa. The retention time of **Orf** in analytical gel filtration analysis with Superose 12™ was 11.44 ml, corresponding to a molecular mass of 125.9 kDa. Its monomer with His tag has been calculated to be 43.8 kDa.

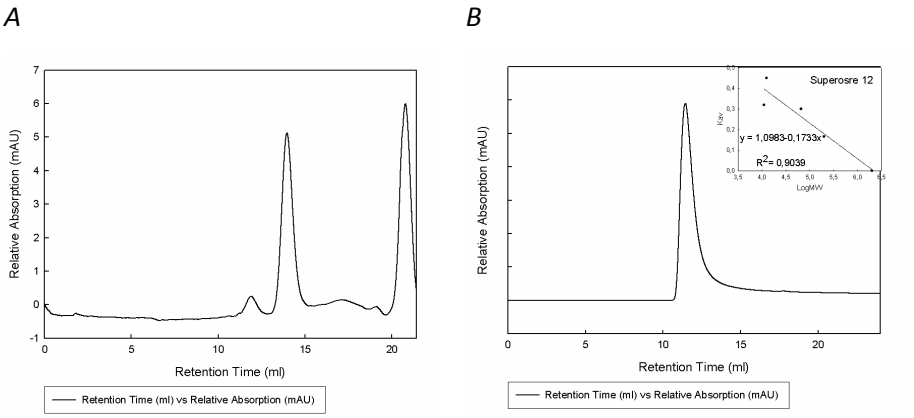

Figure 4.5 Analytical Gel filtration Superose 12 16/60 of purified FlgN (A) and ORF (B)

Dynamic Light Scattering

Recombinant *FlgN*, *FliN*, *FliT*, *HrcA* and *Orf* have been analyzed with Dynamic Light Scattering instrument at DLS Zetasizer Nano ZS (Malven Instruments) using crystallization condition. The analysis was performed at 25°C with a temperature equilibration time of 60 sec. The viscosity of the bulk material was of 0.8872 cP. The cuvette used was a Low Volume Gas Cuvette (Malvern). The measure of Z-Average size (± SD) (d.nm), the polydispersity index (PDI) and the estimation of Molecular weight (Mode ± SD) are reported in table (4.2). In the graphs of proteins analysis, the distribution molecular mass (size nm) compared to the percentage of exclusion volume is reported.

Protein	Concentration (g/l)	Hydrodynamic Radius		Distribution	Theoretical Mass (kDa)
		Hydrodynamic radius (MODE ± SD) (nm)	PDI (%)	Est. MW (kDa) (Mode ± SD)	
FlgN	3.6	**5.61 ±0.9**	34 %	**37.7 ± 6.3**	21.1
FliT	0.2	**7.5 ± 3.7**	41 %	**74.9 ± 47.1**	7.3
FliN	0.5	**58.77 ± 73.39**	73 %		
HrcA	0.35	**50.75 ± 19.17**	39 %		29.7
	3.5	**164.2 ± 77.1**	41 %		
Orf	6.1	**13.54 ± 4.8**	34 %	**295 ± 110**	43.8

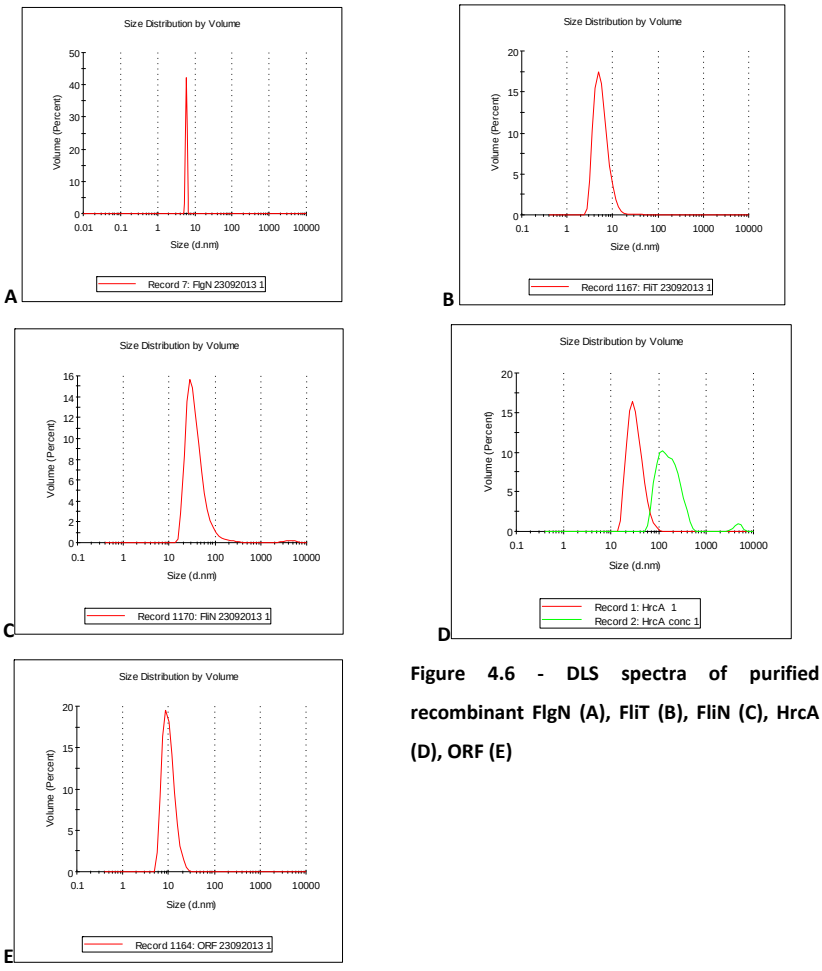

Figure 4.6 - DLS spectra of purified recombinant FlgN (A), FliT (B), FliN (C), HrcA (D), ORF (E)

Results and Discussion

H. pylori colonizes more than half of world population, and severe and lethal diseases have been associated to its infection. Its ability to survive and to colonize the human gastric mucosa are still not fully understood. This study was focused on the pathogenic factors related to motility and on proteins involved in cellular stress response. Pathogenic proteins are possible new pharmaceutical targets, since when their activity is inhibited, the host infection is blocked. More

severe outcomes have been associated to more motile *H. pylori* strains. Hence, bacterial motility has been classified as one of the most important colonization determinants.

H. pylori FliN

H. pylori has evolved a complex system that, owing to its motility and chemotaxis, allows him to move to different micro-niches of the human gastric mucosa and prevent its discharge through peristalsis. Bacterial motility has been studied for more than 30 years, and all components of the flagellar substructure have been identified (Macnab RM, 2003). The flagellar switch mechanism is one of the most fascinating topics of bacterial motility. The C – ring complex of flagellar basal body is constituted by three proteins: FliG, FliM and FliN, each one present in many copies (Thomas DR, 2006). FliN has been observed to interact with type III secretion system components, facilitating the delivery of extracellular components (Gonzales-Pedrajo B, 2006). FliN plays a critical role in switching the movement direction. The binding of phosphorylated CheY mediates the signaling and promotes the clockwise rotation. Even if different structural studies and electron microscopic images of the flagellar basal body complex from *Salmonella* have been captured, the molecular structure of several proteins involved in this complex has not been determined yet. Recently, the crystal complex of *Salmonella* FliM with FliG C – terminal domain has been published (Paul K, 2011), but little is known about the molecular structure of flagellar C- ring component FliN of any species.

H. pylori FliN was cloned and expressed in *E. coli.* After lysis, it resulted to accumulate in inclusion bodies. Denaturation of the lysate insoluble fraction has been performed with Guanidine 6 molar buffer. The unfolded protein was linked on a Ni affinity column and, after different steps with refolding buffer (Tris 20 mM pH 7.5, NaCl 100 mM), was eluted in 300 mM imidazole. With a Sigma PD-10 desalting column, the eluent used for affinity was removed. Purity and concentration of the protein has been measured with UV/Vis spectroscopy. It was possible to estimate that, in these conditions, around 2 g/l of recombinant protein was expressed and purified from 1 liter of *E. coli* culture. Recombinant FliN sequence was analyzed and the monomer resulted to weight 14,788.9 Da, with a theoretical isoelectric point of 5.5. Denaturant sodium dodecyl sulfate gel electrophoresis, stained with Comassie reagent, confirmed protein concentration, purity level and predicted apparent molecular weight (Figure 4.4). The protein was concentrated to 10 g/l and different crystallization screens have been tested. Hard precipitate is present into the crystallization drop. The oligomerization state of the protein has been analyzed. Analytical gel filtration chromatography and DLS measurements revealed that recombinant FliN is polydisperse in solution (73%), suggesting that in these

conditions the protein is not suitable for crystallization. Different approaches need to be investigated to increase the monodispersity of *H. pylori* FliN in solution for structural purposes.

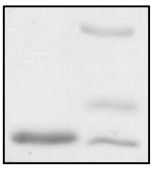

***Image 4.4 FliN SDS-PAGE purified protein*. Purified recombinant FliN sample - LMW (25, 18.4, 14 kDa)**

*Substrate specific chaperones (FlgN - FliT) and **H**ook **A**ssociated **P**roteins (FlgL - FlgK - FliD)*

To prevent axial polymerization of flagellar components involved in an extracellular substructure as the hook junction or the filament cap, specific chaperones are necessary. After the formation of flagellar hook, coordinated by the two hook scaffolding proteins FliK and FlgD, proteins HAP1 (FlgK and FlgL) and HAP2 (FliD) are exported through a flagellar central channel, large around 25 - 30 Å (Ruiz T, 1993). A molecular mechanism controls the folding process and mediates the export of partially unfolded monomers, preventing cytosolic oligomerization (Namba and Vonderviszt, 1997). Type III secretion system components FlgN and FliT have been observed to play this specific role in the flagellar system. The goal of this study was the co-expression of HAPs with its specific chaperone for structural analysis.

Helicobacter pylori G27 strain has been used as template to amplify the nucleotide sequence of FlgN, FliT, FlgK, FlgL, and FliD genes. The primers designed for HAPs contain a N-terminal strep–tag and a restriction site. The primers designed for specific chaperones contained a nucleotide sequence for direct molecular cloning. The amplified DNA of each chaperone has been cloned in a plasmid vector in frame to His–tag in the C-terminal domain and the HAPs have been cloned in a storage vector, for a successive cloning step in an expression plasmid vector. This last step was unsuccessful and the HAPs interaction with their specific chaperones needs to be still investigated. Nevertheless, structural studies on *H. pylori* FlgN and FliT have been deeply investigated. The recombinant FlgN and FliT plasmids have been transformed and expressed in BL21 *E. coli* strain. Bacteria have been lysed with French press and clarified by centrifugation. FlgN was purified by the soluble fraction of the lysed, whilst the FliT pellet was treated with denaturant buffer and refolded during the affinity purification step (Oganesyan N, 2005). The soluble protein fractions have been analyzed with SDS-PAGE, confirming the predicted apparent molecular weight. The secondary structure of these proteins has been investigated with circular

dichroism. A peculiar spectrum for FliT was observed. Analysis with the CDNN 2.0 deconvolution software indicates a predominance of β-strand, a conformation significantly different from that of *Salmonella enterica* FliT (EA7M), characterized by a single α-helix (Imada K, 2010). Analytical gel filtration chromatography revealed that FlgN was eluted as a monomer, experimental data confirmed by dynamic light scattering measurements, where the protein presented a hydrodynamic radius of 5.6 (±0.9) nm and a polydispersity of 34 %. Instead, FliT presents different oligomerization states, observed in gel filtration analysis (Data not shown). The main oligomerization species, estimated by DLS, was of 7.5 (± 3.7) nm with a polydispersity of 41 %. Therefore, preliminary results promote FlgN for a more suitable crystallographic investigation, but even if the protein was concentrated to 10 - 30 - 60 g/l and different tests with crystallization screening were performed, unfortunately no protein crystals were obtained. The investigation of the molecular structure of *H. pylori* specific HAP chaperones have been studied in order to understand how secondary structure of little chaperone proteins could be influenced by the presence of its specific substrate. The missed goal to obtain crystals of the single chaperone protein and HAP-chaperone complex failed. This project presented anyway some preliminary results for further investigation of these housekeeping *H. pylori* flagellar proteins involved in bacterial motility.

Hsps

In order to survive in the gastric environment and establish chronic colonization of the human stomach, the bacterium *H. pylori* had evolved different pathogenic virulence factors, which also include heat shock proteins. The transcription of these proteins is regulated by three operons that encode the major cellular chaperone machineries that include *hspR* and *hrcA* genes. These two transcriptional repressors mediate the expression of these operons. For crystallization purposes these proteins have been expressed and purified. In particular HspR and HrcA, both transcriptional factors, and HP1026, a protein of unknown function. These proteins have been expressed in *E. coli* and purified by IMAC affinity. To determine the level of protein purity and the apparent molecular weight, the purified samples have been checked in sodium dodecyl sulfate polyacrylamide gel electrophoresis (SDS-PAGE), stained in Comassie Brilliant Blue reagent (Figure 4.6 A). They are hardly soluble. In fact, the HspR concentration solubility limit is about 0.7 g/l during sample concentration for crystallization trials. The protein precipitated giving rise to insoluble aggregates. A recent successful strategy to increase protein solubility and prevent protein aggregation was single nucleotide mutagenesis of Cys into neutral residue (Dian C,

2011). Following this result, HspR Cys in position 2 was mutated into a Tyr, using the site directed mutagenesis kit. The presence of a Tyr resulted to be conserved in other *H. pylori* strains, data confirmed by ClustalW sequence alignment (Data not shown). Unfortunately HspR solubility of the HspR mutant did not increase. PDP-blast HspR sequence alignment with the PDB sequence database revealed that *E. coli* CeuR (1Q05, Wang Y, 2007) presents the best sequence similarity with *H. pylori,* 33 %. The molecular structure of this protein has been solved by crystals incubated with 1 g/l of protein solution, suggesting a common solubility limit of this class of proteins. HrcA was insoluble and it was purified from the membranes resuspended in presence of detergents (NP40 0.1%). HrcA behavior was experimentally demonstrated by DLS measurements. Different concentrations of protein solution have been analyzed and it was observed that the hydrodynamic radius of particle aggregates increases when the protein solution is more concentrated. In fact, at 0.35 g/l the particle presents a 50.7 (± 19.2) nm radius and at 3.5 g/l 164.2 (± 77.1) nm with a polydispersity around 40 %. Detergent solubility screening has been performed (Figure 4.6 B) and the best detergent resulted to be NP-40 at 2.5% w/v. In this condition the protein was concentrated and crystallization tests have been performed. Finally Orf (HP1026) has been expressed in *E. coli* and resulted soluble after lysis and clarification. The protein was purified by Ni-IMAC affinity and then gel-filtered with a preparative Superdex 200 GL chromatographic column. Protein characterization by analytical gel filtration, dynamic light scattering and circular dichroism was performed. The secondary structure has been determined by dichroic spectra deconvolution: the protein presents a large content of α-helices (35 %). Analytical gel filtration analysis reveals a possible trimeric oligomerization state, even if DLS measurements predicted a hexameric homoligomeric state. Orf sequence similarity with the whole protein database has been performed with p-Blast , and a possible ATP binding domain has been identified. Therefore, the protein has been concentrated to 15 - 30 - 60 g/l and crystallization trials have been performed with the purified protein (Figure 4.6 C) and in presence of one equivalent ATPγS (SIGMA). No protein crystals have been obtained yet.

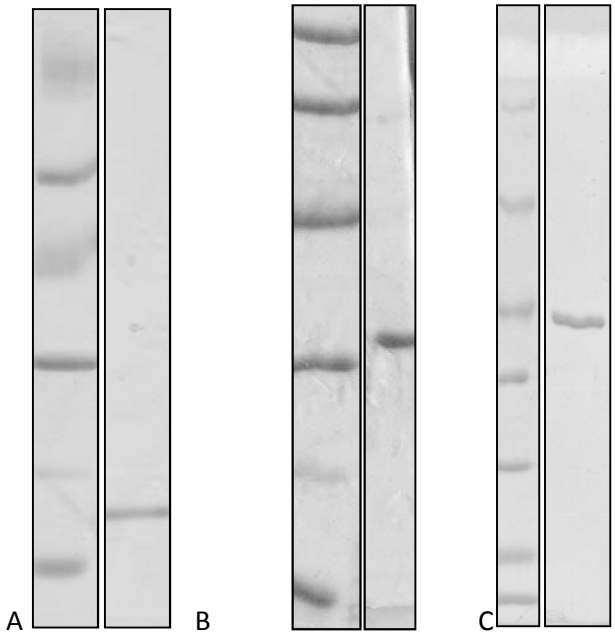

Image 4.5 SDS – PAGE. A) LMW(97, 66, 45, 30, 20 14 kDa) - HspR; B) LMW (97, 66, 45, 30, 20 14 kDa) - HrcA; C) LMW (116, 66, 45, 30, 20, 18, 14 kDa) - Orf (HP1026) purified samples

Appendix

S1P/SKI1

Introduction

Materials and methods

Constructs

Overexpression, purification and crystallization trials

Circular dichroism

Purification and MS analysis

Results and discussion

Introduction

SKI-1/S1P (Site 1 Protease / Subtilisin Kexin Isozyme 1) is a serine protease that belongs to the mammalian family of Proprotein Convertases (PCs) phylogenetically correlated to yeast kexin and bacterial subtilisin. Their function is to mediate the proteolysis of different substrates relevant for the life of the cell (Tourè BB, 2001). Alzheimer disease (Creemers J, 2001), tumorigenesis (Khatib A, 2002), and viral infections as HIV-1 (Muolard M, 1999) have been associated to PCs activity and so they are considered as possible pharmaceutical targets (Couture, F, 2001). Some of the proteases of the family, i.e. furin, PC5/6, PC7, and S1P, are ubiquitously expressed, whilst others are more tissue-specific. In order to be activated, this class of proteases requires an auto-proteolytic activation step (Fùgere M, 2005). The majority of PCs substrates have a highly selective cleavage site at pairs of basic residues: the minimal consensus sequence recognition of the substrate is **R**-X-X-**R**↓, where X could be any residues (Hosaka M, 1991). On the contrary, a unique behavior was observed for S1P/SKI1 enzyme, which does not require a basic amino acid at the cleavage site. In fact, S1P cleavage site could be composed by single or pairs of basic residues, as Lys or Arg or hydrophobic residues as Leu, Phe, Val, or Met, generating a more complex motif R/K-$(X)_n$-R/K↓, where X is any residues except Cys and n = 0, 2, 4, or 6 residues (Seidah N, 1998). Therefore, S1P has been shown to have an unique substrate specificity, preferring cleavage after non-basic amino acids (Bodvard K, 2007).

S1P is synthesized as an inactive precursor of 1052 amino acids in the endoplasmic reticulum (ER), and undergoes three sequential autocatalytic processing steps. In the first process, S1P cleaves the pro-domain at sites B' (**R**KV**F**↓) and B (RKVF**R**SL**K**↓), then in Golgi it processes site C (**K**HQ**K**LL↓), near the transmembrane domain (Elagoz A, 2002). The last cleavage produces a soluble S1P, whose biological role is still not well understood (Pullikotil P, 2007).

S1P substrates are very important for cell homeostasis as well as for endocrine regulation. S1P knockout is lethal and liver-induced knockout produces mice with reduced cholesterol and fatty acid synthesis ability. One of the most important S1P substrates till now identified is SREBP (Sterol Regulatory Element Binding Protein), whose processing occurs in early Golgi apparatus (Brown M, 2000). S1P and S2P process SREBP playing a key role in lipid metabolism and cholesterol by regulating the feedback mechanism of cellular lipid homeostasis. Among identified S1P targets, pro-BDNF (brain derived neural factor) is probably delivered in the correct form at the secretory pathway (Seidah N, 1998). The activation of the major cellular factor ATF-6 involved in unfolded protein response is also mediated by S1P activity (Ye J, 2000). Finally,

related to cellular viral infection, the surface glycoprotein of a Lassa virus (Lenz O, 2001), lymphocytic choriomengitis (Beyer W, 2003) and Crimea Congo hemorrhagic fever virus (Vincent M, 2003) has been identified as S1P substrates.

Kinetic and biochemical information of S1P properties are sparse and not always coherent. The most relevant controversy is related to human S1P as a serine Ca^{2+}-dependent protease (Touré B, 1999), whilst hamster S1P does not require Ca^{2+} (Cheng D, 1999). Structural information of the pro-protein convertases family are confined to kexin progenitor, whilst the three dimensional structure of S1P is not known yet. Therefore, different functional domains of S1P have been produced and purified for crystallographic purposes. Moreover, the processing of an S1P mutant was studied with mass spectrometry to identify a possible alternative cleavage site in the regulatory domain.

Materials and Methods

Construct design, cloning and mutagenesis

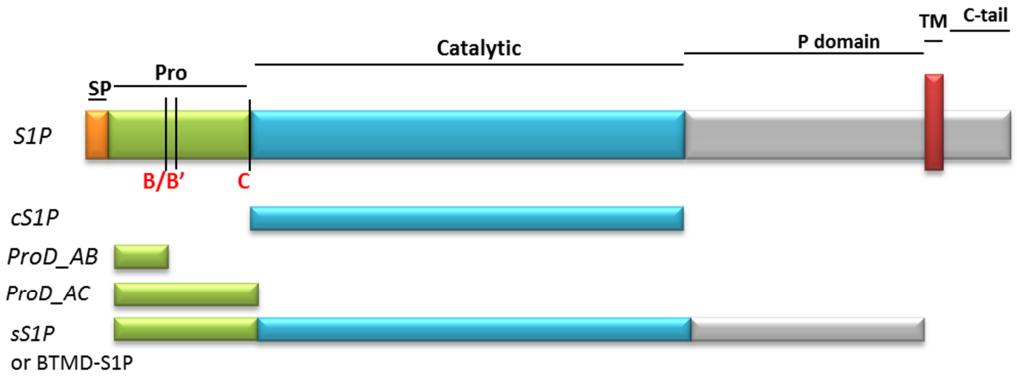

Figure 1.5 S1P synthetized constructs (*cS1P, ProD_AB, ProD_AC, sS1P)* compared to SKI-1/S1P protease domains.

	Amino acids	*Molecular weight*	*Constructs*		*Domain from residue – to residue*
S1P	*1052*	*117,7 kDa*			
cS1P	*296*	*32,2 kDa*	*WT*	*S414A H249A*	*186 - 482*
ProD_AB	*124*	*14,2 kDa*	*WT*		*17 - 129*
ProD_AC	*189*	*21,3 kDa*	*WT*	*Mut C*	*17 - 236*
sS1P or BTMD-S1P	*997*	*111,1 kDa*	*WT*	*Mut C*	*1 - 997*

Table 5.1 S1P/SKI-1 analyzed constructs.

Different S1P domains have been synthesized to be adapted to the codon usage in *E. coli* (Life Technologies™). Optimized genes have been design for 2 protein domains: the catalytic (cS1P) and the pro regulatory domain (ProD_AC). They have been inserted into storage vectors (pMK and pMA). The prodomain corresponding to the fragment processed at the B site (ProD_AB) has been obtained from ProD_AC plasmid. cS1P starts from residue 186 to 482 and ProD from residue 17 to 186 of the S1P amino acids sequence. Nucleotide primers have been designed to amplify the construct present in the *pMK-cS1P* vector (forward: CAC CAT GCG TGC AAT TCC GCG T and reverse 3'-5': CGC CTG CGG TTT ATA GCT ATT). Two constructs starting from *pMA-ProD_AC* vector have been generated to study domain ProD. The first required (forward 5'-3': CAC CAT GTA TCC GTA TGA TGT T and reverse 3'-5': GCC ACC GGT TTC CGG CAG GCT) primers to be amplified and subcloned in an expression plasmid vector ProD_AC construct; the latter was for ProD_AB construct (forward 5'-3' - GAA GGA GAT ATA CAT ATG AAA AAA CAT CTG GGT GA and reverse 3'-5' - GTG ATG GTG GTG ATG ATG TTG CGG TGT AAC ACG). Template DNA was amplified by PCR, using proofreading *pfu* DNA polymerase (Finnzymes). The amplified fragments were cloned into the pET101vector (Invitrogen) and pETite (Lucigen) in frame with a C-terminal His-tag, using a TOPO® Cloning kit to obtain *pET101-cS1P, pET101-ProD_AC and pETite-ProD_AB* plasmids. The appropriate insertion in the expression vector was confirmed by colony PCR and by sequencing with T7 forward and reverse primers.

Double-point mutation of the *pET101-cS1P* was performed with the QuickChange® Site-Directed Mutagenesis Kit (Stratagene) using oligonucleotides to introduce the mutations. The following primers have been used to change from His residue to Asp and then into Ala: cS1P_H294D forward 5'- cS1PH249D: GAT GAT GGT CTG GGT GAT GGC ACC TTT GTT G and reverse 3'- cS1PH249D: CAA CAA AGG TGC CAT CAC CCA GAC CAT CAT C and cS1PD249A_fw: GAT GAT GGT CTG GGT GCT GGC ACC TTT GTT G and cS1PD249A_rev: CAA CAA AGG TGC CAG CAC CCA GAC CAT CAT C respectively. The positive colonies have been verified by DNA sequencing.

Another construct of S1P was design in order to understand the role of aoutoprocessing events during the maturation of the enzyme. **sS1P (s**oluble **S1P) or BTMD-S1P** (**B**efore **T**rans-**M**embrane **D**omain **S1P**) starts from residue 1 to 997 of the S1P sequence excluding the transmembrane and the C-tail domain producing a soluble form of S1P after the processing of the Signal peptide. sS1P was produced in two different forms, a native variant and a mutated form that presents a double mutation at the C cleavage site in order to block that processing event.

Overexpression, purification and crystallization trials

E. coli BL21(DE3) cells (Invitrogen) were transformed with the *pET101-**cS1P**_H294A* plasmid. Protein expression was induced by 0.5 mM IPTG (Sigma) in 2 liters of reach medium for 4h incubation at 28° C, supplemented with Ampicillin (100 µg/ml). Bacteria were collected and resuspended in a lysis buffer 30 mM HEPES, pH 7.5, 200 mM NaCl and NP-40 0.01% containing protease cocktail inhibitors: PMSF 0.2 mM, Complete Mini EDTA free cocktail (Roche) and specific inhibitors: $CuSO_4$ 1 mM, Zn Acetate 1mM and chloromethyl ketone 3µM. The suspension was disrupted by a One Shot Cell breakage system at 1.35psi (Constant System Ltd., UK). The lysate was clarified by centrifugation to remove cell debris at 18,000 g for 30 minutes and loaded into a column containing 1 ml of Ni^{2+} charged Chelating Sepharose™ (GE Healthcare, UK). After washing with 20mM imidazole buffer, the protein was eluted by a linear gradient of 300 mM imidazole. Positive fractions were collected and purified by gel filtration chromatography, using a Superdex 200™ 16/60 GL (GE Healthcare) equilibrated with 30 mM Na Citrate 20 mM pH 7.5, 200 mM NaCl.

Recombinant **ProD_AC** was overexpressed in transformed *E. coli* BL21(DE3) cells, grown in LB for 4 hours at 28° C after induction with 0.5 mM IPTG. The bacteria were collected, suspended in lysis buffer (Na_2HPO_4 20 mM pH 7.5, NaCl 300 mM) supplemented by PMSF 0.2mM and NP-40 0.01%, disrupted by a One Shot Cell breakage system at 1.35psi (Constant System Ltd., UK) and clarified by centrifugation (18,000 g for 30 minutes). Affinity purification was performed with 1 ml Ni-IMAC column (GE-Healthcare) and gel filtration chromatography with Superdex 200 16/60 (GE-Healthcare).

ProD_AB was expressed in *E. coli* BL21(DE3) optimized strain (Lucigen), grown for 3 hours at 37° C after induction (0.5 mM IPTG). The collected bacteria were incubated in a denaturating buffer (Na_2HPO_4 20 mM pH 7.5, NaCl 150 mM, Guanidine 6 M) for 18 hours and then lysed by a One Shot Cell breakage system at 1.4 psi (Constant System Ltd., UK). The lysate was centrifuged (25000 g 30 minutes) and loaded in a 1 ml Ni^{2+} Sepharose column (GE Healthcare). The eluted fractions were subjected to different refolding trials (Table 5.2), without successful results.

In order to understand the importance of the single SKI-1/S1P autoprocessing events and their role on the maturation and activity of the enzyme, we generated the C mutant, by replacing R_{183} and R_{184} with E respectively. **sS1P WT** and **Mutant C** transfections have been performed in serum-free suspension cultures of HEK 293 cells at scales from 10 ml to 500 ml in agitated non-instrumented cultivation systems. Transfection vector derive from a pIRES-S1P-BTMD construct modified to add a His6 tag to the C terminus, pIR-S1P-BTMD(6×His). The recombinant pro-

protein includes its native signal sequence for the appropriate targeting and secretion in the cell culture medium, that is collected for further purification steps, while the cells pellet is discarded. The protein has been isolated from two harvests of cell culture supernatant (3rd and 7th day). These constructs were overexpressed in HEK293 cells which lacks SKI-1/S1P and their auto-processing profile compared to SKI-1/S1P WT (positive ctrl) and SKI-1/S1P H249A (catalytically dead, negative ctrl). Surprisingly, replacement of C site R_{183}, R_{184} with E did not impair maturation. The protein was isolated by IMAC-Co chromatography (Co-TALON resin, GE Healthcare) and eluted with 20 mM Tris-HCl, pH 7.5 containing 150 mM NaCl, 300 mM Imidazole.

Protein quantification was performed by UV/Vis spectroscopy (280nm, Cary 50 Bio UV-Visible spectrophotometer, Varian Inc.) using theoretical absorption coefficient combined to 15% sodium dodecyl sulfate–polyacrylamide gel electrophoresis (SDS–PAGE). The resolved gels were stained with 0.25% Coomassie Brilliant Blue R250 reagents.

Recombinant protein samples have been concentrated to 10 g/l and used for crystallization tests partially automated using an Oryx 8 crystallization robot (Douglas Instruments), but no protein crystals have been obtained so far.

Circular dichroism

Recombinant ProD_AC has been analyzed by circular dichoism using a JASCO J-715 Spectropolarimeter at 298K. Molar ellipticity measurements were performed using a 0.05 cm path quartz cell in Na_2HPO_4 / NaCl, pH 7.5 buffer, in the wavelength interval 190-260 nm. A solution containing the buffer was used as blank.

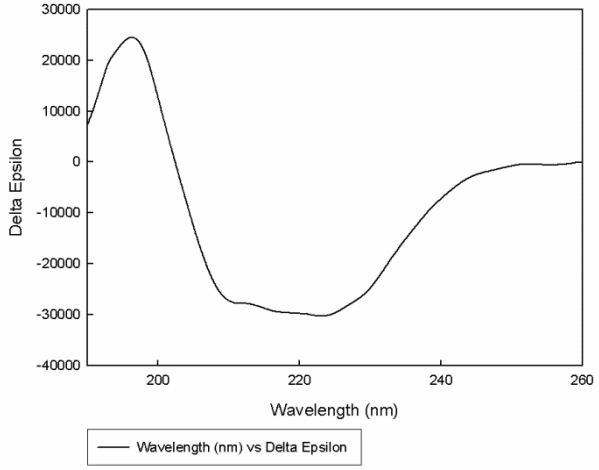

Figure 5.2. **Circular dichroism of soluble fraction of recombinant ProD_AC**

S1P RP-HPLC and MS analysis

Reduction of S1P (WT and Mut C) disulfide bridges was obtained with Tris (2-carboxyethyl) phosphine (TCEP), using a molar ratio of 1:10 (Cys:TCEP) and S-carboxymethylation by using iodoacetamide (IAA) in molar ratio of 1:10 (Cys:IAA). The sample was dissolved in 20 mM Tris-HCl pH 8.5 containing 6 M Guanidine-HCl and treated with TCEP for 30 min at 37°C; after that IAA was added and the sample kept in the dark for 30 min at room temperature. The sample was then subjected to RP-HPLC analysis.

RP-HPLC analysis was performed using a C4 column (150 x 4.6 mm), eluted by a linear gradient (10-70%) in aqueous trifluoroacetic acid/CH_3CN solvent, monitoring at 226 nm at a flow rate of 0.6 ml/min. The sample was denatured in 6 M Guanidine-HCl before loading in RP-HPLC,. The eluted fractions corresponding to the major HPLC peaks were dried out in a speed-vac concentrator, dissolved in 50% acetonitrile, 0.1% formic acid and directly injected in the ESI source. Mass measurements were performed with a quadrupole-TOF spectrometer (Waters, Manchester, UK) (capillary voltage: 2800–3000 V; cone voltage: 45 V; scan time: 1 s; interscan: 0.1 s). Spectra were analyzed using MASSLYNX software (Micromass, Wynthenshow, UK).

Results and Discussion

S1P is a 118 kDa multi-domain protein; therefore, our approach has been focused on two main regions of S1P: the "Pro domain", involved in the inhibition of S1P catalytic activity, and the so called "catalytic domain", which includes the residues responsible for the cleavage reaction itself.

Hence, the sequences corresponding to the before mentioned domains were synthesized as optimized genes for the expression in *E. coli* and sub-cloned in expression plasmids in order to obtain C-term His-tagged fusion proteins. The construct corresponding to the catalytic domain (cS1P) was produced both as wild type and in a mutated form (His249Ala) and (S414A) to abolish its proteolytic activity and increase its stability. The corresponding proteins were expressed and extracted by *E. coli* cells sonication in phosphate buffer, supplemented with detergent and protease inhibitors and the resulting extract clarified by centrifugation. The supernatant was loaded in a His-Trap column and eluted by imidazole gradient. The eluted fractions were pooled and further purified by size exclusion chromatography. The resulting samples were analyzed by SDS-PAGE electrophoresis and those containing the purest and most homogeneous cS1P protein

were concentrated to 10mg/ml for crystallization trials. Sparse matrix crystallization screenings (isothermal vapor diffusion setup) were performed by a semi-automated robot (Oryx8), but no protein crystals have been obtained yet.

Two different constructs of the regulatory ProDomain have been sub-cloned, according to the physiological multi-sites processing events it undergoes upon S1P folding, trafficking and activation: ProD_BB' and ProD_AB, corresponding to 22 and 14 kDa domains, respectively.

While ProD_BB' was soluble but quite unstable if produced in *E. coli* cells, ProD_AB was highly expressed but insoluble and enriched in the inclusion bodies. Therefore, ProD_AB has been expressed in *E. coli*, denatured, isolated by His-tag affinity chromatography and submitted to multiple refolding conditions in order to identify the most promising ones. Unfortunately, the refolding attempts till now tried did not allow to isolate any soluble refolded fractions of such domain. Other purification strategies, as well as different expression systems, need to be explored to overcome the encountered difficulties.

	1	2	3	4	5	6	7	8
Arginina	**400 mM**	**400 mM**	**400 mM**	**400 mM**	**400 mM**			
MgCl2	**2 mM**	**2 mM**	**2 mM**	**2 mM**	**2 mM**			
KCl	**2 mM**	**5 mM**	**5 mM**	**5 mM**	**5 mM**			
MES	**50 mM**	**50 mM**		**50 mM**				
PEG 3350	**0,05%**							
GSSG	**0,1 mM**	**100 mM**	**100 mM**	**100 mM**	**100 mM**			
GSH	**1 mM**	**1 mM**	**1 mM**	**1 mM**	**1 mM**			
CaCl2		**2 mM**	**2 mM**	**2 mM**	**2 mM**			**5 mM**
Sucrose		**300 mM**	**300 mM**	**300 mM**	**300 mM**			
NaCl		**240 mM**	**240 mM**	**10 mM**	**10 mM**	**300 mM**	**300 mM**	**100 mM**
TRIS			**50 mM**		**50 mM**			
NaH2PO4						**50 mM**	**50 mM**	**50 mM**
NP 40						**0, 01 %**	**0,01 %**	**0, 05 %**
DTT						**1 mM**	**2 mM**	**5 mM**
EDTA								**5 mM**
pH	**6.0**	**6.0**	**8.0**	**6.0**	**8.0**	**7.5**	**7,5**	**6.5**

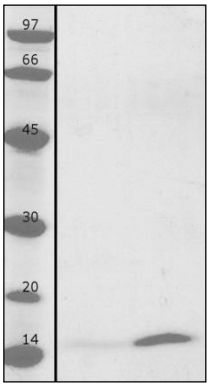

Table 5.2. ProD tested refolding conditions. Figure 5.3 SDS PAGE LMW (97, 66, 45, 30, 20, 14 kDa); Dialyzed ProD_AB (condition n.8); ProD_AB purified from inclusion bodies.

The double substitution of residues at the cleavage site C (sS1P_mut_C) has been studied on a soluble construct of S1P and compared with wild type protease (sS1P_WT). Auto-processing fragments of regulatory ProD domain of both recombinant proteins, expressed and purified from the supernatant of a mammalian HEK293 cells culture, were detected and separated by RP-HPLC (Figure 5.6). Eluted fractions have been analyzed by MALDI-TOF spectrometer and the corresponding profiles compared and further analyzed (Table 5.3).

***Image 5.4. SDS-PAGE purified cS1P and ProD_AB recombinant constructs of human S1P protease* A) cS1P, LMW (97, 66, 45, 30 kDa) B) ProD_AB, LMW (97, 66, 45, 30, 20, 14 kDa)**

Mass Spectrometry analysis

Recently, furin, a member of the PCs family, was also found to have additional processing sites in the prodomain region (Gawlik, 2009). Similarly, it is conceivable that the SKI-1/S1P C is the result of a double cleavage event (C'/C) and that, likewise B'/B, simultaneous blockage of both C and C' processing are required to trap SKI-1/S1P mainly in the intermediate immature form.

To identify the exact C' cleavage site, a MALDI-TOF-MS analysis was performed. A soluble (truncated before the transmembrane domain) SKI-1/S1P C mutant-6His was generated (SKI-1/S1P C-BTMD), produced in HEK293 and purified by IMAC chromatography (Fig. 5.5). Purified wt SKI-1/S1P-BTMD was likewise analyzed in parallel. Using standard MALDI-TOF-MS conditions, both prodomain fragments at site B and B' were found attached to the mature form. Further prodomain fragments of molecular weight higher than the B'/B became visible only upon carboxymethylation, suggesting the existence of a covalent bond between the enzyme and its AC prodomain. In the context of the mutant, multiple C' cleavages were identified, all within the hypothesized region at RRASLSLG$_{170}$↓, WHATGRHS$_{181}$↓, and WHATGRHSSEE$_{184}$↓ motifs. The unusual sequences at the cleavage sites do not fit any specific protease *consensus* motif, although an auto-processing event cannot be ruled out. Accordingly, shedding occurs at QKLL$_{953}$↓

which does not follow the SKI-1/S1P **R**X(**hydrophobic**)X↓ motif (Toure et al, 2000). With the exception of WHATGRHSSEE$_{184}$↓, which is an obvious consequence of the RR$_{184}$↓ replacement by EE, the other fragments found also in the WT enzyme are supportive of a physiological complex processing of SKI-1/S1P prodomain.

We propose that SKI-1/S1P activation occurs through sequential and/or alternative excisions at B'/B and at C'/C without the physical release of the prodomain from the rest of the molecule, thus leading to a heterogeneous population. As a consequence, inhibition of one of the complex auto-processing events alters the relative composition of such population.

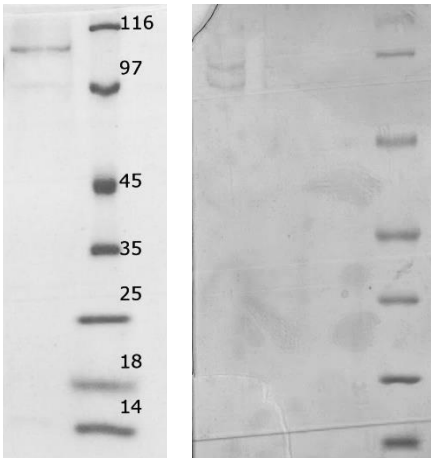

***Image 5.5. SDS-PAGE purified* SKI-1/S1P-BTMD (MUTANT C and WT) *constructs*.**

S1P/SKI1 Mut C					
Theoretical MW (Da)	Experimental MW (Da)	Modification (Da)	Retention time	Protein Domain	Sequence
13211,8	13211,61 ± 0,46		23,8	6 → 120	DRLEKKSFEKAPCPGCSHLTLKVEFSSTVVEYEYIVAFNGYFTAKARNSFISSALKSSEVDNWRIIPRNNPSSDYPSDFEVIQIKEKQKAGLLTLEDHPNIKRVTPQ***RKVFRSLK***
5945,86	5945,18 ± 06		19,2	70 → 120	IIPRNNPSSDYPSDFEVIQIKEKQKAGLLTLEDHPNIKRVTPQ***RKVFRSLK***
4360,08	4361,31 ± 08		19,7	81 → 117	PSDFEVIQIKEKQKAGLLTLEDHPNIKRVTPQ***RKVFR***
13221,08	13325,15 ± 0,17	CM	29,5	6 → 120	DRLEKKSFEKAPCPGCSHLTLKVEFSSTVVEYEYIVAFNGYFTAKARNSFISSALKSSEVDNWRIIPRNNPSSDYPSDFEVIQIKEKQKAGLLTLEDHPNIKRVTPQ***RKVFRSLK***
14064	14122,67 ± 9,74	CM	30,9	46 → 167	YFTAKARNSFISSALKSSEVDNWRIIPRNNPSSDYPSDFEVIQIKEKQKAGLLTLEDHPNIKRVTPQ***RKVFRSLK***YAESDPTVP**C**NETRWSQKWQSSRPLRRASLSLGSGFWHATGRHSS***EE***
13719,4	13781,6 ± 7,6	CM	30,9	46 → 164	YFTAKARNSFISSALKSSEVDNWRIIPRNNPSSDYPSDFEVIQIKEKQKAGLLTLEDHPNIKRVTPQ***RKVFRSLK***YAESDPTVP**C**NETRWSQKWQSSRPLRRASLSLGSGFWHATGRHS
8562,69	8563,12 ± 0,43		28,1	41 → 115	VAFNGYFTAKARNSFISSALKSSEVDNWRIIPRNNPSSDYPSDFEVIQIKEKQKAGLLTLEDHPNIKRVTPQ***RKV***
6935	6992.77 ± 0.33	CM	20,2	94 → 153	KAGLLTLEDHPNIKRVTPQ***RKVFRSLK***YAESDPTVPCNETRWSQKWQSSRPLRRASLSLG

S1P/SKI1WT					
Theoretical MW (Da)	Experimental MW (Da)	Modification (Da)	Retention Time	Protein Domain	Sequence
13211.0847	13209.56 ± 0.3		23,6	6 → 120	DRLEKKSFEKAPCPGCSHLTLKVEFSSTVVEYEYIVAFNGYFTA KARNSFISSALKSSEVDNWRIIPRNNPSSDYPSDFEVIQIKEKQ KAGLLTLEDHPNIKRVTPQ***RKVFRSLK***
13082.9106	13081.39 ± 0.55		23,6	6 → 119	DRLEKKSFEKAPCPGCSHLTLKVEFSSTVVEYEYIVAFNGYFTA KARNSFISSALKSSEVDNWRIIPRNNPSSDYPSDFEVIQIKEKQ KAGLLTLEDHPNIKRVTPQ***RKVFRSL***
9827.0482	9827.29 ± 1.19		25,5	6 → 91	DRLEKKSFEKAPCPGCSHLTLKVEFSSTVVEYEYIVAFNGYFTA KARNSFISSALKSSEVDNWRIIPRNNPSSDYPSDFEVIQIKE
5945.8	5930,07 ± 0,19	cycling	18,9	70 → 120	IIPRNNPSSDYPSDFEVIQIKEKQKAGLLTLEDHPNIKRVTPQ***R KVFRSLK***
5945.8	5946,24 ± 0,55		18,9	70 → 120	IIPRNNPSSDYPSDFEVIQIKEKQKAGLLTLEDHPNIKRVTPQ***R KVFRSLK***
10733.0617	10734.74 ± 1.85		25,5	72 → 164	PRNNPSSDYPSDFEVIQIKEKQKAGLLTLEDHPNIKRVTPQ***RK VFRSLK***YAESDPTVPCNETRWSQKWQSSRPLRRASLSLGSGF WHATGRHS
13211.0847	10734.74 ± 1.85	CM	25,5	72 → 164	DRLEKKSFEKAPCPGCSHLTLKVEFSSTVVEYEYIVAFNGYFTA KARNSFISSALKSSEVDNWRIIPRNNPSSDYPSDFEVIQIKEKQ KAGLLTLEDHPNIKRVTPQ***RKVFRSLK***
	13269.03 ± 0.28	CM 1 CM 2	23,5	6 → 120	KAGLLTLEDHPNIKRVTPQ***RKVFRSLK***YAESDPTVPCNETRW SQKWQSSRPLRRASLSL
6934.9547	6936.64 ± 1.34		19	94 → 153	TAKARNSFISSALKSSEVDNWRIIPRNNPSSDYPSDFEVIQIKE KQKAGLLTLEDHPNIKRVTPQ***RKVFRSLK***YAESDPTVPCNET RWSQ
10360.6662	10361.62 ± 0.33		32	48 → 137	LKSSEVDNWRIIPRNNPSSDYPSDFEVIQIKEKQKAGLLTLED HPNIKRVTPQ***RKVFRSLK***YAESDPTVPCNETRWSQKWQSSR PLRRASLSLGSGFWHATGRHSSRR
12574.1659	12590.27 ± 0.47	OX	32	60 → 167	LKSSEVDNWRIIPRNNPSSDYPSDFEVIQIKEKQKAGLLTLED HPNIKRVTPQ***RKVFRSLK***YAESDPTVPCNETRWSQKWQSSR PLRRASLSLGSGFWHATGRHSSRR

Table 5.3. MALDI-TOF-MS analysis. SKI-1/S1P-BTMD (MUTANT C and WT) prodomain autoprocessing measured molecular masses.

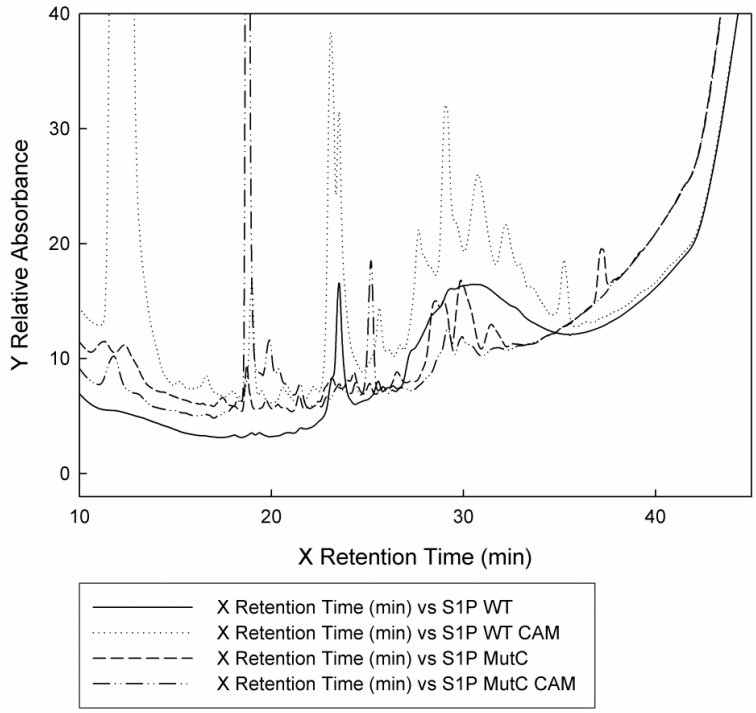

Figure 5.6 HPLC Chromatogram. ProD processing of SKI-1/S1P-BTMD (MUTANT C and WT) constructs.

Bibliography

Addy C, Ohara M, Kawai F, Kidera A, Ikeguchi M, Fuchigami S, Osawa M, Shimada I, Park SY, Tame JR, Heddle JG. Nickel binding to NikA: an additional binding site reconciles spectroscopy, calorimetry and crystallography. Acta Crystallogr D Biol Crystallogr. 2007 Feb;63(Pt 2):221-9. PubMed PMID: 17242515.

Agarwal K, Agarwal S. Helicobacter pylori vaccine: from past to future. Mayo Clin Proc. 2008 Feb;83(2):169-75. PubMed PMID: 18241627.

Andersen LP, Holck S, Janulaityte-Günther D, Kupcinskas L, Kiudelis G, Jonaitis L, Janciauskas D, Holck P, Bennedsen M, Permin H, Norn S, Wadström T. Gastric inflammatory markers and interleukins in patients with functional dyspepsia, with and without Helicobacter pylori infection. FEMS Immunol Med Microbiol. 2005 May 1;44(2):233-8. PubMed PMID: 15866221.

Andersen MT, Brøndsted L, Pearson BM, Mulholland F, Parker M, Pin C, Wells JM, Ingmer H. Diverse roles for HspR in Campylobacter jejuni revealed by the proteome, transcriptome and phenotypic characterization of an hspR mutant. Microbiology. 2005 Mar;151(Pt 3):905-15. PubMed PMID: 15758235.

Anderson DS, Adhikari P, Nowalk AJ, Chen CY, Mietzner TA. The hFbpABC transporter from Haemophilus influenzae functions as a binding-protein-dependent ABC transporter with high specificity and affinity for ferric iron. J Bacteriol. 2004 Sep;186(18):6220-9. PubMed PMID: 15342592; PubMed Central PMCID: PMC515168.

Andrutis KA, Fox JG, Schauer DB, Marini RP, Li X, Yan L, Josenhans C, Suerbaum S. Infection of the ferret stomach by isogenic flagellar mutant strains of Helicobacter mustelae. Infect Immun. 1997 May;65(5):1962-6. PubMed PMID: 9125590; PubMed Central PMCID: PMC175254.

Angelakopoulos H, Hohmann EL. Pilot study of phoP/phoQ-deleted Salmonella enterica serovar typhimurium expressing Helicobacter pylori urease in adult volunteers. Infect Immun. 2000 Apr;68(4):2135-41. PubMed PMID: 10722611; PubMed Central PMCID: PMC97395.

Arnold K, Bordoli L, Kopp J, Schwede T. The SWISS-MODEL workspace: a web-based environment for protein structure homology modelling. Bioinformatics. 2006 Jan 15;22(2):195-201. PubMed PMID: 16301204.

Banaszak K, Martin-Diaconescu V, Bellucci M, Zambelli B, Rypniewski W, Maroney MJ, Ciurli S. Crystallographic and X-ray absorption spectroscopic characterization of Helicobacter pylori UreE bound to Ni^{2+} and Zn^{2+} reveals a role for the disordered C-terminal arm in metal trafficking. Biochem J. 2012 Feb 1;441(3):1017-26. PubMed PMID: 22010876; PubMed Central PMCID: PMC3501991.

Bardhan KD, Bjarnason I, Scott DL, Griffin WM, Fenn GC, Shield MJ, Morant SV. The prevention and healing of acute non-steroidal anti-inflammatory drug-associated gastroduodenal mucosal damage by misoprostol. Br J Rheumatol. 1993 Nov;32(11):990-5. PubMed PMID: 8220939.

Basso D, Zambon CF, Letley DP, Stranges A, Marchet A, Rhead JL, Schiavon S, Guariso G, Ceroti M, Nitti D, Rugge M, Plebani M, Atherton JC. Clinical relevance of Helicobacter pylori cagA and vacA gene polymorphisms. Gastroenterology. 2008 Jul;135(1):91-9. PubMed PMID: 18474244.

Bauerfeind P, Garner RM, Mobley LT. Allelic exchange mutagenesis of nixA in Helicobacter pylori results in reduced nickel transport and urease activity. Infect Immun. 1996 Jul;64(7):2877-80. PubMed PMID: 8698529; PubMed Central PMCID: PMC174160.

Belzer C, Stoof J, Beckwith CS, Kuipers EJ, Kusters JG, van Vliet AH. Differential regulation of urease activity in Helicobacter hepaticus and Helicobacter pylori. Microbiology. 2005 Dec;151(Pt 12):3989-95. PubMed PMID: 16339943.

Benoit S, Maier RJ. Dependence of Helicobacter pylori urease activity on the nickel-sequestering ability of the UreE accessory protein. J Bacteriol. 2003 Aug;185(16):4787-95. PubMed PMID: 12896998; PubMed Central PMCID: PMC166491.

Benoit SL, Mehta N, Weinberg MV, Maier C, Maier RJ. Interaction between the Helicobacter pylori accessory proteins HypA and UreE is needed for urease maturation. Microbiology. 2007 May;153(Pt 5):1474-82. PubMed PMID: 17464061; PubMed Central PMCID: PMC2553680.

Benoit SL, Maier RJ. Mua (HP0868) is a nickel-binding protein that modulates urease activity in Helicobacter pylori. MBio. 2011;2(2):e00039-11. PubMed PMID: 21505055; PubMed Central PMCID: PMC3086059.

Benoit SL, Zbell AL, Maier RJ. Nickel enzyme maturation in Helicobacter hepaticus: roles of accessory proteins in hydrogenase and urease activities. Microbiology. 2007 Nov;153(Pt 11):3748-56. PubMed PMID: 17975083; PubMed Central PMCID: PMC2562792.

Benoit SL, Maier RJ. Hydrogen and nickel metabolism in helicobacter species. Ann N Y Acad Sci. 2008 Mar;1125:242-51. PubMed PMID: 18378596.

Benoit SL, McMurry JL, Hill SA, Maier RJ. Helicobacter pylori hydrogenase accessory protein HypA and urease accessory protein UreG compete with each other for UreE recognition. Biochim Biophys Acta. 2012 Oct;1820(10):1519-25. PubMed PMID: 22698670.

Benoit SL, Miller EF, Maier RJ. Helicobacter pylori stores nickel to aid its host colonization. Infect Immun. 2013 Feb;81(2):580-4. PubMed PMID: 23230291; PubMed Central PMCID: PMC3553817.

Beyer WR, Pöpplau D, Garten W, von Laer D, Lenz O. Endoproteolytic processing of the lymphocytic choriomeningitis virus glycoprotein by the subtilase SKI-1/S1P. J Virol. 2003 Mar;77(5):2866-72. PubMed PMID: 12584310; PubMed Central PMCID: PMC149737.

Bina JE, Alm RA, Uria-Nickelsen M, Thomas SR, Trust TJ, Hancock RE. Helicobacter pylori uptake and efflux: basis for intrinsic susceptibility to antibiotics in vitro. Antimicrob Agents Chemother. 2000 Feb;44(2):248-54. PubMed PMID: 10639345; PubMed Central PMCID: PMC89666.

Blaser MJ. Helicobacters are indigenous to the human stomach: duodenal ulceration is due to changes in gastric microecology in the modern era. Gut. 1998 Nov;43(5):721-7. PubMed PMID: 9824358; PubMed Central PMCID: PMC1727310.

Bodvard K, Mohlin J, Knecht W. Recombinant expression, purification, and kinetic and inhibitor characterisation of human site-1-protease. Protein Expr Purif. 2007 Feb;51(2):308-19. PubMed PMID: 16973377.

Boncristiano M, Paccani SR, Barone S, Ulivieri C, Patrussi L, Ilver D, Amedei A, D'Elios MM, Telford JL, Baldari CT. The Helicobacter pylori vacuolating toxin inhibits T cell activation by two independent mechanisms. J Exp Med. 2003 Dec 15;198(12):1887-97. PubMed PMID: 14676300; PubMed Central PMCID: PMC2194151.

Brown MS, Goldstein JL. A proteolytic pathway that controls the cholesterol content of membranes, cells, and blood. Proc Natl Acad Sci U S A. 1999 Sep 28;96(20):11041-8. PubMed PMID: 10500120; PubMed Central PMCID: PMC34238.

Bruggraber SF, French G, Thompson RP, Powell JJ. Selective and effective bactericidal activity of the cobalt (II) cation against Helicobacter pylori. Helicobacter. 2004 Oct;9(5):422-8. PubMed PMID: 15361081.

Bucca G, Ferina G, Puglia AM, Smith CP. The dnaK operon of Streptomyces coelicolor encodes a novel heat-shock protein which binds to the promoter region of the operon. Mol Microbiol. 1995 Aug;17(4):663-74. PubMed PMID: 8801421.

Bukau B. Regulation of the Escherichia coli heat-shock response. Mol Microbiol. 1993 Aug;9(4):671-80. PubMed PMID: 7901731.

Bumann D, Metzger WG, Mansouri E, Palme O, Wendland M, Hurwitz R, Haas G, Aebischer T, von Specht BU, Meyer TF. Safety and immunogenicity of live recombinant Salmonella enterica serovar Typhi Ty21a expressing urease A and B from Helicobacter pylori in human volunteers. Vaccine. 2001 Dec 12;20(5-6):845-52. PubMed PMID: 11738748.

Cavazza C, Martin L, Laffly E, Lebrette H, Cherrier MV, Zeppieri L, Richaud P, Carrière M, Fontecilla-Camps JC. Histidine 416 of the periplasmic binding protein NikA is essential for nickel uptake in Escherichia coli. FEBS Lett. 2011 Feb 18;585(4):711-5. PubMed PMID: 21281641.

Censini S, Lange C, Xiang Z, Crabtree JE, Ghiara P, Borodovsky M, Rappuoli R, Covacci A. cag, a pathogenicity island of Helicobacter pylori, encodes type I-specific and disease-associated virulence factors. Proc Natl Acad Sci U S A. 1996 Dec 10;93(25):14648-53. PubMed PMID: 8962108; PubMed Central PMCID: PMC26189.

Cheng D, Espenshade PJ, Slaughter CA, Jaen JC, Brown MS, Goldstein JL. Secreted site-1 protease cleaves peptides corresponding to luminal loop of sterol regulatory element-binding proteins. J Biol Chem. 1999 Aug 6;274(32):22805-12. PubMed PMID: 10428865.

Cheng T, Li H, Xia W, Sun H. Multifaceted SlyD from Helicobacter pylori: implication in [NiFe] hydrogenase maturation. J Biol Inorg Chem. 2012 Mar;17(3):331-43. PubMed PMID: 22045417; PubMed Central PMCID: PMC3292732.

Cherrier MV, Martin L, Cavazza C, Jacquamet L, Lemaire D, Gaillard J, Fontecilla-Camps JC. Crystallographic and spectroscopic evidence for high affinity binding of FeEDTA(H2O)- to the periplasmic nickel transporter NikA. J Am Chem Soc. 2005 Jul 20;127(28):10075-82. PubMed PMID: 16011372.

Cherrier MV, Cavazza C, Bochot C, Lemaire D, Fontecilla-Camps JC. Structural characterization of a putative endogenous metal chelator in the periplasmic nickel transporter NikA. Biochemistry. 2008 Sep 23;47(38):9937-43. PubMed PMID: 18759453.

Chivers PT, Benanti EL, Heil-Chapdelaine V, Iwig JS, Rowe JL. Identification of Ni-(L-His)$_2$ as a substrate for NikABCDE-dependent nickel uptake in Escherichia coli. Metallomics. 2012 Oct;4(10):1043-50. PubMed PMID: 22885853.

Chu BC, Vogel HJ. A structural and functional analysis of type III periplasmic and substrate binding proteins: their role in bacterial siderophore and heme transport. Biol Chem. 2011 Jan;392(1-2):39-52. PubMed PMID: 21194366.

Clarke TE, Rohrbach MR, Tari LW, Vogel HJ, Köster W. Ferric hydroxamate binding protein FhuD from Escherichia coli: mutants in conserved and non-conserved regions. Biometals. 2002 Jun;15(2):121-31. PubMed PMID: 12046920.

Clarke TE, Braun V, Winkelmann G, Tari LW, Vogel HJ. X-ray crystallographic structures of the Escherichia coli periplasmic protein FhuD bound to hydroxamate-type siderophores and the antibiotic albomycin. J Biol Chem. 2002 Apr 19;277(16):13966-72. PubMed PMID: 11805094.

Clarke TE, Tari LW, Vogel HJ. Structural biology of bacterial iron uptake systems. Curr Top Med Chem. 2001 May;1(1):7-30. PubMed PMID: 11895294.

Cole C, Barber JD, Barton GJ. The Jpred 3 secondary structure prediction server. Nucleic Acids Res. 2008 Jul 1;36(Web Server issue):W197-201. PubMed PMID: 18463136; PubMed Central PMCID: PMC2447793.

Colland F, Rain JC, Gounon P, Labigne A, Legrain P, De Reuse H. Identification of the Helicobacter pylori anti-sigma28 factor. Mol Microbiol. 2001 Jul;41(2):477-87. PubMed PMID: 11489132.

Contreras M, Thiberge JM, Mandrand-Berthelot MA, Labigne A. Characterization of the roles of NikR, a nickel-responsive pleiotropic autoregulator of Helicobacter pylori. Mol Microbiol. 2003 Aug;49(4):947-63. PubMed PMID: 12890020.

Couture F, D'Anjou F, Desjardins R, Boudreau F, Day R. Role of proprotein convertases in prostate cancer progression. Neoplasia. 2012 Nov;14(11):1032-42. PubMed PMID: 23226097; PubMed Central PMCID: PMC3514743.

Covacci A, Censini S, Bugnoli M, Petracca R, Burroni D, Macchia G, Massone A, Papini E, Xiang Z, Figura N. Molecular characterization of the 128-kDa immunodominant antigen of Helicobacter pylori associated with cytotoxicity and duodenal ulcer. Proc Natl Acad Sci U S A. 1993 Jun 15;90(12):5791-5. PubMed PMID: 8516329; PubMed Central PMCID: PMC46808.

Cover TL, Blaser MJ. Purification and characterization of the vacuolating toxin from Helicobacter pylori. J Biol Chem. 1992 May 25;267(15):10570-5. PubMed PMID: 1587837.

Cover TL, Hanson PI, Heuser JE. Acid-induced dissociation of VacA, the Helicobacter pylori vacuolating cytotoxin, reveals its pattern of assembly. J Cell Biol. 1997 Aug 25;138(4):759-69. PubMed PMID: 9265644; PubMed Central PMCID: PMC2138037.

Cover TL, Blaser MJ. Helicobacter pylori in health and disease. Gastroenterology. 2009 May;136(6):1863-73. PubMed PMID: 19457415; PubMed Central PMCID: PMC3644425.

Craig EA, Gambill BD, Nelson RJ. Heat shock proteins: molecular chaperones of protein biogenesis. Microbiol Rev. 1993 Jun;57(2):402-14. PubMed PMID: 8336673; PubMed Central PMCID: PMC372916.

Craig TA, Lutz WH, Kumar R. Association of prokaryotic and eukaryotic chaperone proteins with the human 1alpha,25-dihydroxyvitamin D(3) receptor. Biochem Biophys Res Commun. 1999 Jul 5;260(2):446-52. PubMed PMID: 10403788.

Creemers JW, Ines Dominguez D, Plets E, Serneels L, Taylor NA, Multhaup G, Craessaerts K, Annaert W, De Strooper B. Processing of beta-secretase by furin and other members of the proprotein convertase family. J Biol Chem. 2001 Feb 9;276(6):4211-7. PubMed PMID: 11071887.

Cun S, Li H, Ge R, Lin MC, Sun H. A histidine-rich and cysteine-rich metal-binding domain at the C terminus of heat shock protein A from Helicobacter pylori: implication for nickel homeostasis and bismuth susceptibility. J Biol Chem. 2008 May 30;283(22):15142-51. PubMed PMID: 18364351; PubMed Central PMCID: PMC3258894.

D'Elios MM, Andersen LP. Helicobacter pylori inflammation, immunity, and vaccines. Helicobacter. 2007 Oct;12 Suppl 1:15-9. PubMed PMID: 17727455.

Davis GS, Flannery EL, Mobley HL. Helicobacter pylori HP1512 is a nickel-responsive NikR-regulated outer membrane protein. Infect Immun. 2006 Dec;74(12):6811-20. PubMed PMID: 17030579; PubMed Central PMCID: PMC1698071.

de Pina K, Navarro C, McWalter L, Boxer DH, Price NC, Kelly SM, Mandrand-Berthelot MA, Wu LF. Purification and characterization of the periplasmic nickel-binding protein NikA of Escherichia coli K12. Eur J Biochem. 1995 Feb 1;227(3):857-65. PubMed PMID: 7867647.

de Reuse H, Vinella D, Cavazza C. Common themes and unique proteins for the uptake and trafficking of nickel, a metal essential for the virulence of Helicobacter pylori. Front Cell Infect Microbiol. 2013 Dec 9;3:94. PubMed PMID: 24367767; PubMed Central PMCID: PMC3856676.

Delany I, Spohn G, Rappuoli R, Scarlato V. The Fur repressor controls transcription of iron-activated and -repressed genes in Helicobacter pylori. Mol Microbiol. 2001 Dec;42(5):1297-309. PubMed PMID: 11886560.

Dian C, Vitale S, Leonard GA, Bahlawane C, Fauquant C, Leduc D, Muller C, de Reuse H, Michaud-Soret I, Terradot L. The structure of the Helicobacter pylori ferric uptake regulator Fur reveals three functional metal binding sites. Mol Microbiol. 2011 Mar;79(5):1260-75. PubMed PMID: 21208302.

DiPetrillo MD, Tibbetts T, Kleanthous H, Killeen KP, Hohmann EL. Safety and immunogenicity of phoP/phoQ-deleted Salmonella typhi expressing Helicobacter pylori urease in adult volunteers. Vaccine. 1999 Oct 14;18(5-6):449-59. PubMed PMID: 10519934.

Dosanjh NS, Michel SL. Microbial nickel metalloregulation: NikRs for nickel ions. Curr Opin Chem Biol. 2006 Apr;10(2):123-30. PubMed PMID: 16504569.

Eaton KA, Radin MJ, Kramer L, Wack R, Sherding R, Krakowka S, Morgan DR. Gastric spiral bacilli in captive cheetahs. Scand J Gastroenterol Suppl. 1991;181:38-42. PubMed PMID: 1866593.

Eaton KA, Brooks CL, Morgan DR, Krakowka S. Essential role of urease in pathogenesis of gastritis induced by Helicobacter pylori in gnotobiotic piglets. Infect Immun. 1991 Jul;59(7):2470-5. PubMed PMID: 2050411; PubMed Central PMCID: PMC258033.

Eitinger T, Mandrand-Berthelot MA. Nickel transport systems in microorganisms. Arch Microbiol. 2000 Jan;173(1):1-9. PubMed PMID: 10648098.

Elagoz A, Benjannet S, Mammarbassi A, Wickham L, Seidah NG. Biosynthesis and cellular trafficking of the convertase SKI-1/S1P: ectodomain shedding requires SKI-1 activity. J Biol Chem. 2002 Mar 29;277(13):11265-75. PubMed PMID: 11756446.

Englert DL, Adase CA, Jayaraman A, Manson MD. Repellent taxis in response to nickel ion requires neither Ni2+ transport nor the periplasmic NikA binding protein. J Bacteriol. 2010 May;192(10):2633-7. PubMed PMID: 20233931; PubMed Central PMCID: PMC2863559.

Ernst FD, Kuipers EJ, Heijens A, Sarwari R, Stoof J, Penn CW, Kusters JG, van Vliet AH. The nickel-responsive regulator NikR controls activation and repression of gene transcription in Helicobacter pylori. Infect Immun. 2005 Nov;73(11):7252-8. PubMed PMID: 16239520; PubMed Central PMCID: PMC1273850.

Ernst FD, Stoof J, Horrevoets WM, Kuipers EJ, Kusters JG, van Vliet AH. NikR mediates nickel-responsive transcriptional repression of the Helicobacter pylori outer membrane proteins FecA3 (HP1400) and FrpB4 (HP1512). Infect Immun. 2006 Dec;74(12):6821-8. PubMed PMID: 17015456; PubMed Central PMCID: PMC1698083.

Evans DG, Evans DJ Jr, Graham DY. Adherence and internalization of Helicobacter pylori by HEp-2 cells. Gastroenterology. 1992 May;102(5):1557-67. PubMed PMID: 1568565.

Evans DJ Jr, Evans DG, Engstrand L, Graham DY. Urease-associated heat shock protein of Helicobacter pylori. Infect Immun. 1992 May;60(5):2125-7. PubMed PMID: 1348725; PubMed Central PMCID: PMC257126.

Evans DJ Jr, Evans DG, Lampert HC, Nakano H. Identification of four new prokaryotic bacterioferritins, from Helicobacter pylori, Anabaena variabilis, Bacillus subtilis and Treponema pallidum, by analysis of gene sequences. Gene. 1995 Feb 3;153(1):123-7. PubMed PMID: 7883175.

Evans P. Scaling and assessment of data quality. Acta Crystallogr D Biol Crystallogr. 2006 Jan;62(Pt 1):72-82. PubMed PMID: 16369096.

Farinha P, Gascoyne RD. Molecular pathogenesis of mucosa-associated lymphoid tissue lymphoma. J Clin Oncol. 2005 Sep 10;23(26):6370-8. PubMed PMID: 16155022.

Fauquant C, Diederix RE, Rodrigue A, Dian C, Kapp U, Terradot L, Mandrand-Berthelot MA, Michaud-Soret I. pH dependent Ni(II) binding and aggregation of Escherichia coli and Helicobacter pylori NikR. Biochimie. 2006 Nov;88(11):1693-705. PubMed PMID: 16930800.

Fiedorek SC, Casteel HB, Pumphrey CL, Evans DJ Jr, Evans DG, Klein PD, Graham DY. The role of Helicobacter pylori in recurrent, functional abdominal pain in children. Am J Gastroenterol. 1992 Mar;87(3):347-9. PubMed PMID: 1539570.

Fong YH, Wong HC, Chuck CP, Chen YW, Sun H, Wong KB. Assembly of preactivation complex for urease maturation in Helicobacter pylori: crystal structure of UreF-UreH protein complex. J Biol Chem. 2011 Dec 16;286(50):43241-9. PubMed PMID: 22013070; PubMed Central PMCID: PMC3234868.

Fong YH, Wong HC, Yuen MH, Lau PH, Chen YW, Wong KB. Structure of UreG/UreF/UreH complex reveals how urease accessory proteins facilitate maturation of Helicobacter pylori urease. PLoS Biol. 2013 Oct;11(10):e1001678. PubMed PMID: 24115911; PubMed Central PMCID: PMC3792862.

Fugère M, Day R. Cutting back on pro-protein convertases: the latest approaches to pharmacological inhibition. Trends Pharmacol Sci. 2005 Jun;26(6):294-301. PubMed PMID: 15925704.

Fulkerson JF Jr, Garner RM, Mobley HL. Conserved residues and motifs in the NixA protein of Helicobacter pylori are critical for the high affinity transport of nickel ions. J Biol Chem. 1998 Jan 2;273(1):235-41. PubMed PMID: 9417070.

Fulkerson JF Jr, Mobley HL. Membrane topology of the NixA nickel transporter of Helicobacter pylori: two nickel transport-specific motifs within transmembrane helices II and III. J Bacteriol. 2000 Mar;182(6):1722-30. PubMed PMID: 10692379; PubMed Central PMCID: PMC94471.

Galmiche A, Rassow J, Doye A, Cagnol S, Chambard JC, Contamin S, de Thillot V, Just I, Ricci V, Solcia E, Van Obberghen E, Boquet P. The N-terminal 34 kDa fragment of Helicobacter pylori vacuolating cytotoxin targets mitochondria and induces cytochrome c release. EMBO J. 2000 Dec 1;19(23):6361-70. PubMed PMID: 11101509; PubMed Central PMCID: PMC305856.

Garcia-Herrero A, Peacock RS, Howard SP, Vogel HJ. The solution structure of the periplasmic domain of the TonB system ExbD protein reveals an unexpected structural homology with siderophore-binding proteins. Mol Microbiol. 2007 Nov;66(4):872-89. PubMed PMID: 17927700.

Ge R, Watt RM, Sun X, Tanner JA, He QY, Huang JD, Sun H. Expression and characterization of a histidine-rich protein, Hpn: potential for Ni2+ storage in Helicobacter pylori. Biochem J. 2006 Jan 1;393(Pt 1):285-93. PubMed PMID: 16164421; PubMed Central PMCID: PMC1383687.

Ge RG, Wang DX, Hao MC, Sun XS. Nickel trafficking system responsible for urease maturation in Helicobacter pylori. World J Gastroenterol. 2013 Dec 7;19(45):8211-8218. PubMed PMID: 24363511; PubMed Central PMCID: PMC3857443.

Geis G, Suerbaum S, Forsthoff B, Leying H, Opferkuch W. Ultrastructure and biochemical studies of the flagellar sheath of Helicobacter pylori. J Med Microbiol. 1993 May;38(5):371-7. PubMed PMID: 8487294.

Gilbert JV, Ramakrishna J, Sunderman FW Jr, Wright A, Plaut AG. Protein Hpn: cloning and characterization of a histidine-rich metal-binding polypeptide in Helicobacter pylori and Helicobacter mustelae. Infect Immun. 1995 Jul;63(7):2682-8. PubMed PMID: 7790085; PubMed Central PMCID: PMC173359.

Gilbreath JJ, Pich OQ, Benoit SL, Besold AN, Cha JH, Maier RJ, Michel SL, Maynard EL, Merrell DS. Random and site-specific mutagenesis of the Helicobacter pylori ferric uptake regulator provides insight into Fur structure-function relationships. Mol Microbiol. 2013 Jul;89(2):304-23. PubMed PMID: 23710935; PubMed Central PMCID: PMC3713617.

González-Pedrajo B, Minamino T, Kihara M, Namba K. Interactions between C ring proteins and export apparatus components: a possible mechanism for facilitating type III protein export. Mol Microbiol. 2006 May;60(4):984-98. PubMed PMID: 16677309.

Goodwin CS, Bell B, McCullough C, Turner M. Sensitivity of Campylobacter pylori to colloidal bismuth subcitrate. J Clin Pathol. 1989 Feb;42(2):216-7. PubMed PMID: 2921366; PubMed Central PMCID: PMC1141833.

Goodwin CS, McCulloch RK, Armstrong JA, Wee SH. Unusual cellular fatty acids and distinctive ultrastructure in a new spiral bacterium (Campylobacter pyloridis) from the human gastric mucosa. J Med Microbiol. 1985 Apr;19(2):257-67. PubMed PMID: 3981612.

Graham DY, Go MF, Evans DJ Jr. Review article: urease, gastric ammonium/ammonia, and Helicobacter pylori--the past, the present, and recommendations for future research. Aliment Pharmacol Ther. 1992 Dec;6(6):659-69. PubMed PMID: 1486153.

Graham DY, Lew GM, Klein PD, Evans DG, Evans DJ Jr, Saeed ZA, Malaty HM. Effect of treatment of Helicobacter pylori infection on the long-term recurrence of gastric or duodenal ulcer A randomized, controlled study. Ann Intern Med. 1992 May 1;116(9):705-8. PubMed PMID: 1558340.

Graham DY, Lew GM, Malaty HM, Evans DG, Evans DJ Jr, Klein PD, Alpert LC, Genta RM. Factors influencing the eradication of Helicobacter pylori with triple therapy. Gastroenterology. 1992 Feb;102(2):493-6. PubMed PMID: 1732120.

Groeger W, Köster W. Transmembrane topology of the two FhuB domains representing the hydrophobic components of bacterial ABC transporters involved in the uptake of siderophores, haem and vitamin B12. Microbiology. 1998 Oct;144 (Pt 10):2759-69. PubMed PMID: 9802017.

Ha NC, Oh ST, Sung JY, Cha KA, Lee MH, Oh BH. Supramolecular assembly and acid resistance of Helicobacter pylori urease. Nat Struct Biol. 2001 Jun;8(6):505-9. PubMed PMID: 11373617.

Haas R, Meyer TF, van Putten JP. Aflagellated mutants of Helicobacter pylori generated by genetic transformation of naturally competent strains using transposon shuttle mutagenesis. Mol Microbiol. 1993 May;8(4):753-60. PubMed PMID: 8332066.

Hatakeyama M. The role of Helicobacter pylori CagA in gastric carcinogenesis. Int J Hematol. 2006 Nov;84(4):301-8. PubMed PMID: 17118755.

Hatakeyama M. Helicobacter pylori causes gastric cancer by hijacking cell growth signaling. Discov Med. 2004 Dec;4(24):476-81. PubMed PMID: 20704951.

Hatakeyama M, Higashi H. Helicobacter pylori CagA: a new paradigm for bacterial carcinogenesis. Cancer Sci. 2005 Dec;96(12):835-43. PubMed PMID: 16367902.

Hatakeyama M. Helicobacter pylori and gastric carcinogenesis. J Gastroenterol. 2009;44(4):239-48. PubMed PMID: 19271114.

Hazell SL, Eichberg JW, Lee DR, Alpert L, Evans DG, Evans DJ Jr, Graham DY. Selection of the chimpanzee over the baboon as a model for Helicobacter pylori infection. Gastroenterology. 1992 Sep;103(3):848-54. PubMed PMID: 1499934.

Heddle J, Scott DJ, Unzai S, Park SY, Tame JR. Crystal structures of the liganded and unliganded nickel-binding protein NikA from Escherichia coli. J Biol Chem. 2003 Dec 12;278(50):50322-9. PubMed PMID: 12960164.

Hendricks JK, Mobley HL. Helicobacter pylori ABC transporter: effect of allelic exchange mutagenesis on urease activity. J Bacteriol. 1997 Sep;179(18):5892-902. PubMed PMID: 9294450; PubMed Central PMCID: PMC179482.

Herbst RW, Perovic I, Martin-Diaconescu V, O'Brien K, Chivers PT, Pochapsky SS, Pochapsky TC, Maroney MJ. Communication between the zinc and nickel sites in dimeric HypA: metal recognition and pH sensing. J Am Chem Soc. 2010 Aug 4;132(30):10338-51. PubMed PMID: 20662514; PubMed Central PMCID: PMC2934764.

Heyl KA, Fischer A, Göbel UB, Henklein P, Heimesaat MM, Bereswill S. Inhibition of Helicobacter pylori urease activity in vivo by the synthetic nickel binding protein Hpn. Eur J Microbiol Immunol (Bp). 2013 Mar;3(1):77-80. PubMed PMID: 24265922; PubMed Central PMCID: PMC3832076.

Higashi H, Tsutsumi R, Muto S, Sugiyama T, Azuma T, Asaka M, Hatakeyama M. SHP-2 tyrosine phosphatase as an intracellular target of Helicobacter pylori CagA protein. Science. 2002 Jan 25;295(5555):683-6. PubMed PMID: 11743164.

Higgins KA, Carr CE, Maroney MJ. Specific metal recognition in nickel trafficking. Biochemistry. 2012 Oct 9;51(40):7816-32. PubMed PMID: 22970729; PubMed Central PMCID: PMC3502001.

Ho WW, Li H, Eakanunkul S, Tong Y, Wilks A, Guo M, Poulos TL. Holo- and apo-bound structures of bacterial periplasmic heme-binding proteins. J Biol Chem. 2007 Dec 7;282(49):35796-802. PubMed PMID: 17925389.

Hoffman PS, Vats N, Hutchison D, Butler J, Chisholm K, Sisson G, Raudonikiene A, Marshall JS, Veldhuyzen van Zanten SJ. Development of an interleukin-12-deficient mouse model that is permissive for colonization by a motile KE26695 strain of Helicobacter pylori. Infect Immun. 2003 May;71(5):2534-41. PubMed PMID: 12704125; PubMed Central PMCID: PMC153236.

Homma M, Iino T, Kutsukake K, Yamaguchi S. In vitro reconstitution of flagellar filaments onto hooks of filamentless mutants of Salmonella typhimurium by addition of hook-associated proteins. Proc Natl Acad Sci U S A. 1986 Aug;83(16):6169-73. PubMed PMID: 3526353; PubMed Central PMCID: PMC386461.

Homma M, DeRosier DJ, Macnab RM. Flagellar hook and hook-associated proteins of Salmonella typhimurium and their relationship to other axial components of the flagellum. J Mol Biol. 1990 Jun 20;213(4):819-32. PubMed PMID: 2193164.

Homma M, Kutsukake K, Iino T, Yamaguchi S. Hook-associated proteins essential for flagellar filament formation in Salmonella typhimurium. J Bacteriol. 1984 Jan;157(1):100-8. PubMed PMID: 6360991; PubMed Central PMCID: PMC215136.

Hosaka M, Nagahama M, Kim WS, Watanabe T, Hatsuzawa K, Ikemizu J, Murakami K, Nakayama K. Arg-X-Lys/Arg-Arg motif as a signal for precursor cleavage catalyzed by furin within the constitutive secretory pathway. J Biol Chem. 1991 Jul 5;266(19):12127-30. PubMed PMID: 1905715.

Howlett RM, Hughes BM, Hitchcock A, Kelly DJ. Hydrogenase activity in the foodborne pathogen Campylobacter jejuni depends upon a novel ABC-type nickel transporter (NikZYXWV) and is SlyD-independent. Microbiology. 2012 Jun;158(Pt 6):1645-55. PubMed PMID: 22403188.

Hu LT, Mobley HL. Expression of catalytically active recombinant Helicobacter pylori urease at wild-type levels in Escherichia coli. Infect Immun. 1993 Jun;61(6):2563-9. PubMed PMID: 8500893; PubMed Central PMCID: PMC280885.

Hu Y, Jiang F, Guo Y, Shen X, Zhang Y, Zhang R, Guo G, Mao X, Zou Q, Wang DC. Crystal structure of HugZ, a novel heme oxygenase from Helicobacter pylori. J Biol Chem. 2011 Jan 14;286(2):1537-44. PubMed PMID: 21030596; PubMed Central PMCID: PMC3020762.

Imada K, Minamino T, Kinoshita M, Furukawa Y, Namba K. Structural insight into the regulatory mechanisms of interactions of the flagellar type III chaperone FliT with its binding partners. Proc Natl Acad Sci U S A. 2010 May 11;107(19):8812-7. PubMed PMID: 20421493; PubMed Central PMCID: PMC2889304.

Jin UH, Chung TW, Lee YC, Ha SD, Kim CH. Molecular cloning and functional expression of the rfaE gene required for lipopolysaccharide biosynthesis in Salmonella typhimurium. Glycoconj J. 2001 Oct;18(10):779-87. PubMed PMID: 12441667.

Jones AC, Logan RP, Foynes S, Cockayne A, Wren BW, Penn CW. A flagellar sheath protein of Helicobacter pylori is identical to HpaA, a putative N-acetylneuraminyllactose-binding hemagglutinin, but is not an adhesin for AGS cells. J Bacteriol. 1997 Sep;179(17):5643-7. PubMed PMID: 9287032; PubMed Central PMCID: PMC179448.

Josenhans C, Labigne A, Suerbaum S. Comparative ultrastructural and functional studies of Helicobacter pylori and Helicobacter mustelae flagellin mutants: both flagellin subunits, FlaA and FlaB, are necessary for full motility in Helicobacter species. J Bacteriol. 1995 Jun;177(11):3010-20. PubMed PMID: 7768796; PubMed Central PMCID: PMC176987.

Jubier-Maurin V, Rodrigue A, Ouahrani-Bettache S, Layssac M, Mandrand-Berthelot MA, Köhler S, Liautard JP. Identification of the nik gene cluster of Brucella suis: regulation and contribution to urease activity. J Bacteriol. 2001 Jan;183(2):426-34. PubMed PMID: 11133934; PubMed Central PMCID: PMC94896.

Kang JM, Iovine NM, Blaser MJ. A paradigm for direct stress-induced mutation in prokaryotes. FASEB J. 2006 Dec;20(14):2476-85. PubMed PMID: 17142797.

Kansau I, Labigne A. Heat shock proteins of Helicobacter pylori. Aliment Pharmacol Ther. 1996 Apr;10 Suppl 1:51-6. PubMed PMID: 8730259.

Kansau I, Guillain F, Thiberge JM, Labigne A. Nickel binding and immunological properties of the C-terminal domain of the Helicobacter pylori GroES homologue (HspA). Mol Microbiol. 1996 Dec;22(5):1013-23. PubMed PMID: 8971721.

Kao CY, Sheu BS, Sheu SM, Yang HB, Chang WL, Cheng HC, Wu JJ. Higher motility enhances bacterial density and inflammatory response in dyspeptic patients infected with Helicobacter pylori. Helicobacter. 2012 Dec;17(6):411-6. PubMed PMID: 23066970.

Karpowich NK, Huang HH, Smith PC, Hunt JF. Crystal structures of the BtuF periplasmic-binding protein for vitamin B12 suggest a functionally important reduction in protein mobility upon ligand binding. J Biol Chem. 2003 Mar 7;278(10):8429-34. PubMed PMID: 12468528.

Kavermann H, Burns BP, Angermuller K, Odenbreit S, Fischer W, Melchers K, Haas R. Identification and characterization of Helicobacter pylori genes essential for gastric colonization. J Exp Med. 2003 Apr 7;197(7):813-22. PubMed PMID: 12668646; PubMed Central PMCID: PMC2193887.

Kawagishi I, Homma M, Williams AW, Macnab RM. Characterization of the flagellar hook length control protein fliK of Salmonella typhimurium and Escherichia coli. J Bacteriol. 1996 May;178(10):2954-9. PubMed PMID: 8631687; PubMed Central PMCID: PMC178034.

Kersulyte D, Mukhopadhyay AK, Shirai M, Nakazawa T, Berg DE. Functional organization and insertion specificity of IS607, a chimeric element of Helicobacter pylori. J Bacteriol. 2000 Oct;182(19):5300-8. PubMed PMID: 10986230; PubMed Central PMCID: PMC110970.

Khatib AM, Siegfried G, Chrétien M, Metrakos P, Seidah NG. Proprotein convertases in tumor progression and malignancy: novel targets in cancer therapy. Am J Pathol. 2002 Jun;160(6):1921-35. PubMed PMID: 12057895; PubMed Central PMCID: PMC1850825.

Klein PD, Graham DY, Gaillour A, Opekun AR, Smith EO. Water source as risk factor for Helicobacter pylori infection in Peruvian children Gastrointestinal Physiology Working Group. Lancet. 1991 Jun 22;337(8756):1503-6. PubMed PMID: 1675369.

Krakowka S, Eaton KA, Rings DM, Morgan DR. Gastritis induced by Helicobacter pylori in gnotobiotic piglets. Rev Infect Dis. 1991 Jul-Aug;13 Suppl 8:S681-5. PubMed PMID: 1925308.

Krewulak KD, Vogel HJ. TonB or not TonB: is that the question?. Biochem Cell Biol. 2011 Apr;89(2):87-97. PubMed PMID: 21455261.

Krukonis ES, Yu RR, Dirita VJ. The Vibrio cholerae ToxR/TcpP/ToxT virulence cascade: distinct roles for two membrane-localized transcriptional activators on a single promoter. Mol Microbiol. 2000 Oct;38(1):67-84. PubMed PMID: 11029691.

Kubori T, Shimamoto N, Yamaguchi S, Namba K, Aizawa S. Morphological pathway of flagellar assembly in Salmonella typhimurium. J Mol Biol. 1992 Jul 20;226(2):433-46. PubMed PMID: 1640458.

Kuo WT, Chin KH, Lo WT, Wang AH, Chou SH. Crystal structure of the C-terminal domain of a flagellar hook-capping protein from Xanthomonas campestris. J Mol Biol. 2008 Aug 1;381(1):189-99. PubMed PMID: 18599076.

Kurihara N, Kamiya S, Yamaguchi H, Osaki T, Shinohara H, Kitahora T, Ishida H, Ozawa A, Otani Y, Kubota T, Kumai K, Kitajima M. Characteristics of Helicobacter pylori strains isolated from patients with different gastric diseases. J Gastroenterol. 1998;33 Suppl 10:10-3. PubMed PMID: 9840009.

Kutsukake K, Minamino T, Yokoseki T. Isolation and characterization of FliK-independent flagellation mutants from Salmonella typhimurium. J Bacteriol. 1994 Dec;176(24):7625-9. PubMed PMID: 8002586; PubMed Central PMCID: PMC197219.

Lam R, Romanov V, Johns K, Battaile KP, Wu-Brown J, Guthrie JL, Hausinger RP, Pai EF, Chirgadze NY. Crystal structure of a truncated urease accessory protein UreF from Helicobacter pylori. Proteins. 2010 Oct;78(13):2839-48. PubMed PMID: 20635345; PubMed Central PMCID: PMC2978904.

Lebrette H, Iannello M, Fontecilla-Camps JC, Cavazza C. The binding mode of Ni-(L-His)2 in NikA revealed by X-ray crystallography. J Inorg Biochem. 2013 Apr;121:16-8. PubMed PMID: 23314594.

Lee TH, Yang JC, Lee SC, Farn SS, Wang TH. Effect of mouth washing on the. J Gastroenterol Hepatol. 2001 Mar;16(3):261-3. PubMed PMID: 11339415.

Lenz O, ter Meulen J, Klenk HD, Seidah NG, Garten W. The Lassa virus glycoprotein precursor GP-C is proteolytically processed by subtilase SKI-1/S1P. Proc Natl Acad Sci U S A. 2001 Oct 23;98(22):12701-5. PubMed PMID: 11606739; PubMed Central PMCID: PMC60117.

Lertsethtakarn P, Ottemann KM, Hendrixson DR. Motility and chemotaxis in Campylobacter and Helicobacter . Annu Rev Microbiol. 2011;65:389-410. PubMed PMID: 21939377.

Leslie AG. The integration of macromolecular diffraction data. Acta Crystallogr D Biol Crystallogr. 2006 Jan;62(Pt 1):48-57. PubMed PMID: 16369093.

Leunk RD, Johnson PT, David BC, Kraft WG, Morgan DR. Cytotoxic activity in broth-culture filtrates of Campylobacter pylori. J Med Microbiol. 1988 Jun;26(2):93-9. PubMed PMID: 3385767.

Liu J, Huang C, Shin DH, Yokota H, Jancarik J, Kim JS, Adams PD, Kim R, Kim SH. Crystal structure of a heat-inducible transcriptional repressor HrcA from Thermotoga maritima: structural insight into DNA binding and dimerization. J Mol Biol. 2005 Jul 29;350(5):987-96. PubMed PMID: 15979091.

Losonsky GA, Kotloff KL, Walker RI. B cell responses in gastric antrum and duodenum following oral inactivated Helicobacter pylori whole cell (HWC) vaccine and LT(R192G) in H pylori seronegative individuals. Vaccine. 2003 Jan 17;21(5-6):562-5. PubMed PMID: 12531656.

Lowenthal AC, Hill M, Sycuro LK, Mehmood K, Salama NR, Ottemann KM. Functional analysis of the Helicobacter pylori flagellar switch proteins. J Bacteriol. 2009 Dec;191(23):7147-56. PubMed PMID: 19767432; PubMed Central PMCID: PMC2786559.

Mahdavi J, Sondén B, Hurtig M, Olfat FO, Forsberg L, Roche N, Angstrom J, Larsson T, Teneberg S, Karlsson KA, Altraja S, Wadström T, Kersulyte D, Berg DE, Dubois A, Petersson C, Magnusson KE, Norberg T, Lindh F, Lundskog BB, Arnqvist A, Hammarström L, Borén T. Helicobacter pylori SabA adhesin in persistent infection and chronic inflammation. Science. 2002 Jul 26;297(5581):573-8. PubMed PMID: 12142529; PubMed Central PMCID: PMC2570540.

Maier RJ, Benoit SL, Seshadri S. Nickel-binding and accessory proteins facilitating Ni-enzyme maturation in Helicobacter pylori. Biometals. 2007 Jun;20(3-4):655-64. PubMed PMID: 17205208; PubMed Central PMCID: PMC2665251.

Malaty HM, Engstrand L, Pedersen NL, Graham DY. Helicobacter pylori infection: genetic and environmental influences A study of twins. Ann Intern Med. 1994 Jun 15;120(12):982-6. PubMed PMID: 8185146.

Malaty HM, Evans DJ Jr, Abramovitch K, Evans DG, Graham DY. Helicobacter pylori infection in dental workers: a seroepidemiology study. Am J Gastroenterol. 1992 Dec;87(12):1728-31. PubMed PMID: 1449133.

Malaty HM, Evans DG, Evans DJ Jr, Graham DY. Helicobacter pylori in Hispanics: comparison with blacks and whites of similar age and socioeconomic class. Gastroenterology. 1992 Sep;103(3):813-6. PubMed PMID: 1499931.

Malfertheiner P, Megraud F, O'Morain C, Bazzoli F, El-Omar E, Graham D, Hunt R, Rokkas T, Vakil N, Kuipers EJ. Current concepts in the management of Helicobacter pylori infection: the Maastricht III Consensus Report. Gut. 2007 Jun;56(6):772-81. PubMed PMID: 17170018; PubMed Central PMCID: PMC1954853.

Marcus EA, Sachs G, Scott DR. The role of ExbD in periplasmic pH homeostasis in Helicobacter pylori. Helicobacter. 2013 Oct;18(5):363-72. PubMed PMID: 23600974; PubMed Central PMCID: PMC3742559.

Marcus EA, Sachs G, Wen Y, Feng J, Scott DR. Role of the Helicobacter pylori sensor kinase ArsS in protein trafficking and acid acclimation. J Bacteriol. 2012 Oct;194(20):5545-51. PubMed PMID: 22865848; PubMed Central PMCID: PMC3458681.

Marshall BJ, Warren JR. Unidentified curved bacilli in the stomach of patients with gastritis and peptic ulceration. Lancet. 1984 Jun 16;1(8390):1311-5. PubMed PMID: 6145023.

Mattle D, Zeltina A, Woo JS, Goetz BA, Locher KP. Two stacked heme molecules in the binding pocket of the periplasmic heme-binding protein HmuT from Yersinia pestis. J Mol Biol. 2010 Nov 26;404(2):220-31. PubMed PMID: 20888343.

McGee DJ, Coker C, Testerman TL, Harro JM, Gibson SV, Mobley HL. The Helicobacter pylori flbA flagellar biosynthesis and regulatory gene is required for motility and virulence and modulates urease of H pylori and Proteus mirabilis. J Med Microbiol. 2002 Nov;51(11):958-70. PubMed PMID: 12448680.

McGee DJ, May CA, Garner RM, Himpsl JM, Mobley HL. Isolation of Helicobacter pylori genes that modulate urease activity. J Bacteriol. 1999 Apr;181(8):2477-84. PubMed PMID: 10198012; PubMed Central PMCID: PMC93674.

Mehta N, Olson JW, Maier RJ. Characterization of Helicobacter pylori nickel metabolism accessory proteins needed for maturation of both urease and hydrogenase. J Bacteriol. 2003 Feb;185(3):726-34. PubMed PMID: 12533448; PubMed Central PMCID: PMC142838.

Mehta N, Benoit S, Maier RJ. Roles of conserved nucleotide-binding domains in accessory proteins, HypB and UreG, in the maturation of nickel-enzymes required for efficient Helicobacter pylori colonization. Microb Pathog. 2003 Nov;35(5):229-34. PubMed PMID: 14521881.

Mitchell HM, Li YY, Hu PJ, Liu Q, Chen M, Du GG, Wang ZJ, Lee A, Hazell SL. Epidemiology of Helicobacter pylori in southern China: identification of early childhood as the critical period for acquisition. J Infect Dis. 1992 Jul;166(1):149-53. PubMed PMID: 1607687.

Mobley HL, Garner RM, Bauerfeind P. Helicobacter pylori nickel-transport gene nixA: synthesis of catalytically active urease in Escherichia coli independent of growth conditions. Mol Microbiol. 1995 Apr;16(1):97-109. PubMed PMID: 7651142.

Molinari M, Salio M, Galli C, Norais N, Rappuoli R, Lanzavecchia A, Montecucco C. Selective inhibition of Ii-dependent antigen presentation by Helicobacter pylori toxin VacA. J Exp Med. 1998 Jan 5;187(1):135-40. PubMed PMID: 9419220; PubMed Central PMCID: PMC2199184.

Montecucco C, Rappuoli R. Living dangerously: how Helicobacter pylori survives in the human stomach. Nat Rev Mol Cell Biol. 2001 Jun;2(6):457-66. PubMed PMID: 11389469.

Morris A, Nicholson G, Lloyd G, Haines D, Rogers A, Taylor D. Seroepidemiology of Campylobacter pyloridis. N Z Med J. 1986 Sep 10;99(809):657-9. PubMed PMID: 3463897.

Morris A, Lloyd G, Nicholson G. Campylobacter pyloridis serology among gastroendoscopy clinic staff. N Z Med J. 1986 Oct 22;99(812):819-20. PubMed PMID: 3466096.

Moulard M, Hallenberger S, Garten W, Klenk HD. Processing and routage of HIV glycoproteins by furin to the cell surface. Virus Res. 1999 Mar;60(1):55-65. PubMed PMID: 10225274.

Namavar F, Roosendaal R, Kuipers EJ, de Groot P, van der Bijl MW, Peña AS, de Graaff J. Presence of Helicobacter pylori in the oral cavity, oesophagus, stomach and faeces of patients with gastritis. Eur J Clin Microbiol Infect Dis. 1995 Mar;14(3):234-7. PubMed PMID: 7614967.

Namba K, Vonderviszt F. Molecular architecture of bacterial flagellum. Q Rev Biophys. 1997 Feb;30(1):1-65. PubMed PMID: 9134575.

Narberhaus F. Negative regulation of bacterial heat shock genes. Mol Microbiol. 1999 Jan;31(1):1-8. PubMed PMID: 9987104.

Navarro C, Wu LF, Mandrand-Berthelot MA. The nik operon of Escherichia coli encodes a periplasmic binding-protein-dependent transport system for nickel. Mol Microbiol. 1993 Sep;9(6):1181-91. PubMed PMID: 7934931.

Niehus E, Gressmann H, Ye F, Schlapbach R, Dehio M, Dehio C, Stack A, Meyer TF, Suerbaum S, Josenhans C. Genome-wide analysis of transcriptional hierarchy and feedback regulation in the flagellar system of Helicobacter pylori. Mol Microbiol. 2004 May;52(4):947-61. PubMed PMID: 15130117.

Norris V, Baisley K, Dunn K, Warrington S, Morocutti A. Combined analysis of three crossover clinical pharmacology studies of effects of rabeprazole and esomeprazole on 24-h intragastric pH in healthy volunteers. Aliment Pharmacol Ther. 2007 Feb 15;25(4):501-10. PubMed PMID: 17270006.

O'Toole PW, Lane MC, Porwollik S. Helicobacter pylori motility. Microbes Infect. 2000 Aug;2(10):1207-14. PubMed PMID: 11008110.

Oganesyan N, Kim SH, Kim R. On-column protein refolding for crystallization. J Struct Funct Genomics. 2005;6(2-3):177-82. PubMed PMID: 16211516.

Ohnishi K, Ohto Y, Aizawa S, Macnab RM, Iino T. FlgD is a scaffolding protein needed for flagellar hook assembly in Salmonella typhimurium. J Bacteriol. 1994 Apr;176(8):2272-81. PubMed PMID: 8157595; PubMed Central PMCID: PMC205349.

Olson JW, Mehta NS, Maier RJ. Requirement of nickel metabolism proteins HypA and HypB for full activity of both hydrogenase and urease in Helicobacter pylori. Mol Microbiol. 2001 Jan;39(1):176-82. PubMed PMID: 11123699.

Pallen MJ, Penn CW, Chaudhuri RR. Bacterial flagellar diversity in the post-genomic era. Trends Microbiol. 2005 Apr;13(4):143-9. PubMed PMID: 15817382.

Parsonnet J, Replogle M, Yang S, Hiatt R. Seroprevalence of CagA-positive strains among Helicobacter pylori-infected, healthy young adults. J Infect Dis. 1997 May;175(5):1240-2. PubMed PMID: 9129095.

Paul K, Gonzalez-Bonet G, Bilwes AM, Crane BR, Blair D. Architecture of the flagellar rotor. EMBO J. 2011 Jun 14;30(14):2962-71. PubMed PMID: 21673656; PubMed Central PMCID: PMC3160249.

Peek RM Jr, Blaser MJ. Helicobacter pylori and gastrointestinal tract adenocarcinomas. Nat Rev Cancer. 2002 Jan;2(1):28-37. PubMed PMID: 11902583.

Peek RM Jr. Helicobacter pylori strain-specific modulation of gastric mucosal cellular turnover: implications for carcinogenesis. J Gastroenterol. 2002;37 Suppl 13:10-6. PubMed PMID: 12109657.

Penagini R, Carmagnola S, Cantu P. Review article: gastro-oesophageal reflux disease--pathophysiological issues of clinical relevance. Aliment Pharmacol Ther. 2002 Jul;16 Suppl 4:65-71. PubMed PMID: 12047263.

Perez-Perez GI, Rothenbacher D, Brenner H. Epidemiology of Helicobacter pylori infection. Helicobacter. 2004;9 Suppl 1:1-6. PubMed PMID: 15347299.

Pfeiffer J, Guhl J, Waidner B, Kist M, Bereswill S. Magnesium uptake by CorA is essential for viability of the gastric pathogen Helicobacter pylori. Infect Immun. 2002 Jul;70(7):3930-4. PubMed PMID: 12065537; PubMed Central PMCID: PMC128062.

Pflock M, Dietz P, Schär J, Beier D. Genetic evidence for histidine kinase HP165 being an acid sensor of Helicobacter pylori. FEMS Microbiol Lett. 2004 May 1;234(1):51-61. PubMed PMID: 15109719.

Pflock M, Kennard S, Finsterer N, Beier D. Acid-responsive gene regulation in the human pathogen Helicobacter pylori. J Biotechnol. 2006 Oct 20;126(1):52-60. PubMed PMID: 16713649.

Phadnis SH, Parlow MH, Levy M, Ilver D, Caulkins CM, Connors JB, Dunn BE. Surface localization of Helicobacter pylori urease and a heat shock protein homolog requires bacterial autolysis. Infect Immun. 1996 Mar;64(3):905-12. PubMed PMID: 8641799; PubMed Central PMCID: PMC173855.

Richardson PT, Park SF. Enterochelin acquisition in Campylobacter coli: characterization of components of a binding-protein-dependent transport system. Microbiology. 1995 Dec;141 (Pt 12):3181-91. PubMed PMID: 8574410.

Robertson BR, Button DK. Toluene induction and uptake kinetics and their inclusion in the specific-affinity relationship for describing rates of hydrocarbon metabolism. Appl Environ Microbiol. 1987 Sep;53(9):2193-205. PubMed PMID: 16347440; PubMed Central PMCID: PMC204080.

Romaniuk PJ, Zoltowska B, Trust TJ, Lane DJ, Olsen GJ, Pace NR, Stahl DA. Campylobacter pylori, the spiral bacterium associated with human gastritis, is not a true Campylobacter sp. J Bacteriol. 1987 May;169(5):2137-41. PubMed PMID: 3571163; PubMed Central PMCID: PMC212113.

Roncarati D, Spohn G, Tango N, Danielli A, Delany I, Scarlato V. Expression, purification and characterization of the membrane-associated HrcA repressor protein of Helicobacter pylori. Protein Expr Purif. 2007 Feb;51(2):267-75. PubMed PMID: 16997572.

Ruiz T, Francis NR, Morgan DG, DeRosier DJ. Size of the export channel in the flagellar filament of Salmonella typhimurium. Ultramicroscopy. 1993 Feb;49(1-4):417-25. PubMed PMID: 8475605.

Sarkar MK, Paul K, Blair D. Chemotaxis signaling protein CheY binds to the rotor protein FliN to control the direction of flagellar rotation in Escherichia coli. Proc Natl Acad Sci U S A. 2010 May 18;107(20):9370-5. PubMed PMID: 20439729; PubMed Central PMCID: PMC2889077.

Saunders NJ, Peden JF, Hood DW, Moxon ER. Simple sequence repeats in the Helicobacter pylori genome. Mol Microbiol. 1998 Mar;27(6):1091-8. PubMed PMID: 9570395.

Schauer K, Gouget B, Carrière M, Labigne A, de Reuse H. Novel nickel transport mechanism across the bacterial outer membrane energized by the TonB/ExbB/ExbD machinery. Mol Microbiol. 2007 Feb;63(4):1054-68. PubMed PMID: 17238922.

Schauer K, Muller C, Carrière M, Labigne A, Cavazza C, De Reuse H. The Helicobacter pylori GroES cochaperonin HspA functions as a specialized nickel chaperone and sequestration protein through its unique C-terminal extension. J Bacteriol. 2010 Mar;192(5):1231-7. PubMed PMID: 20061471; PubMed Central PMCID: PMC2820833.

Sebbane F, Mandrand-Berthelot MA, Simonet M. Genes encoding specific nickel transport systems flank the chromosomal urease locus of pathogenic yersiniae. J Bacteriol. 2002 Oct;184(20):5706-13. PubMed PMID: 12270829; PubMed Central PMCID: PMC139606.

Seidah NG, Day R, Marcinkiewicz M, Chrétien M. Precursor convertases: an evolutionary ancient, cell-specific, combinatorial mechanism yielding diverse bioactive peptides and proteins. Ann N Y Acad Sci. 1998 May 15;839:9-24. PubMed PMID: 9629127.

Seshadri S, Benoit SL, Maier RJ. Roles of His-rich hpn and hpn-like proteins in Helicobacter pylori nickel physiology. J Bacteriol. 2007 Jun;189(11):4120-6. PubMed PMID: 17384182; PubMed Central PMCID: PMC1913394.

Shaik MM, Cendron L, Salamina M, Ruzzene M, Zanotti G. Helicobacter pylori periplasmic receptor CeuE (HP1561) modulates its nickel affinity via organic metallophores. Mol Microbiol. 2013 Dec 12;PubMed PMID: 24330328.

Shepherd M, Heath MD, Poole RK. NikA binds heme: a new role for an Escherichia coli periplasmic nickel-binding protein. Biochemistry. 2007 May 1;46(17):5030-7. PubMed PMID: 17411076.

Shi R, Munger C, Asinas A, Benoit SL, Miller E, Matte A, Maier RJ, Cygler M. Crystal structures of apo and metal-bound forms of the UreE protein from Helicobacter pylori: role of multiple metal binding sites. Biochemistry. 2010 Aug 24;49(33):7080-8. PubMed PMID: 20681615.

Shomer NH, Dangler CA, Schrenzel MD, Whary MT, Xu S, Feng Y, Paster BJ, Dewhirst FE, Fox JG. Cholangiohepatitis and inflammatory bowel disease induced by a novel urease-negative Helicobacter species in A/J and Tac:ICR:HascidfRF mice. Exp Biol Med (Maywood). 2001 May;226(5):420-8. PubMed PMID: 11393169.

Skorupski K, Taylor RK. Control of the ToxR virulence regulon in Vibrio cholerae by environmental stimuli. Mol Microbiol. 1997 Sep;25(6):1003-9. PubMed PMID: 9350858.

Sorger PK, Nelson HC. Trimerization of a yeast transcriptional activator via a coiled-coil motif. Cell. 1989 Dec 1;59(5):807-13. PubMed PMID: 2686840.

Souza RC, Lima JH. Helicobacter pylori and gastroesophageal reflux disease: a review of this intriguing relationship. Dis Esophagus. 2009;22(3):256-63. PubMed PMID: 19425207.

Spohn G, Danielli A, Roncarati D, Delany I, Rappuoli R, Scarlato V. Dual control of Helicobacter pylori heat shock gene transcription by HspR and HrcA. J Bacteriol. 2004 May;186(10):2956-65. PubMed PMID: 15126455; PubMed Central PMCID: PMC400627.

Spohn G, Scarlato V. The autoregulatory HspR repressor protein governs chaperone gene transcription in Helicobacter pylori. Mol Microbiol. 1999 Nov;34(4):663-74. PubMed PMID: 10564507.

Spohn G, Scarlato V. Motility of Helicobacter pylori is coordinately regulated by the transcriptional activator FlgR, an NtrC homolog. J Bacteriol. 1999 Jan;181(2):593-9. PubMed PMID: 9882675; PubMed Central PMCID: PMC93415.

Stähler FN, Odenbreit S, Haas R, Wilrich J, Van Vliet AH, Kusters JG, Kist M, Bereswill S. The novel Helicobacter pylori CznABC metal efflux pump is required for cadmium, zinc, and nickel resistance, urease modulation, and gastric colonization. Infect Immun. 2006 Jul;74(7):3845-52. PubMed PMID: 16790756; PubMed Central PMCID: PMC1489693.

Stoof J, Kuipers EJ, Klaver G, van Vliet AH. An ABC transporter and a TonB ortholog contribute to Helicobacter mustelae nickel and cobalt acquisition. Infect Immun. 2010 Oct;78(10):4261-7. PubMed PMID: 20643857; PubMed Central PMCID: PMC2950367.

Stoof J, Kuipers EJ, van Vliet AH. Characterization of NikR-responsive promoters of urease and metal transport genes of Helicobacter mustelae. Biometals. 2010 Feb;23(1):145-59. PubMed PMID: 19894125.

Suerbaum S, Michetti P. Helicobacter pylori infection. N Engl J Med. 2002 Oct 10;347(15):1175-86. PubMed PMID: 12374879.

Suerbaum S, Josenhans C. Helicobacter pylori evolution and phenotypic diversification in a changing host. Nat Rev Microbiol. 2007 Jun;5(6):441-52. PubMed PMID: 17505524.

Suerbaum S, Josenhans C, Labigne A. Cloning and genetic characterization of the Helicobacter pylori and Helicobacter mustelae flaB flagellin genes and construction of H pylori flaA- and flaB-negative mutants by electroporation-mediated allelic exchange. J Bacteriol. 1993 Jun;175(11):3278-88. PubMed PMID: 8501031; PubMed Central PMCID: PMC204724.

Suerbaum S, Thiberge JM, Kansau I, Ferrero RL, Labigne A. Helicobacter pylori hspA-hspB heat-shock gene cluster: nucleotide sequence, expression, putative function and immunogenicity. Mol Microbiol. 1994 Dec;14(5):959-74. PubMed PMID: 7715457.

Suganuma M, Kurusu M, Okabe S, Sueoka N, Yoshida M, Wakatsuki Y, Fujiki H. Helicobacter pylori membrane protein 1: a new carcinogenic factor of Helicobacter pylori. Cancer Res. 2001 Sep 1;61(17):6356-9. PubMed PMID: 11522625.

Sydor AM, Lebrette H, Ariyakumaran R, Cavazza C, Zamble DB. Relationship between Ni(II) and Zn(II) coordination and nucleotide binding by the Helicobacter pylori [NiFe]-hydrogenase and urease maturation factor HypB. J Biol Chem. 2013 Dec 12;PubMed PMID: 24338018.

Sydor AM, Liu J, Zamble DB. Effects of metal on the biochemical properties of Helicobacter pylori HypB, a maturation factor of [NiFe]-hydrogenase and urease. J Bacteriol. 2011 Mar;193(6):1359-68. PubMed PMID: 21239585; PubMed Central PMCID: PMC3067625.

Szeto ML, Lee CK, Yee YK, Li KF, Lee WK, Lee CC, Que TL, Wong BC. Evaluation of five commercial serological tests for the detection of Helicobacter pylori infection in Chinese. Aliment Pharmacol Ther. 2001 May;15(5):703-6. PubMed PMID: 11328265.

Thomas J, Stafford GP, Hughes C. Docking of cytosolic chaperone-substrate complexes at the membrane ATPase during flagellar type III protein export. Proc Natl Acad Sci U S A. 2004 Mar 16;101(11):3945-50. PubMed PMID: 15001708; PubMed Central PMCID: PMC374349.

Tomb JF, White O, Kerlavage AR, Clayton RA, Sutton GG, Fleischmann RD, Ketchum KA, Klenk HP, Gill S, Dougherty BA, Nelson K, Quackenbush J, Zhou L, Kirkness EF, Peterson S, Loftus B, Richardson D, Dodson R, Khalak HG, Glodek A, McKenney K, Fitzegerald LM, Lee N, Adams MD, Hickey EK, Berg DE, Gocayne JD, Utterback TR, Peterson JD, Kelley JM, Cotton MD, Weidman JM, Fujii C, Bowman C, Watthey L, Wallin E, Hayes WS, Borodovsky M, Karp PD, Smith HO, Fraser CM, Venter JC. The complete genome sequence of the gastric pathogen Helicobacter pylori. Nature. 1997 Aug 7;388(6642):539-47. PubMed PMID: 9252185.

Touré BB, Munzer JS, Basak A, Benjannet S, Rochemont J, Lazure C, Chrétien M, Seidah NG. Biosynthesis and enzymatic characterization of human SKI-1/S1P and the processing of its inhibitory prosegment. J Biol Chem. 2000 Jan 28;275(4):2349-58. PubMed PMID: 10644685.

Tran AX, Karbarz MJ, Wang X, Raetz CR, McGrath SC, Cotter RJ, Trent MS. Periplasmic cleavage and modification of the 1-phosphate group of Helicobacter pylori lipid A. J Biol Chem. 2004 Dec 31;279(53):55780-91. PubMed PMID: 15489235; PubMed Central PMCID: PMC2552395.

Tummuru MK, Cover TL, Blaser MJ. Cloning and expression of a high-molecular-mass major antigen of Helicobacter pylori: evidence of linkage to cytotoxin production. Infect Immun. 1993 May;61(5):1799-809. PubMed PMID: 8478069; PubMed Central PMCID: PMC280768.

Uemura N, Okamoto S, Yamamoto S, Matsumura N, Yamaguchi S, Yamakido M, Taniyama K, Sasaki N, Schlemper RJ. Helicobacter pylori infection and the development of gastric cancer. N Engl J Med. 2001 Sep 13;345(11):784-9. PubMed PMID: 11556297.

Vagin A, Teplyakov A. Molecular replacement with MOLREP. Acta Crystallogr D Biol Crystallogr. 2010 Jan;66(Pt 1):22-5. PubMed PMID: 20057045.

van Vliet AH, Stoof J, Poppelaars SW, Bereswill S, Homuth G, Kist M, Kuipers EJ, Kusters JG. Differential regulation of amidase- and formamidase-mediated ammonia production by the Helicobacter pylori fur repressor. J Biol Chem. 2003 Mar 14;278(11):9052-7. PubMed PMID: 12499381.

van Vliet AH, Kuipers EJ, Waidner B, Davies BJ, de Vries N, Penn CW, Vandenbroucke-Grauls CM, Kist M, Bereswill S, Kusters JG. Nickel-responsive induction of urease expression in Helicobacter pylori is mediated at the transcriptional level. Infect Immun. 2001 Aug;69(8):4891-7. PubMed PMID: 11447165; PubMed Central PMCID: PMC98579.

van Vliet AH, Poppelaars SW, Davies BJ, Stoof J, Bereswill S, Kist M, Penn CW, Kuipers EJ, Kusters JG. NikR mediates nickel-responsive transcriptional induction of urease expression in Helicobacter pylori. Infect Immun. 2002 Jun;70(6):2846-52. PubMed PMID: 12010971; PubMed Central PMCID: PMC128006.

Velayudhan J, Hughes NJ, McColm AA, Bagshaw J, Clayton CL, Andrews SC, Kelly DJ. Iron acquisition and virulence in Helicobacter pylori: a major role for FeoB, a high-affinity ferrous iron transporter. Mol Microbiol. 2000 Jul;37(2):274-86. PubMed PMID: 10931324.

Vergauwen B, Van der Meeren R, Dansercoer A, Savvides SN. Delineation of the Pasteurellaceae-specific GbpA-family of glutathione-binding proteins. BMC Biochem. 2011 Nov 16;12:59. PubMed PMID: 22087650; PubMed Central PMCID: PMC3295651.

Vincent MJ, Sanchez AJ, Erickson BR, Basak A, Chretien M, Seidah NG, Nichol ST. Crimean-Congo hemorrhagic fever virus glycoprotein proteolytic processing by subtilase SKI-1. J Virol. 2003 Aug;77(16):8640-9. PubMed PMID: 12885882; PubMed Central PMCID: PMC167219.

Watanabe S, Takagi A, Tada U, Kabir AM, Koga Y, Kamiya S, Osaki T, Miwa T. Cytotoxicity and motility of Helicobacter pylori. J Clin Gastroenterol. 1997;25 Suppl 1:S169-71. PubMed PMID: 9479644.

West AL, Evans SE, González JM, Carter LG, Tsuruta H, Pozharski E, Michel SL. Ni(II) coordination to mixed sites modulates DNA binding of HpNikR via a long-range effect. Proc Natl Acad Sci U S A. 2012 Apr 10;109(15):5633-8. PubMed PMID: 22451934; PubMed Central PMCID: PMC3326501.

Windle HJ, Fox A, Ní Eidhin D, Kelleher D. The thioredoxin system of Helicobacter pylori. J Biol Chem. 2000 Feb 18;275(7):5081-9. PubMed PMID: 10671551.

Wolfram L, Bauerfeind P. Conserved low-affinity nickel-binding amino acids are essential for the function of the nickel permease NixA of Helicobacter pylori. J Bacteriol. 2002 Mar;184(5):1438-43. PubMed PMID: 11844775; PubMed Central PMCID: PMC134868.

Wolfram L, Bauerfeind P. Activities of urease and nickel uptake of Helicobacter pylori proteins are media- and host-dependent. Helicobacter. 2009 Aug;14(4):264-70. PubMed PMID: 19674130.

Worst DJ, Otto BR, de Graaff J. Iron-repressible outer membrane proteins of Helicobacter pylori involved in heme uptake. Infect Immun. 1995 Oct;63(10):4161-5. PubMed PMID: 7558334; PubMed Central PMCID: PMC173585.

Wu LF, Mandrand MA. Microbial hydrogenases: primary structure, classification, signatures and phylogeny. FEMS Microbiol Rev. 1993 Apr;10(3-4):243-69. PubMed PMID: 8318259.

Xia W, Li H, Sze KH, Sun H. Structure of a nickel chaperone, HypA, from Helicobacter pylori reveals two distinct metal binding sites. J Am Chem Soc. 2009 Jul 29;131(29):10031-40. PubMed PMID: 19621959.

Xia W, Li H, Yang X, Wong KB, Sun H. Metallo-GTPase HypB from Helicobacter pylori and its interaction with nickel chaperone protein HypA. J Biol Chem. 2012 Feb 24;287(9):6753-63. PubMed PMID: 22179820; PubMed Central PMCID: PMC3307304.

Yamaoka Y, Ojo O, Fujimoto S, Odenbreit S, Haas R, Gutierrez O, El-Zimaity HM, Reddy R, Arnqvist A, Graham DY. Helicobacter pylori outer membrane proteins and gastroduodenal disease. Gut. 2006 Jun;55(6):775-81. PubMed PMID: 16322107; PubMed Central PMCID: PMC1856239.

Ye J, Rawson RB, Komuro R, Chen X, Davé UP, Prywes R, Brown MS, Goldstein JL. ER stress induces cleavage of membrane-bound ATF6 by the same proteases that process SREBPs. Mol Cell. 2000 Dec;6(6):1355-64. PubMed PMID: 11163209.

Yoshida N, Granger DN, Evans DJ Jr, Evans DG, Graham DY, Anderson DC, Wolf RE, Kvietys PR. Mechanisms involved in Helicobacter pylori-induced inflammation. Gastroenterology. 1993 Nov;105(5):1431-40. PubMed PMID: 7901109.

Yoshiyama H, Nakamura H, Kimoto M, Okita K, Nakazawa T. Chemotaxis and motility of Helicobacter pylori in a viscous environment. J Gastroenterol. 1999;34 Suppl 11:18-23. PubMed PMID: 10616760.

Zambelli B, Turano P, Musiani F, Neyroz P, Ciurli S. Zn2+-linked dimerization of UreG from Helicobacter pylori, a chaperone involved in nickel trafficking and urease activation. Proteins. 2009 Jan;74(1):222-39. PubMed PMID: 18767150.

Zambelli B, Danielli A, Romagnoli S, Neyroz P, Ciurli S, Scarlato V. High-affinity Ni2+ binding selectively promotes binding of Helicobacter pylori NikR to its target urease promoter. J Mol Biol. 2008 Nov 28;383(5):1129-43. PubMed PMID: 18790698.

Zambelli B, Berardi A, Martin-Diaconescu V, Mazzei L, Musiani F, Maroney MJ, Ciurli S. Nickel binding properties of Helicobacter pylori UreF, an accessory protein in the nickel-based activation of urease. J Biol Inorg Chem. 2013 Nov 30;PubMed PMID: 24292245.

Zambelli B, Musiani F, Benini S, Ciurli S. Chemistry of Ni2+ in urease: sensing, trafficking, and catalysis. Acc Chem Res. 2011 Jul 19;44(7):520-30. PubMed PMID: 21542631.

Zanotti G, Papinutto E, Dundon W, Battistutta R, Seveso M, Giudice G, Rappuoli R, Montecucco C. Structure of the neutrophil-activating protein from Helicobacter pylori. J Mol Biol. 2002 Oct 11;323(1):125-30. PubMed PMID: 12368104.

Zhang Y, Rodionov DA, Gelfand MS, Gladyshev VN. Comparative genomic analyses of nickel, cobalt and vitamin B12 utilization. BMC Genomics. 2009 Feb 10;10:78. PubMed PMID: 19208259; PubMed Central PMCID: PMC2667541.

Zhang Y. I-TASSER server for protein 3D structure prediction. BMC Bioinformatics. 2008 Jan 23;9:40. PubMed PMID: 18215316; PubMed Central PMCID: PMC2245901.

Zhou H, Luo M, Cai X, Tang J, Niu S, Zhang W, Hu Y, Yin Y, Huang A, Wang D, Wang D. Crystal structure of a novel dimer form of FlgD from P aeruginosa PAO1. Proteins. 2011 Jul;79(7):2346-51. PubMed PMID: 21604306.